FLAWED PHOSPHOLIPID FORMATION OR FAULTY FATTY ACID OXIDATION: DETERMINING THE CAUSE OF MITOCHONDRIAL DYSFUNCTION IN HEARTS LACKING ACSL1

Trisha J. Grevengoed

A dissertation submitted to the faculty at the University of North Carolina at Chapel Hill in partial fulfillment of the requirements for the degree of Doctor of Philosophy in the Department of Nutrition (Biochemistry) in the School of Public Health.

Chapel Hill
2015

Approved by:

Rosalind A. Coleman

Stephen D. Hursting

Liza Makowski

Leslie V. Parise

Steven H. Zeisel

© 2015
Trisha J. Grevengoed
ALL RIGHTS RESERVED

ABSTRACT

Trisha J. Grevengoed: Fatty acid activation in cardiac mitochondria: The role of ACSL1 in phospholipid formation and remodeling, substrate switching, and autophagic flux
(Under the direction of Rosalind A. Coleman)

Cardiovascular disease is the number one cause of death worldwide. In the heart, mitochondria provide up to 95% of energy, with most of this energy coming from metabolism of fatty acids (FA). FA must be converted to acyl-CoAs by acyl-CoA synthetases (ACS) before entry into pathways of β-oxidation or glycerolipid synthesis. ACSL1 contributes more than 90% of total cardiac ACSL activity, and mice with an inducible knockout of ACSL1 (*Acsl1*$^{T-/-}$) have impaired cardiac FA oxidation. The effects of loss of ACSL1 on mitochondrial respiratory function, phospholipid formation, or autophagic flux have not yet been studied.

Acsl1$^{T-/-}$ hearts contained 3-fold more mitochondria with abnormal structure and displayed lower respiratory function. Because ACSL1 exhibited a strong substrate preference for linoleate (18:2), we investigated the composition of mitochondrial phospholipids. *Acsl1*$^{T-/-}$ hearts contained 83% less tetralinoleoyl-cardiolipin (CL), the major form present in control hearts. Modulating ACSL1 expression in cell lines confirmed that ACSL1 is necessary for linoleate incorporation into CL. To determine whether increasing content of linoleate in CL would improve mitochondrial respiratory function, control and *Acsl1*$^{T-/-}$ mice were fed a high linoleate diet, which normalized amount of tetralinoleoyl-CL, but did not improve respiratory function.

The metabolic switch from FA use to high glucose use activates mechanistic target of rapamycin complex 1 (mTORC1), which initiates growth by increasing protein and RNA synthesis and FA metabolism while decreasing autophagy. Short-term mTORC1 inhibition normalized mitochondrial structure, number, and maximal respiration rate in *Acsl1*$^{T-/-}$ hearts but not ADP-stimulated oxygen

consumption, which was likely caused by lower ATP synthase activity present in both vehicle- and rapamycin-treated *Acsl1*$^{T-/-}$ hearts. The autophagic rate was 88% lower in *Acsl1*$^{T-/-}$ hearts. mTORC1 inhibition increased autophagy to a rate that was 3.1-fold higher than in controls, allowing clearance of damaged mitochondria. ACSL1 deficiency in heart activated mTORC1, thereby inhibiting autophagy and increasing the number of damaged mitochondria with impaired respiratory capacity.

ACSL1 is required for the normal composition of phospholipid species and maintenance of FA oxidation to prevent low autophagic rate. Loss of ACSL1 causes impaired mitochondrial respiratory function, which can be partially improved by clearing damaged mitochondria but not by normalizing CL.

ACKNOWLEDGEMENTS

I would like to thank Dr. Rosalind Coleman for helping me develop the skills needed to become an independent researcher. She has instilled the value of critical thinking in every aspect of science. Her support and guidance has been invaluable to my development as a scientist.

Rosalind has also provided me with a laboratory of people that I can learn from: Jessica Ellis's support through my first years of graduate school was vital to that time. Daniel Cooper has gone through much of the process with me and has been a useful critic of experiments as well a sympathetic ear when experiments inevitably did not work. Others in the lab, including David Paul, Angela Wendel, Matthew Keogh, and Florencia Pascual have provided guidance and support that I could not have done without.

I also want to acknowledge my parents' support of me through a process which was completely foreign to them. They told me I could be anything I wanted when I grew up, and helped me along every step of the process. Their support has made it possible for me to complete this work.

PREFACE

Parts of this dissertation have been or will be published in peer-reviewed journals. The majority of Chapter 1 is taken from a review written in collaboration with Dr. Eric Klett and Dr. Rosalind Coleman that has been published in the *Annual Review of Nutrition* (1). Chapter 2 is work that has been submitted to the *Journal of Lipid Research* in which I designed and performed the majority of experiments under the supervision of Dr. Coleman and collaborated with Sarah Martin and Dr. Robert Murphy for measurement of lipid species and with Lalage Katunga and Dr. Ethan Anderson for measurement of mitochondrial function in muscle fibers. Chapter 3 is work that has been submitted to the *FASEB Journal* and is under review. I performed the majority of this work with technical assistance from Daniel Cooper and Jessica Ellis under the supervision of Dr. Coleman.

TABLE OF CONTENTS

LIST OF TABLES

LIST OF FIGURES

LIST OF ABBREVIATIONS

ACBP	Acyl-CoA binding protein
ACC	Acetyl-CoA carboxylase
ACOT	Acyl-CoA thioesterase
ACS	Acyl-CoA synthetase
ACSBg	ACS bubblegum
ACSL	Long-chain ACS
ACSVL	Very-long-chain ACS
AGPAT	Acyl-CoA:1-acylglycerol-3-phosphate acyltransferase
ANT	Adenine nucleotide transferase
ASM	Acid soluble metabolites
Atg	Autophagic protein
CDP-DAG	Cytidine diphosphate-DAG
CEPT	Diacylglycerol choline/ethanolamine phosphotransferase
CMC	Critical micellar concentration
CL	Cardiolipin
CPT1	Carnitine palmitoyltransferase-1
DAG	Diacylglycerol
DGAT	Diacylglycerol acyltransferase
ER	Endoplasmic reticulum
FA	Fatty acid
FABP	FA binding protein
FATP	Fatty acid transport protein
FCCP	Carbonyl cyanide-4-(trifluoromethoxy)-phenylhydrazone
GLUT1	Glucose transporter 1

HSL	Hormone sensitive lipase
LC3b	Microtubule associated protein light chain 3b
mTOR	Mechanistic target of rapamycin
mTORC1	Mechanistic target of rapamycin complex 1
p62/SQSTM1	Sequestome 1
OCR	Oxygen consumption rate
PA	Phosphatidic acid
PC	Phosphatidylcholine
PE	Phosphatidylethanolamine
PEMT	Phosphatidylethanolamine N-methyltransferase
PG	Phosphatidylglycerol
PGPP	Phosphatidylglycerophosphate phosphatase
PGPS	Phosphatidylglycerophosphate synthase
PI	Phosphatidylinositol
PIS	Phosphatidylinositol synthase
PS	Phosphatidylserine
PSD	Phosphatidylserine decarboxylase
PSS	Phosphatidylserine synthase
SNP	Single nucleotide polymorphism
T3	Triiodothyronine
TAG	Triacylglycerol
TCA cycle	Tricarboxylic acid cycle
ULK1	Unc51-like kinase

CHAPTER 1: BACKGROUND

Partitioning of fatty acids and the formation of fatty acyl-CoAs

Long-chain FAs derived from either *de novo* synthesis, dietary sources, or from the turnover of triacylglycerol, phospholipids, and cholesterol esters have multiple metabolic fates. These fates include the entry of FAs into pathways of degradation, incorporation or reincorporation into complex lipids, esterification to proteins, and the synthesis of eicosanoids. Long-chain FAs have additional roles in activating transcription factors, functioning as intracellular signals, and allosterically modulating enzyme reactions (**Fig. 1.1**). Each of these outcomes except for some of those related to signaling and eicosanoid formation require the formation of a long-chain acyl-CoA by one of least 13 acyl-CoA synthetases (ACS) that use long-chain and very-long-chain FAs (ACSL, ACSVL, ACSBg). The 13 ACS isoforms are part of the 26-member ACS family, all of which contain related nucleotide (AMP/ATP) and FA binding motifs, and most of which include a transmembrane domain anchor at the N-terminus.

The long-chain ACS isoforms activate FA of 16-22 carbons (2,3) in an energetically costly two-step reaction that uses the equivalent of two high-energy bonds:

$$\text{Fatty acid} + \text{ATP} \rightarrow \text{acyl-AMP} + \text{PPi}$$

$$\text{Acyl-AMP} + \text{CoASH} \rightarrow \text{acyl-CoA} + \text{AMP}$$

In addition to their uses in β-oxidation and glycerolipids synthesis (**Fig. 1.2**), acyl-CoAs are critical signaling molecules as allosteric inhibitors of adenosine nucleotide translocase (ANT) (4,5), liver glucokinase (6), acetyl-CoA carboxylase (ACC) (7,8), HMG-CoA reductase (9), phosphofructokinase-1 (10), and hormone sensitive lipase (HSL) (10). Acyl-CoAs can also stimulate the release of transport vesicles (11,12). Long-chain acyl-CoAs are excellent detergents that form

micelles in aqueous solutions with the CoA groups exposed to the water phase (13). The measured critical micellar concentrations (CMC) for the most common long-chain acyl-CoAs, 18:1-CoA and 16:0-CoA are about 32 and 42 μM, respectively (14,15). However, within cells, acyl-CoAs are probably bound to proteins and membranes so that the concentration of acyl-CoAs would be too low to self-aggregate. Because of their amphipathic nature, acyl-CoAs can interfere with membrane integrity by acting as detergents; when high concentrations of acyl-CoAs are present, the permeability of membranes to small molecules like sucrose and citrate is altered (16). Myristoylation or palmitoylation of proteins requires acyl-CoAs, but to our knowledge, no changes in protein acylation have been found in mice or cells with a deficiency of an ACS.

Because most mammalian cells contain several different long-chain ACS isoforms, it has been hypothesized that each isoform may partition or channel its long-chain FA substrates into specific downstream pathways. In addition, several of the isoforms have two different start sites, one of which lacks an N-terminal transmembrane anchor, or have alternative internal exons that result from differential splicing (17). Hypothesized differences in cell function include the use of the activated FA for pathways that synthesize glycerolipids and cholesterol esters, for pathways of FA elongation or desaturation, for degradative pathways in the mitochondria, ER, and peroxisomes, for protein acylation, and for transcriptional regulation.

Fatty acid use by acyl-CoA synthetases

FAs are carboxylic acids with long-chain hydrocarbon side groups. In animals, the predominant long-chain FAs are those of 16 and 18 carbons with varying degrees of saturation. FAs of 20 carbons, like 20:4ω6 and 20:5ω3 form a small percent of the total FA content in animals, but are precursors for multiple subfamilies of eicosanoids. The question of how FAs are transported into cells remains controversial, but whether FAs enter via transport proteins or flip-flop across the plasma membrane, their thioesterification to coenzyme A almost certainly prevents their exit. It has been variously speculated that entry might occur via junctions between the plasma membrane and the ER.

Alternatively, entry might be mediated by fatty acid binding protein (FABP) isoforms (18), or facilitated by the FA transport proteins (FATP) (19) that are themselves acyl-CoA synthetases. Several groups, however, have shown that the rapidity of FA entry or "vectorial transport" is driven by intracellular metabolism of the FA (18,20,21).

Understanding the process that channels FAs into specific metabolic pathways requires consideration of the physical chemistry of hydrophobic FAs which must move in an aqueous environment. Further, in order to minimize futile cycles, synthetic and degradative pathways must be separated from one another both spatially and temporally. Cells overcome the problem of hydrophobicity by converting the FA to an amphipathic molecule by the thioesterification of Coenzyme A to the carboxyl group. The ability of the cell to vectorially channel fatty acyl-CoAs towards or away from a metabolic pathway forms the basis of partitioning, and is likely to vary with cell type, intracellular location of carriers and enzymes, cellular energy status, and hormonal signals.

Acyl-CoA binding protein and fatty acid binding proteins

Selective partitioning of acyl-CoAs within cells requires methods of overcoming hydrophobicity, because the amphipathic fatty acyl-CoAs can move freely both in the aqueous cytosol and in membrane monolayers. Two protein families, FABPs and acyl-CoA binding protein (ACBP), aid in FA and acyl-CoA movement within cells and are believed to protect cell membranes from the detergent effects of the acyl-CoAs. FABPs are isoforms of a 10 member intracellular lipid-binding protein family which reversibly binds hydrophobic ligands and, in theory, traffics them throughout the cytosol to various organelles (22). A recent comprehensive review of FABP isoforms identifies metabolic alterations in knockout models, but definitive functions have not been established (23). FABP isoforms are ubiquitously expressed, but differ in stoichiometry, affinity and specificity toward related ligands that include FAs, acyl-CoAs, eicosanoids, and peroxisome proliferator-activated receptor ligands. The amount of an FABP isoform in any tissue appears to reflect the tissue's lipid-metabolizing capacity. For example, in hepatocytes, adipocytes and cardiomyocytes, which

specialize in lipid metabolism, FABPs make up 1–5% of all cytosolic proteins (24). Evidence for the importance of FABPs in lipid metabolism comes from loss-of-function studies in mice. FABP1, which is strongly expressed in liver and intestine, is the only isoform that binds both FA and fatty acyl-CoA; the other FABP isoforms bind only FA (24,25). Two independent *Fabp1*$^{-/-}$ mouse models have been generated but, despite the importance of lipid metabolism in liver and intestine, neither model has an overt phenotype (26,27). When mice are fed low fat chow, *Fabp1*$^{-/-}$ liver appears normal histologically, and serum TAG and total free FA levels are unchanged, although alterations in specific FAs are observed (28). In one of the *Fabp1*$^{-/-}$ models, the hepatic content of phospholipid, cholesterol, and cholesterol ester is greater than in the controls (28). Although the loss of *Fabp1* reduces hepatic FA binding capacity, total liver lipid content, including TAG and free FA, is unchanged. Only under extreme fasting conditions (48 hours) does the reduced FA binding capacity in the knockout mice cause a reduction in hepatic FA uptake, FA oxidation, and TAG levels (27). Although differences were observed in the effects of knockouts of the FABP1 and the intestinal FABP isoform, information related to acyl-CoAs was not provided (29). The adipose-type FABP4 (also known as aP2) is the major isoform in white and brown adipose tissue and macrophages (30,31). Because disruption of the *Fabp4* gene in mice increases the cytosolic content of free FA, FABP4 is generally thought to facilitate FA transport between intracellular compartments for storage or export (32,33), however this model provides no evidence for mistargeted intracellular FA. The heart-type FABP3, which is most abundantly expressed in heart, skeletal muscle, and brain, is induced by acute cold exposure in rat brown adipose tissue (BAT) (34,35), by a 5-day cold exposure, or by a β_3-adrenergic receptor agonist in mouse subcutaneous white adipose as cells became “beiged” (36). Physiologically, the *Fabp3*$^{-/-}$ model is the one knockout that most strongly supports a specific function for FABP in FA partitioning; *Fabp3* deficient mice have defective FA oxidation and are more reliant on glucose as a substrate for energy production in both cardiomyocytes and muscle (37,38). In addition, *Fabp3*$^{-/-}$ mice are extremely cold intolerant (39).

ACBPs bind medium- and long-chain acyl-CoAs with high affinity, but does not bind free FA, acyl-carnitine, or cholesterol (40). The affinity for acyl-CoAs is so much higher for ACBP than for liver-type FABP1 that it was suggested that ACBP is the major carrier of acyl-CoA in all cells including hepatocytes (41). ACBP expression and concentration are highest in liver, but ACBP is also present in high levels in the adrenal cortex, testis and epithelial cells. Because these tissues and cells specialize in secretion, they have high energy needs and may require ACBP to shuttle fatty acyl-CoAs towards energy producing oxidative pathways (42). Disruption of the ACBP homologue in yeast (ACB1), does not affect phospholipid synthesis or turnover, indicating that ACBP is not required for glycerolipid synthesis in yeast. However, yeast deficient in ACB1 have disordered plasma membrane structures as a result of aberrant and reduced sphingolipid synthesis (43). Highlighting the importance of ACBP in *in vivo* metabolism are studies from two separate *Acbp* deficient mouse models. In the first model, the authors concluded that ACBP is an essential protein required for embryonic development because an implantation defect results in embryonic lethality (44). The second knockout was viable, but did not indicate a role for ACBP in trafficking acyl-CoAs, although liver acyl-CoA levels were ~40% lower than in controls; instead, the main effect of the knockout was an impaired skin barrier and the development of alopecia (45). In addition to their skin phenotype, $Acbp^{-/-}$ mice undergo a crisis around the weaning period, exhibiting weakness and poor weight gain (46). At this time point, SREBP maturation is impaired and SREBP target genes involved in cholesterol biogenesis are not appropriately upregulated. It is unclear why two separately generated *Acbp* knockout models express these two disparate phenotypes, but these models indicate that ACBP and the acyl-CoAs they bind are essential for normal growth and development.

Complex lipid synthesis and degradation

Exogenous FAs and those synthesized *de novo* primarily enter pathways of complex lipid synthesis to produce stored energy depots and phospholipid membranes or they enter degradative pathways; degradation includes mitochondrial β-oxidation, peroxisomal β- or α-oxidation (47), and

ER ω-oxidation (48,49). Evolutionarily, the cell has developed organelles that perform each of these processes, evidence of an additional level of fatty acyl-CoA partitioning. Further evidence for this type of partitioning lies in the organelle localization of synthetic and oxidative enzymes. However, although one generally thinks of each organelle as specializing in a single function, in fact, both glycerolipid synthesis and ω-oxidation occur in the ER, both alkyl lipid synthesis and β-oxidation take place in peroxisomes, and both FA synthesis and β-oxidation occur in mitochondria. It is not known how FA and acyl-CoAs are independently directed into these separate pathways.

Glycerolipid Synthesis

The initial and committed step for the *de novo* synthesis of TAG and all glycerophospholipids is the acylation of *sn*-glycerol-3-phosphate with a fatty acyl-CoA to form 1-acyl-*sn*-glycerol-3-phosphate (lysophosphatidic acid) catalyzed by glycerol-3-phosphate acyltransferase (GPAT) (50). GPAT isoforms are present in the outer mitochondrial membrane (GPAT1 and -2) and in the endoplasmic reticulum (GPAT3 and -4) (51). Overexpression of GPAT1 in either isolated primary rat hepatocytes or *in vivo* in rats causes steatosis, confirming the important role of GPAT in initiating hepatic TAG synthesis (52,53). Mouse knockout models of the GPAT isoforms have provided clues as to the partitioning of acyl-CoAs towards synthetic or oxidative pathways. In studies comparing *Gpat1*$^{-/-}$ and *Gpat4*$^{-/-}$ mice, for example, GPAT1, but not GPAT4, is required to incorporate *de novo* synthesized FA into TAG and to divert FA away from oxidation (54). The ER GPATs are likely to channel exogenously derived acyl-CoAs towards TAG or phospholipid synthesis. It is possible that the location of GPAT1 at the outer mitochondrial membrane serves to divert *de novo* synthesized fatty acyl-CoAs away from carnitine palmitoyltransferase-1 (CPT1)-mediated entrance into the mitochondria where they would be oxidized. This hypothesis makes sense from a cellular homeostatic standpoint in that newly synthesized FA would not be oxidized but, instead, stored for later use when energy stores are low. This example of acyl-CoA partitioning at the level of the mitochondria is at least partly controlled by the energy status of the cell and by the animal's hormonal

status. With low cellular energy, activated AMP-activated kinase inhibits GPAT1 and favors mitochondrial β-oxidation, whereas dietary carbohydrate and insulin upregulate GPAT1 and promote TAG synthesis (54,55).

After lysophosphatidic acid is synthesized, it is used in synthesis of TAG for storage or phospholipids for membrane synthesis (**Fig. 1.3**). In the next step, an acyl-CoA:1-acylglycerol-3-phosphate acyltransferase (AGPAT) will add a second acyl-CoA to form phosphatidic acid (PA). At this point, the PA can either be hydrolyzed by PA phosphatase (lipin) to form diacylglycerol (DAG) or be combined with cytidine triphosphate (CTP) to form cytidine diphosphate DAG (CDP-DAG). CDP-DAG is then combined with an inositol by phosphatidylinositol synthase (PIS) to form phosphatidylinositol (PI) at the ER. In the mitochondria, CDP-DAG is converted by phosphatidylglycerophosphate synthase (PGPS) to phosphatidylglycerophosphate, which is then converted to phosphatidylglycerol (PG) by phosphatidylglycerophosphate phosphatase (PGPP). To form cardiolipin (CL), PG is combined with the phosphatidyl group of CDP-DAG by CL synthase in the mitochondrial matrix.

In the other branch of the synthesis pathway, DAG can be used by diacylglycerol acyltransferase (DGAT) to form TAG. DAG is also used to form phosphatidylserine (PS), phosphatidylcholine (PC), or phosphatidylethanolamine (PE). To make PC, the most abundant mammalian phospholipid, CDP-choline is combined with DAG by diacylglycerol choline/ethanolamine phosphotransferase (CEPT) on the ER. PC can also be synthesized from PE by phosphatidylethanolamine N-methyltransferase (PEMT) at the mitochondria-associated membrane. PE is synthesized from DAG and CDP-ethanolamine by CEPT. PS is made from PE or PC by exchange of the headgroups by phosphatidylserine synthase 1 and 2 (PSS1 and PSS2). In the mitochondria, PS can be converted to PE by decarboxylation by phosphatidylserine decarboxylase (PSD) (56). Understanding where these synthesis reactions takes place helps us see how lipid metabolism is compartmentalized within the cell (**Table 1.1**).

CL is highly remodeled after synthesis, typically to contain polyunsaturated fatty acids (**Fig. 1.4**). In heart, the predominant fatty acid is linoleate (18:2). Because CL synthase lacks a preference for phosphatidylglycerol or CDP-diacylglycerol species that contain linoleate (57,58), the acyl-chains of the nascent CL are more highly saturated than those of mature cardiac CL. CL is remodeled by successive removal of acyl-chains by a phospholipase, the identity of which is currently unknown, followed by replacement via transacylation from donor phospholipids, such as PC and PE, or by acyltransferase-mediated esterification of an acyl-CoA. Mutations in tafazzin cause Barth syndrome, an X-linked disorder characterized by skeletal muscle weakness and heart failure in childhood and low tetralinoleoyl-CL and high MLCL (59). In mammalian cells, two additional enzymes, lysocardiolipin acyltransferase 1 (ALCAT1) and MLCL acyltransferase 1 (MLCL AT-1), can use acyl-CoAs to esterify MLCL (60). ALCAT1, however, is located on the ER, which would prevent its interaction with most CL (61), but MLCL AT-1 is found in mitochondria (62). Although overexpressing MLCL AT-1 in tafazzin-deficient lymphoblasts increases both linoleate incorporation into CL and total CL content (62), the importance of MLCL AT-1 for normal CL remodeling in heart cells remains unclear.

Acyl-CoA degradation

The regulation of mitochondrial β-oxidation depends on cellular energy status. When ATP levels are low, acyl-CoAs are transported into the mitochondria by carnitine palmitoyltransferase-1 (CPT1). Mitochondrial β-oxidation of fatty acyl-CoAs is the major route of FA degradation, but very-long-chain FAs and branched-chain FAs are poorly oxidized in mitochondria, and, instead, are degraded in peroxisomes. The β-oxidation capability of peroxisomes terminates at medium-chain acyl-CoAs and produces chain-shortened acyl-CoAs and acetyl- and propionyl-CoAs, which are transported out of the peroxisome as short- to medium-chain acyl-carnitines to be completely oxidized in the mitochondria (63). Depending on its chain length, the acyl-CoA is converted to the

corresponding carnitine ester by one of two peroxisomal enzymes, carnitine acetyltransferase or carnitine octanoyltransferase (CRAT and CROT) (64).

Despite the high-energy cost of acyl-CoA synthesis, numerous acyl-CoA thioesterases (ACOT) reverse this reaction. Because several ACOTs are upregulated by PPARα under the same conditions that promote acyl-CoA synthesis and oxidation, their physiological function remains unclear. The requirement for free CoASH within mitochondria is very high, reflecting the importance of CoASH in both the citric acid cycle and β-oxidation, so it is possible that ACOT operates to ensure free CoASH sufficient to maintain optimal mitochondrial function.

Two distinct types of ACOT proteins (type I and II) have arisen by convergent evolution (65). Type I ACOTs (ACOTs 1–6) contain N-terminal β-sandwich and C-terminal α/β hydrolase domains. Type II ACOTs (ACOTs 7–13) use N-terminal hotdog-fold thioesterase domains (66). The organelle distribution is distinct for each type. Of the type I ACOTs, ACOT1 is located in the cytosol, ACOT2 in mitochondria, and ACOT3-6 in peroxisomes. Of the type II ACOTs, ACOT8 is located in peroxisomes, ACOTs 7, -11, -12 and -13 are in the cytosol, and ACOT9, -10, and -13 are mitochondrial (66). Each of the ACOT isoforms has an acyl-chain length preference; recombinant ACOT3 prefers long-chain acyl-CoAs (12 - 18 carbons), whereas ACOT5 prefers medium-chain acyl-CoAs (C10-CoA) (67). ACOT8 uses acyl-CoA substrates ranging from 2 to 20 carbons, both saturated and unsaturated (63,68), and is strongly inhibited by CoASH (68). This broad substrate specificity and CoASH inhibition suggest that ACOT8 may sense CoASH content and regulate intra-peroxisomal acyl-CoA levels in order to ensure optimal flux through the cellular β-oxidation system. Because few knockout models have been reported, it is difficult to understand the specific roles of the ACOTs. However, ACOT13 (Them2) deficient mice fed a high fat diet are protected from weight gain, hepatic steatosis and glucose intolerance, implying that ACOT13 is important for hepatic β-oxidation and gluconeogenesis (69). Additionally, ACOT13 deficient mice are better able to adapt to acute cold exposure, suggesting that ACOT13 in brown adipose (BAT) may diminish FA channeling into heat production or UCP1 activation (69). The studies involving both ACOT8 and ACOT13

suggest that ACOTs modulate acyl-CoA flux through oxidative pathways. Thus, there may be a reciprocal relationship between the ACSLs and ACOTs to regulate the metabolic fates of acyl-CoAs via either mitochondrial or peroxisomal oxidation.

In hepatocytes, the ω-hydroxylation of medium and long-chain saturated FAs, mediated by the family of Cyp450 4A fatty acid omega hydroxylases, represents an important secondary pathway for FA metabolism in liver under conditions in which hepatocellular fatty acid flux rates exceed the capacities of the normally dominant esterification and mitochondrial β-oxidation pathways (49). This alternative pathway, which synthesizes dicarboxylic fatty acids, diminishes acyl-CoA flux through both the mitochondrial and peroxisomal β-oxidative pathways, perhaps preventing mitochondrial dysfunction. The ω-oxidation of 20:4ω6 initiates the synthesis of the eicosanoid family of signaling molecules (70).

Acyl-CoA synthetases and fatty acid transport proteins

The 26 enzymes that comprise the ACS family have significant sequence homology with highly conserved domains that correspond to an ATP/AMP binding site and a FA binding site (2). Crystallization studies of bacterial and yeast acyl-CoA synthetases (71-73) suggest that the enzyme binds ATP, which induces a conformational change that opens a "gate" to the FA binding site (71). Once bound, the FA is converted to a FA-AMP intermediate. Coenzyme A (CoA) is then bound to the FA-AMP, and AMP is removed. Finally, the acyl-CoA and AMP are released, and the enzyme reverts to its original form.

Acyl-CoA synthetases are named for the FA chain length of the preferred substrate. Short-chain acyl-CoA synthetases (ACSS) activate acetate, propionate, and butyrate. Medium-chain acyl-CoA synthetases (ACSM) prefer FAs of 6-10 carbons, but can also activate longer-chain FAs. Long chain acyl-CoA synthetases (ACSL) activate FAs of 12-20 carbons. Very-long-chain acyl-CoA synthetases (ACSVL) can activate FAs longer than 20 carbons, but prefer 16 and 18 carbon FAs. ACSBg activate both long- and very-long chain fatty acids (74). Overlap in FA preference between

the groups is common, and within each subfamily, individual isoforms have preferences for a specific chain length or saturation. The FA saturation and chain length preference of each ACS enzyme has been hypothesized to relate to the size and shape of the FA-binding site (71). Site-directed mutagenesis of ACSL4 confirmed the FA-binding site and showed that specific amino acids in this site help to determine FA preference (75). In addition to FAs, certain ACSVL isoforms can use other molecules as substrates. ACSVL6 (FATP5) activates bile acids (76,77), and ACSVL1 (FATP2) activates 3α, 7α, 12α-trihydroxy-5β-cholestanoate (78).

Although it has been hypothesized that the subcellular location of each acyl-CoA synthetase determines acyl-CoA partitioning, several of the ACS isoforms have been found on multiple membranes. For example, ACSL1 has been identified on the plasma membrane, ER, nucleus, mitochondria, peroxisomes, GLUT4 vesicles, and lipid droplets (79-84). Several explanations are possible for the abundance of putative subcellular locations. The location of ACSL1 may actually differ in different cell types, perhaps related to splice variants (17). Alternatively, the localization studies may not have examined purified organelles. With overexpression studies, the protein may have been mislocated. Finally, the ACS may move from one location to another under different physiological conditions. For example, FATP1 may translocate from ER to the plasma membrane after insulin stimulation (85).

Supporting the relationship between location and function, the endogenous ACSL1 in liver has been found on ER and mitochondria, corresponding to its effects on neutral lipid synthesis and FA oxidation (86), and cardiac ACSL1 has been identified on mitochondria, consistent with its large effect on FA oxidation (87). If one assumes that the identified location is accurate, one might suggest that ACSL3, which has been found on lipid droplets and ER, participates in FA uptake and glycerolipid biosynthesis (88,89). In liver, FATP4 is located on the ER (90), ACSL4 is located on the ER, mitochondrial associated membrane, and peroxisomes (82,90), and ACSL5 has been found on the mitochondria (82,91). Specific functions related to these sites have not been investigated.

Because changing the expression level of intracellular ACSLs or FATPs alters cellular FA retention, FA uptake may be an exception to the idea that location dictates function (18,90,92). In 3T3-L1 cells, overexpression of FATP1 or FATP4 on the ER or ACSL1 on the mitochondria increases FA uptake and retention by 40% (92). This result may be due to changing the concentration gradient as intracellular FAs are converted to acyl-CoAs or trapping of FAs in the cell with the addition of the CoA.

A mechanism by which substrates are sequentially channeled through a pathway is via multi-enzyme complexes (93). Thus, the location of ACSL1 may dictate where fatty acyl-CoAs are next directed by allowing the ACSL to interact with proteins involved in downstream processing of fatty acyl-CoAs. For example, ACSL1 co-immunoprecipitates with CPT1a and voltage-dependent anionic channel (VDAC) on the outer mitochondrial membrane (94). CPT1a catalyzes the conversion of acyl-CoA to an acyl-carnitine, which is required for transport into the mitochondrial matrix for oxidation (95). This complex of ACSL1, CPT1a, and VDAC could facilitate the transfer of the acyl-CoA product to VDAC and then to CPT1 which would convert it to an acyl-carnitine. Similar protein interactions could exist between ACSL1 or other ACS isoforms and acyltransferases on the ER. An alternative to a direct protein-to-protein transfer might be an ACS-mediated increase in the local concentration of its acyl-CoA product, thereby effecting a localized increase in the amount of substrate available for the downstream pathway.

Regulation of long-chain ACS isoforms

ACSL expression is highly regulated by both nutrient status of the cell and by the developmental stage of the animal. ACSL activity in rat liver increases 7-fold from birth to adulthood (96), suggesting a marked increase in fatty acid metabolism after birth. In liver, *Acsl1* and *Acsl4* are upregulated with fasting and down-regulated with refeeding of a high sucrose diet. *Acsl5* shows the opposite pattern with higher expression during fasting and lower expression with refeeding (97), indicating the potential for different functions or preference for endogenous or exogenous FA of the

different isoforms. A high fat diet increases the expression of liver *Acsl1* (97,98). In liver, a 48-hour fast decreases the amount of ACSL1 on microsomes, whereas a fasting-refeeding regimen increases microsomal ACSL1 (82). A fasting–sucrose refeeding protocol increases *Acsl5* mRNA in liver, but not in intestine (99). In hamster liver, *Acsl3* expression decreases with high fructose feeding (100) and increases with high fat, high cholesterol diet (101).

ACSL activity in adipose is decreased by exercise and noradrenaline, stimuli which increase lipolysis (102,103). Fasting, a time of diminished TAG synthesis, decreases adipose ACSL activity 52% (97). PPARγ agonists increase *Acsl1* expression in adipocytes (104). PPARγ is necessary for adipocyte differentiation, a time of high lipid accumulation, indicating that ACSL1 may play a role in early lipid accumulation in adipocytes. However, loss of ACSL1 does not prevent accumulation of TAG in adipocytes (105), indicating that the majority of TAG synthesis is not dependent on ACSL1. *Acsl1* gene transcription in adipocytes is increased by overeating, insulin, triiodothyronine (T3), and PPARα and PPARγ agonists (102,104,106).

In the heart, peroxisome proliferator-activated receptor α (PPARα) increases the transcription of *Acsl1* (107). Incubation with either insulin or oleate also increases *Acsl1* and *Acsl3* expression in rat cardiomyocytes (107). The predominant ACSL isoform in the heart changes with maturation. In the embryonic day 16 mouse heart, *Acsl3* mRNA predominates, but decreases 3.5-fold by adulthood. Conversely, *Acsl1* mRNA expression is low in the embryonic heart, but increases 2.5-fold with maturation. *Acsl4*, *Acsl5*, and *Acsl6* mRNA abundances remain steady throughout development. During heart maturation, phospholipid acyl chains shift to a more unsaturated profile with 18:2 and 22:6 increasing by 5% and 23%, respectively, of total acyl chains, and 16:0 and 18:1 decreasing by 9% and 5%, respectively (108). Phospholipid acyl chain saturation and length are likely coupled to the fatty acid preference of the predominant ACSL isoform present. During this same period, the heart switches from primarily glucose to FA as the preferred substrate for energy production, consistent with ACSL1-mediated activation of FAs destined for oxidation (87). *Acsl3* expression

decreases more than 2-fold between embryonic day 16 and post-natal day 7, indicating a potential importance in heart development (108).

Acsl3 mRNA is upregulated under disparate conditions, including induction by poliovirus protein 2A infection of HeLa cells; the requirement of ACSL3 for viral proliferation appears to be related to the incorporation of activated FAs into phosphatidylcholine (109). ER stress via activated GSK-3b induces the expression of *Acsl3* in the hepatocarcinoma cell line HuH-7 and in mouse liver, and knocking down *Acsl3*, but not *Acsl1*, with shRNA, blocks ER stress-related lipid accumulation (110).

Norepinephrine or glucagon treatment rapidly decreases ACSL activity in adipocytes, and insulin quenches the effect of norepinephrine on ACSL activity within minutes (103). This rapid change in ACSL activity suggests that post-translational modifications occur to modulate ACSL activity in response to nutritional status and other stimuli. Using mass spectrometry, 25 phosphorylation and 15 acetylation sites were identified on ACSL1 in liver and brown adipocytes. When seven of these sites were mutated to mimic phosphorylation or acetylation, the activity of ACSL1 decreased, confirming the importance of post-translational modifications in regulating ACSL1 activity (111). The phosphorylation of ACSL1 and ACSL4 is also altered by fasting and *ob/ob* genotype in the liver (112), but how these changes in phosphorylation affect activity has not been studied.

Channeling.

Evidence that acyl-CoAs are channeled or partitioned into different pathways was first obtained in *Saccharomyces cerevisiae*, which expresses three well-studied long-chain ACS isoforms (termed Faa1-3p). Analyses of null alleles showed that the ability to use exogenous FA required Faa1p, that Faa2p and Faa3p activate only endogenous FA, and that none of these Faa proteins channel FA towards β-oxidation (113). Replacing yeast Faa null mutants with rodent ACSL or FATP isoforms showed that complementation varies for FA uptake and incorporation (114,115). Similarly,

in ACS-deficient *Escherichia coli* complementation studies showed that each of the 5 rat ACSL isoforms differs in its ability to channel FA into phospholipid synthesis and β-oxidation (116).

The differential effects of inhibiting FA incorporation into triacylglycerol and phospholipid in cultured rat hepatocytes and human fibroblasts also suggested the possibility of channeling in mammalian cells. Thus, the FA acid analog triacsin C decreases [1-^{14}C]oleic acid incorporation into TAG relative to phospholipid and oxidation products (117,118). Because triacsin C is a competitive inhibitor of ACSL1, ACSL3, and ACSL4 (119,120), inhibition studies could not identify specific roles for the individual ACSL isoforms.

Knockout and knockdown of ACSL1

One way to learn about function is to observe the effect on animal or cell physiology and biochemistry in the absence of a particular gene. Knockouts have been made for several of the genes that encode proteins able to activate long-chain fatty acids. Multiple caveats impede firm conclusions based on knockout models. Problems include the fact that many of the ACSL isoforms have splice variants or different start sites, that the expression or activity of other ACSL isoforms may increase to compensate for the absent enzyme, that the long-term absence of a particular enzyme may induce changes in the cell or animal that modify or distort the effect of the missing protein, and that an ACSL isoform may not only be located on several subcellular membranes, but its location and function may differ in different tissues. Thus, the interpretation of function derived from knockout animals remains tentative.

ACSL1, the most extensively studied isoform, is highly expressed in liver, heart, white and brown adipose, and skeletal muscle (107). Multi-tissue and tissue-specific knockouts indicate that ACSL1 has different functions in different tissues (**Table 1.2**). In liver, the knockout causes a 50% decrease in total ACSL activity and a 25-35% decrease in hepatic acyl-CoA content and a 20% decrease in the incorporation of [^{14}C]oleate into TAG (86). Although incorporation of oleate into phospholipids appeared to be unaffected, analysis of phospholipid species suggested that ACSL1

contributes specifically to the incorporation of 18:0-CoA (86). Long-chain acyl-carnitines are 50% lower than controls, suggesting that trafficking of acyl-CoAs into both TAG and oxidation pathways is impaired by the knockout. These data could be interpreted as consistent with an enzyme that either does not target its acyl-CoA product into a specific pathway or that, because of its dual location on both the mitochondria and the ER, ACSL1 partitions its product into both synthetic and degradative pathways.

In contrast, tissue-specific knockouts of ACSL1 in highly oxidative tissues like heart (87) or white or brown adipose (105) strongly suggest that channeling towards β-oxidation is primary. In these tissues, the knockout causes an 80-90% decrease in total ACSL activity and profound decreases in the oxidation of long-chain fatty acids, without altering the incorporation of [^{14}C]oleate into TAG or phospholipid. In *Acsl1*$^{-/-}$ heart, the uptake of the FA analog Br-[^{14}C]palmitate is lower than controls, whereas uptake of 2-deoxy-[^{14}C]glucose increases 8-fold. In ACSL1-deficient brown adipose, the defect in FA oxidation impairs the ability of the mice to maintain a normal body temperature when placed at 4 ºC. In both heart and brown adipose, although *Acsl3* mRNA is upregulated, this isoform is apparently ineffective in supplying acyl-CoA for oxidation and thermogenesis. Similarly, in white adipose, the loss of ACSL1 activity causes a 50% decrease in [^{14}C]18:1 oxidation, but no alteration in FA incorporation into TAG or phospholipid; in fact, compared to controls, white adipose depots are 40% larger (105). Interestingly, an shRNA-mediated knockdown of ACSL1 in 3T3-L1 adipocytes supported a role in FA re-esterification, suggesting that the function of ACSL1 in these cells may differ from that in mouse adipose tissue (121).

In macrophages from diabetic mice and humans, ACSL1 is upregulated; it increases the metabolism of 20:4ω6 and enhances inflammation and atherosclerosis (122). Unlike the deficiency in liver, adipose, and heart, ACSL1 deficiency in macrophages did not impair either FA oxidation or the accumulation of neutral lipid (122). Surprisingly, the deficiency caused a reduction in the levels of 20:4ω6-CoA and prevented the increased production of PGE2 that is usually observed in mice with type-1 diabetes. It was speculated that this finding was the result either of limited uptake and

activation of 20:4 and depletion of the membrane phospholipid pool available as a substrate for phospholipase A2 (123) or caused by lack of ACSL1-mediated activation of 18:2 as a substrate for the elongation and desaturation enzymes that convert 18:2-CoA to 20:4-CoA (124). In addition, when macrophages are activated by a variety of inflammatory signals, *Acsl1* mRNA and protein increase markedly, and the absence of ACSL1 reduced lipopolysaccharide (LPS)-stimulated increase in 16:0-, 18:1-, and 20:4-CoA levels, diminished multiple acyl- and alkyl-PC species, and reduced the turnover of 20:4 in several phospholipids, but did not affect the LPS-stimulated increase in ceramide species (125). Similarly, the absence of ACSL1 in endothelial cells resulted in a >50% decrease in ACSL total activity, but no change in 16:0 oxidation (126). These data show clearly that the function of ACSL1 in macrophages differs fundamentally from its function in oxidative tissues and liver.

Overexpression of ACSL1

When a protein has been over-expressed, the interpretation of its function is problematic. The transfected protein may be located in a membrane or organelle with which it is not normally associated. If adenovirus-mediated over-expression is used, virus toxicity may cause cells to function abnormally and, ultimately, even to lyse. With transgenic over-expression, the gene can insert into the DNA at a position that interrupts an unrelated function. The situations most likely to present problems in interpretation are those in which an over-expressed enzyme synthesizes large amounts of a product for which the downstream cellular machinery is unprepared to handle. Thus, the synthesis of a large amount of acyl-CoA may overwhelm downstream pathways that can neither use the acyl-CoAs for synthetic purposes nor degrade them quickly (126). The detergent properties of acyl-CoAs may then damage cell membranes and alter the functions of membrane-associated receptors, enzymes and transporters. One example of such acyl-CoA toxicity occurs when ACSL1 is over-expressed in heart (127,128). As might be expected, the resulting lipotoxic cardiomyopathy is ameliorated by cardiac over-expression of diacylglycerol acyltransferase, a downstream enzyme that can use the

accumulating acyl-CoAs to synthesize triacylglycerol and sequester the excess acyl-CoAs in cytoprotective lipid droplets (129).

In other studies in which ACSL and FATP/ACSVL isoforms are over-expressed in cultured cells, a common result has been to increase the incorporation of FA into glycerolipids. Thus, over-expression of FATP1 causes an increase in FA incorporation into TAG in in HEK293 cells (130) and skeletal muscle (131) and the overexpression of ACSL1 increases FA incorporation into TAG. These overexpression studies led to a radically different interpretation of function than subsequent studies, which showed that the absence of either FATP1 or ACSL1 impairs FA oxidation. For a comprehensive review of ACSL over-expression studies, see (132).

Role of acyl-CoAs in disease

Cancer

A hallmark of tumorigenesis is the upregulation of genes that encode enzymes that synthesize FAs and complex lipids (133,134). Although lipids are required for enhanced membrane biosynthesis in rapidly proliferating cells, a role beyond that of simple cellular growth is suggested by the upregulation of isoforms that are specific for lipids with specialized properties. For example, upregulated *Acsl4* is particularly associated with hepatocellular carcinoma and aggressive cancers in breast, prostate, and colon (135-138). ACSL4 prefers to activate 20:4ω6 (139) and promotes tumor cell survival by two separate mechanisms. In colon cancer, ACSL4 overexpression may prevent apoptosis by depleting pro-apoptotic unesterified 20:4ω6 (140,141). In hepatocellular carcinoma, ACSL4 overexpression generates 20:4ω6-CoAs that might promote cell proliferation and growth by regulating signaling molecules like atypical protein kinase C (aPKC) or by binding a transcription factor like hepatic nuclear factor-4α (HNF-4α), antagonizing its activity, and enhancing tumor growth (47,142,143). In addition, chemical inhibition of ACS activity by triacsin C, which inhibits ACSL1, ACSL3, and ACSL4, but not ACSL5 or ACSL6, induces apoptosis in lung, colon and brain cancer cells (144). Although it appears that 20:4ω6-CoA is important for tumorigenesis, cell growth, and

proliferation, more studies will be needed to elucidate the mechanism by which 20:4ω6-CoA enhances growth.

Obesity and type 2 diabetes mellitus

Obesity and type 2 diabetes mellitus are associated disorders that share the underlying features of insulin resistance and dyslipidemia. The dyslipidemia is characterized by hypertriglyceridemia, low HDL, and elevated free FA. Although the pathogenesis of the insulin resistance syndrome is controversial, three factors are held in common: 1) hypersecretion of insulin by pancreatic β-cells; 2) increases in intra-abdominal adiposity, with high circulating levels of free FA; and 3) insulin resistance in skeletal muscle. All three of these factors are associated with disordered FA metabolism and, secondarily, with disordered acyl-CoA metabolism.

In an attempt to mechanistically link the three commonly held factors, Prentki and Corkey hypothesized that elevated cytosolic long-chain acyl-CoAs cause the insulin resistance syndrome. This hypothesis is based on the work of McGarry and Foster who showed that malonyl-CoA, the "signal of plenty," inhibits CPT1, thereby blocking acyl-CoA transport into the mitochondria for β-oxidation (145,146). Prentki and Corkey hypothesize that with nutrient surfeit, glucose metabolism increases in pancreatic β-cells, liver, and muscle, causing cytosolic malonyl-CoA levels to rise, which then inhibits the mitochondrial β-oxidation of acyl-CoAs, allowing acyl-CoAs to accumulate (147).

The accumulation of cytosolic long-chain acyl-CoAs in β-cells can modify the acylation state of key regulatory proteins involved in the regulation of ion channels and exocytosis of insulin (148). Indeed, in both cultured β-cells and rodent pancreatic islets, adding exogenous FA and glucose increases long-chain acyl-CoA content concomitantly with increased insulin secretion, basal hyperinsulinemia, and reduced prandial insulin release (149-151). It is unclear whether the resultant hyperinsulinemia results from insulin resistance or is the driver of insulin resistance (152).

Insulin resistance in liver and muscle has been attributed to long-chain acyl-CoA activation of protein kinase Cθ, which phosphorylates the insulin receptor and/or insulin receptor substrate-1 (IRS-

1) and reduces the cells' ability to respond to insulin (153). Despite an associative study linking elevated hepatic long-chain-acyl-CoA content and plasma insulin levels (154), two knockout mouse models have not confirmed a direct link between elevated hepatic acyl-CoA content and hepatic insulin resistance. In mice with liver-specific deficiency of *Acsl1*, a 25-35% decrease in hepatic acyl-CoA content does not protect the mice from developing diet-induced insulin resistance (86), and in *Gpat1* deficient liver, which has a nearly 2-fold increase in acyl-CoA content, the mice are protected from diet-induced insulin resistance (155). Thus, at least in liver, acyl-CoA accumulation does not necessarily result in insulin resistance.

Evidence for muscle acyl-CoA accumulation as a cause of insulin resistance is better supported by studies in both rats and humans, in which high fat feeding or direct lipid infusion increases intramuscular acyl-CoA levels and diminishes muscle uptake of glucose in response to insulin (154,156). Conversely, when morbidly obese subjects lose weight, insulin sensitivity improves together with a reduction in intramuscular acyl-CoA levels (157). This indirect evidence associates the accumulation of cytosolic long-chain acyl-CoAs in muscle with the development of insulin resistance.

These studies do not support a direct role for long-chain acyl-CoA accumulation in the development insulin resistance. While it is appealing to identify a single molecule as a unifying cause for the development of insulin resistance, it is more likely that long-chain acyl-CoAs are merely a marker for metabolically dysfunctional tissues.

Cardiovascular Disease

The normal heart obtains 60-90% of its energy from fatty acids (158), but excess acyl-CoA formation causes lipid accumulation that can cause heart failure (159), implying that the balance between energy production and storage is critical. Several disease states alter the ratio of fatty acid use to glucose use. Glucose use increases with heart failure and pathologic hypertrophy caused by pressure overload (160-163). The diabetic heart uses high amounts of fatty acid because glucose

uptake is low (164,165). Diabetic cardiomyopathy is defined as contractile dysfunction that cannot be accounted for exclusively by arterial hypertension or coronary artery disease in individuals with diabetes (166). Diabetic cardiomyopathy is also associated with impaired insulin signaling and mitochondrial dysfunction (166). In heart, mitochondria produce up to 95% of the total ATP (167). In addition to energy production, mitochondria are a site of phospholipid synthesis (56), calcium uptake (168), and induction of apoptosis (168). Therefore, these organelles are critical to heart health.

Mitochondria are the site of both the TCA cycle and the electron transport chain. Whereas glycolysis can produce 2 net ATP from a glucose molecule, oxidative phosphorylation can produce up to 36 ATP molecules, showing the importance of mitochondria to energy production. The high efficiency of ATP production from glucose or fatty acids is especially important in the heart, which is constantly beating and thus in demand of continuous ATP. When one acetyl-CoA, the end product of both glycolysis (after conversion of pyruvate by pyruvate dehydrogenase (PDH)) and fatty acid breakdown, is used in the TCA cycle, 3 NADH and 1 $FADH_2$ molecules are formed, which can be used by the electron transport chain. The electron transport chain (ETC) consists of five complexes (I-V) on the inner mitochondrial membrane. These complexes form a proton gradient by transferring electrons to acceptors, such as oxygen, and coupling this gradient to ATP production in the complex V, which is also known as ATP synthase (**Fig. 1.4**).

Impairments to any part of the ETC can be catastrophic for energy production. Complex I receives 2 electrons from NADH, which are then transferred through iron-sulfur clusters to form ubiquinol and transports 2 hydrogen ions across the inner mitochondrial membrane to the mitochondrial matrix. Deficiency of complex I is the most common childhood-onset mitochondrial disease and typically results in death in childhood (169). The disease can present with lactic acidosis, mitochondrial encephalomyopathy, hypertrophic cardiomyopathy, or an optic neuropathy (169). Complex II forms ubiquinol using energy from conversion of $FADH_2$ to FAD^+. Complex II deficiency is very rare, accounting for 2% of human respiratory chain deficiencies and has been associated with cardiomyopathy, leukoencephalopathy, and neurological disorders (170). Complex III

oxidizes ubiquinol to pump 4 hydrogen ions across the inner mitochondrial membrane. Deficiency of complex III can cause hearing loss, acidosis, liver disease, encephalopathy, and death (171). Complex IV transfers electrons to oxygen, which then combines with two hydrogen ions on the inside of the membrane to form water. Four hydrogen ions are pumped across the membrane, further contributing to the proton gradient. Complex IV deficiency is the second most common respiratory chain deficiency and can present with severe myopathy, cardiomyopathy, liver failure, and encephalopathy (172). Complex V uses the proton gradient formed to produce ATP. Deficiency of complex V is found in about 1% of mitochondrial disorders, and this deficiency is associated with neuropathy, ataxia, and early death (173). Deficiency of any mitochondrial complex has the potential to decrease ATP synthesis and increase reactive oxygen species formation (174).

Cardiolipin in Mitochondrial Function

In the inner mitochondrial membrane, CL closely associates with the ETC complexes, and a small number of CL molecules are tightly bound to the complexes (175,176) (**Fig. 1.4**). Complexes III and IV are found in CL-rich portions of the inner mitochondrial membrane, and this high amount of CL is necessary for their normal function (175,177,178). Providing CL to the ischemic rat heart using liposomes can improve complex III activity (179). CL is necessary for cristae membrane curvature, dimerization of complex V, and normal ATP synthase activity (180,181). Mitochondrial complexes also aggregate in the membrane to form supercomplexes, and CL is necessary for their stability (182,183). In addition to ETC complexes, adenine nucleotide translocase (184), carnitine palmitoyltransferase-I (185), mitochondrial phosphate carrier (186), and carnitine acyltransferase (187) interact with CL and display increased activity when these enzymes are in CL-containing membranes compared to CL-deficient liposomes or membranes.

The acyl-chain composition of CL, which is primarily linoleate (18:2) in mammalian heart, increases membrane fluidity, potentially improving ETC function (188). These unsaturated acyl chains act as acceptors of electrons from reactive oxygen species formed by the ETC, forming lipid

peroxides, or have oxygen added via action of lipoxygenases or peroxidases (189). Impaired ETC function, blocking electron flow, can increase formation of reactive oxygen species and oxidize CL (179). The peroxidation of CL may cause apoptosis (190) and excess formation of MLCL if not counteracted by remodeling (191). CL is especially prone to oxidative damage if linoleate acyl chains are replaced with arachidonate or DHA, such as occurs with heart failure and aging (189). Thus, the acyl chain composition may be important in CL's function in mitochondria.

CL content and acyl chain composition are altered in several heart diseases. Total CL content decreases during regional ischemia (192). Linoleate content of CL is diminished with pressure overload in mice and in spontaneously hypertensive rats (193,194). Due to the high amount of linoleate in CL and its loss in disease states, it has been hypothesized that a specific acyl-chain composition is necessary for normal mitochondrial function. However, recent studies in *Saccharomyces cerevisiae* in which CL is not remodeled nor converted to MLCL, contain acyl chains with a mixture of lengths and degrees of unsaturation and retain normal mitochondrial function (195,196). These studies suggest that the respiratory defect in *S. cerevisiae* was caused by the accumulation of MLCL and/or the decrease in the mitochondrial content of CL, but not to changes in the saturation of the CL acyl chains.

Mitochondrial quality control

Cardiomyocytes are at high risk of damage because of their high metabolic rate and long lifespan. Mitochondria are the source of the majority of reactive oxygen species, and due to this proximity can be greatly damaged. Therefore, the cell must remove these damaged mitochondria by either general autophagy or specific mitophagy. Impaired removal of damaged mitochondria can exacerbate damage after ischemia (197) or myocardial infarction (198) and cause heart failure (199,200). Generalized autophagy is highly regulated to prevent degradation of key cellular components. Autophagy can be triggered by inflammation, reactive oxygen species, hypoxia, ER stress, and nutrient deprivation (201). Under normal conditions, mechanistic target of rapamycin

complex (mTORC1) binds unc-51-like protein (ULK1), preventing formation of the autophagosome (202) (**Fig. 1.6**). When mTORC1 is inactivated by AMPK or low nutrient status, ULK1 is dephosphorylated and activated, allowing it to activate autophagy proteins (Atg) for autophagosome formation. LC3 is a protein involved in the formation of the autophagosome and in cargo recognition. LC3-I is inactive and must be cleaved and lipidated by the addition of a phosphatidylethanolamine (PE) to form LC3-II. The ratio of active to inactive LC3 is a commonly used measure of autophagic rate. Once the autophagosome is fully formed, the autophagosome fuses with lysosomes, forming the autophagolysosome, in which enzymatic degradation of proteins, nucleic acids, lipids, and carbohydrates occurs (201).

When mitochondria are subjected to stress, CL translocates to the outer mitochondrial membrane and acts as a signal for mitophagy or fission (203,204). Mitochondrial fusion and fission allow the damaged portions to be combined and sequestered into one small mitochondria with a low membrane potential to be degraded by mitophagy. CL contributes to this process because it can strongly bind proteins necessary for these processes. For mitochondrial fission, CL on the outer mitochondrial membrane anchors dynamin-related protein 1 (DRP1), a fission protein normally found in the cytosol (205). Once on the outer mitochondrial membrane, DRP1 can be activated and initiate mitochondrial fission. CL also binds LC3, (203), and this CL-LC3 conjugation acts as a signal for degradation of the mitochondria (203). Under more extreme stress, oxidation of CL by Cytochrome c can induce the formation of a pore in the mitochondrial membranes to allow the release of Cytochrome c and induces apoptosis (206).

The Pink1-Parkin pathway is another way to specifically degrade damaged mitochondria. In healthy mitochondria, Pink1 is imported into the mitochondria and proteolytically degraded. In damaged mitochondria with low membrane potential, Pink1 accumulates at the outer mitochondrial membrane, where it can recruit Parkin. Parkin then ubiquitinates mitochondrial proteins such as mitofusin 1/2 (Mfn 1/2), voltage-dependent anion channel (VDAC), and translocase of the outer mitochondrial membrane (TOM). The ubiquitination of these proteins prevents their normal function

and allows binding of the cytosolic autophagy adaptor p62 (sequestome 1, SQSTM1), which can then bind LC3 to recruit the autophagosome for degradation of the damaged mitochondria (207). Having two pathways for specifically targeting mitochondria for degradation allows the cell to clear out damaged mitochondria without removing healthy mitochondria, which could compromise the energy-producing capabilities of the cell.

In summary, acyl-CoA trafficking is necessary to maintaining cellular viability through providing substrate for both ATP production and glycerolipid synthesis. It has been hypothesized that each ACS isoform is able to target the acyl-CoA to a specific fate, potentially based on its subcellular location or fatty acid preference. By altering the amount of ACS isoforms in cells and tissues, we have begun to understand the function of these enzymes. The expression and activity of different ACS isoforms are altered in different disease states, prompting us to question the importance of ACS enzymes in the development of these diseases. This dissertation work focuses on how loss of ACSL1, the major ACSL isoform in the heart, impacts heart health with an emphasis on mitochondrial respiratory function.

Background Figures

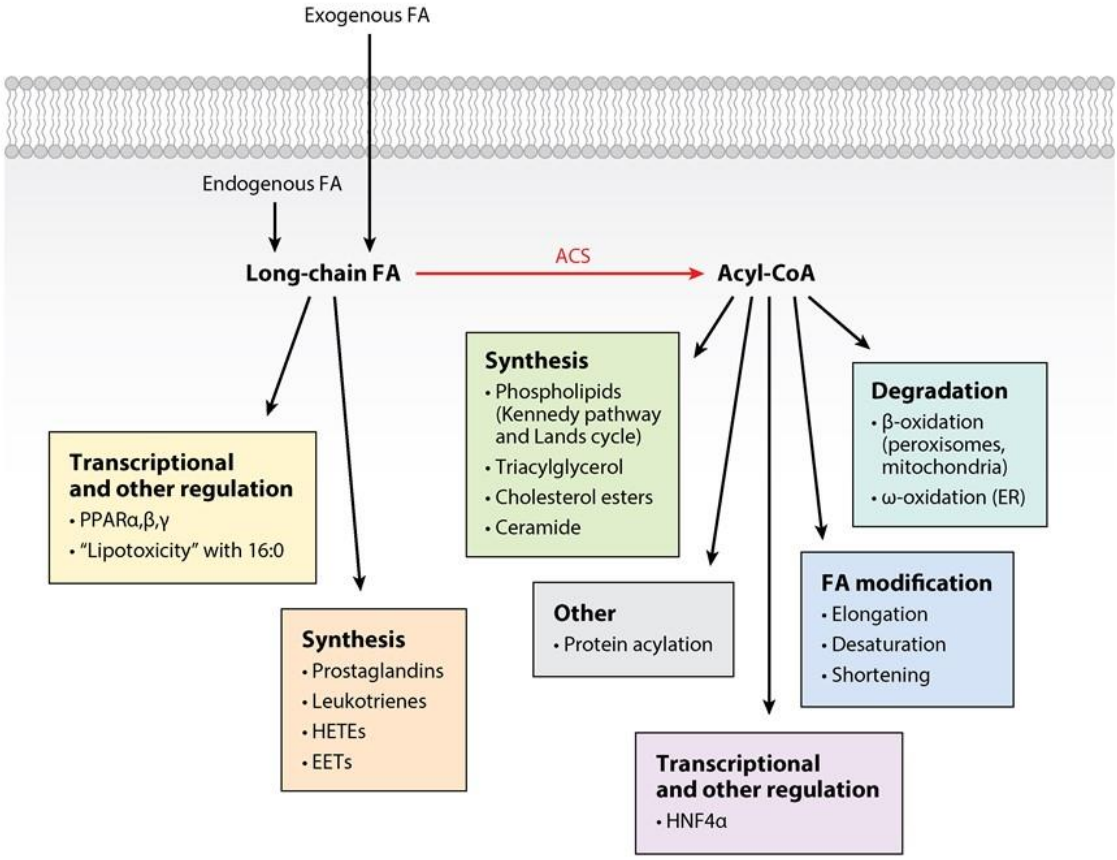

Figure 1.1 Metabolic fates of long-chain fatty acids. Long-chain fatty acids from exogenous or endogenous sources are activated to acyl-coenzyme As (CoAs) by one of 13 acyl-CoA synthetase isoforms. The free fatty acids are ligands for nuclear transcription factors, and 20-carbon fatty acids can be converted to a variety of signaling eicosanoids. The acyl-CoAs are transcriptional ligands and substrates for β- and ω-oxidation, and can be incorporated into complex lipids or used to modify proteins. Abbreviations: ACS, acyl-CoA synthetase; CoA, coenzyme A; EETs, epoxyeicosatrienoic acids; ER, endoplasmic reticulum; FA, fatty acid; HETEs, hydroxyeicosatetraenoic acids; HNF4, hepatic nuclear factor-4; PPAR, peroxisome proliferator-activated receptor. Published in (1).

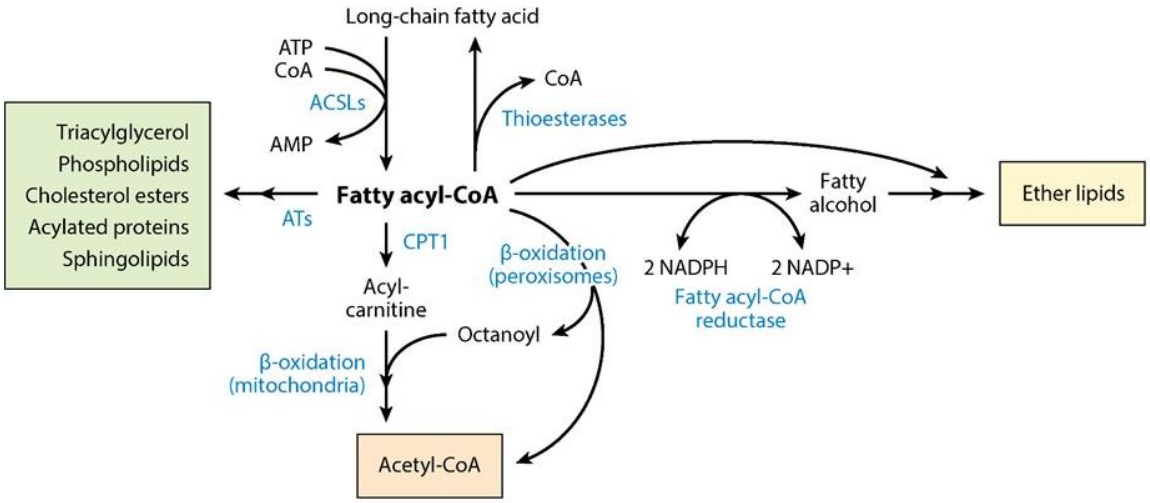

Figure 1.2 Acyl-CoA metabolism. The major initial enzymatic steps in the metabolism of long-chain acyl-CoAs include 13 independent thioesterases to hydrolyze acyl-CoAs, fatty acyl-CoA reductase, which converts the acyl-CoA to a fatty alcohol that will be incorporated into ether lipids, and ATs, which incorporate fatty acids into complex lipids and acylated proteins. In the major degradative pathways, CPT1 converts acyl-CoAs to acylcarnitines that enter the mitochondria for β-oxidation, whereas very-long-chain acyl-CoAs begin to be oxidized in peroxisomes, releasing acetyl-CoAs, until they are chain-shortened to eight carbons, which complete their oxidation in the mitochondria. Abbreviations: ACSLs, long-chain acyl-CoA synthetases; AMP, adenosine monophosphate; ATP, adenosine triphosphate; ATs, acyl-CoA acyltransferases; CoA, coenzyme A; CPT1, carnitine palmitoyltransferase-1; ER, endoplasmic reticulum; FA, fatty acid; NADP, nicotinamide adenine dinucleotide phosphate; NADPH, reduced NADP. Published in (1).

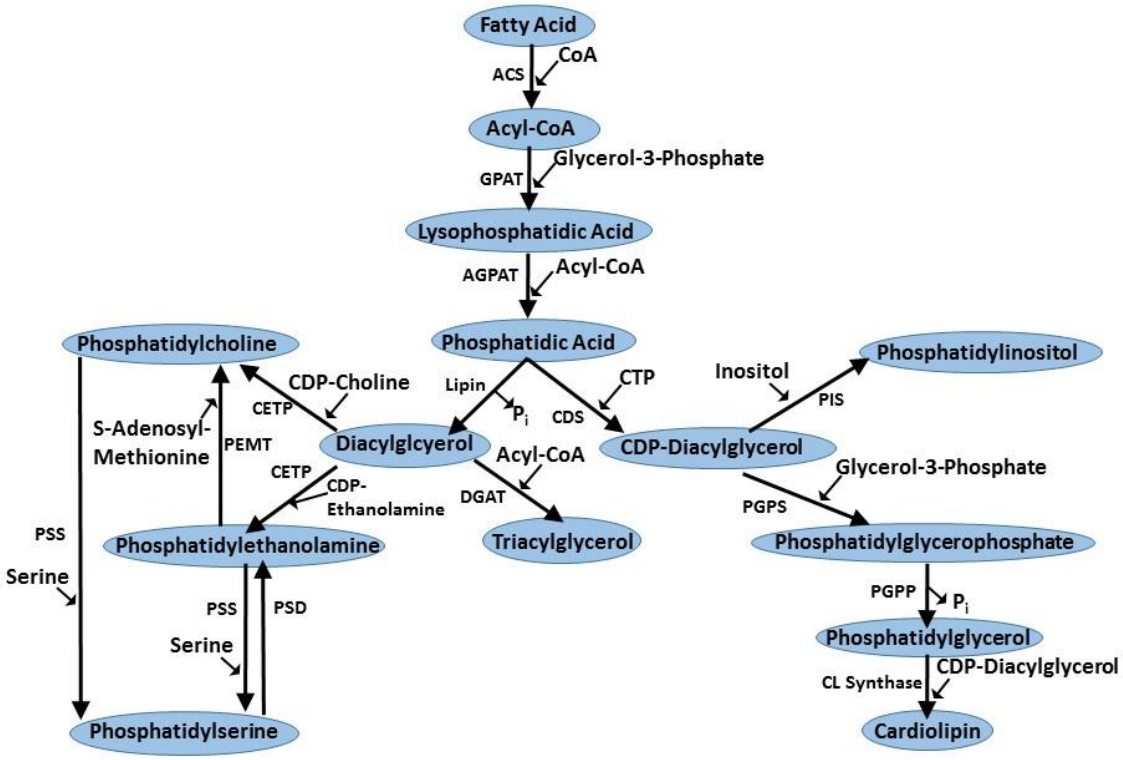

Figure 1.3 Glycerolipid synthesis. Abbreviations: AGPAT - acyl-CoA:1-acylglycerol-3-phosphate acyltransferase; CDP-DAG - cytidine diphosphate-DAG; CEPT - diacylglycerol choline/ethanolamine phosphotransferase; CL – cardiolipin; DAG – diacylglycerol; DGAT – diacylglycerol acyltransferase; MAM- mitochondria-associated membrane; PA – phosphatidic acid; PC- phosphatidylcholine; PE – phosphatidylethanolamine; PEMT - phosphatidylethanolamine N-methyltransferase; PG – phosphatidylglycerol; PGPP - phosphatidylglycerophosphate phosphatase; PGPS - phosphatidylglycerophosphate synthase; PI – phosphatidylinositol; PIS - phosphatidylinositol synthase; PS – phosphatidylserine; PSD - phosphatidylserine decarboxylase; PSS - phosphatidylserine synthase; TAG - triacylglycerol. Adapted from (56).

Table 1.1 Site of phospholipid synthesis.

Phospholipid	Enzyme	Precursor	Site of Synthesis
PC	CEPT	CDP-choline + DAG	ER
	PEMT	PE	ER (MAM)
PE	CEPT	CDP-ethanolamine + DAG	ER
	PSD	PS	Mito
PS	PSS	PC + serine	ER
	PSS	PE + serine	ER
PG	PGPP	PGP	Mito
CL	CL synthase	PG + CDP-DAG	Mito
	Tafazzin; MLCL AT1; ALCAT1	MLCL	Mito
PI	PIS	CDP-DAG + inositol	ER

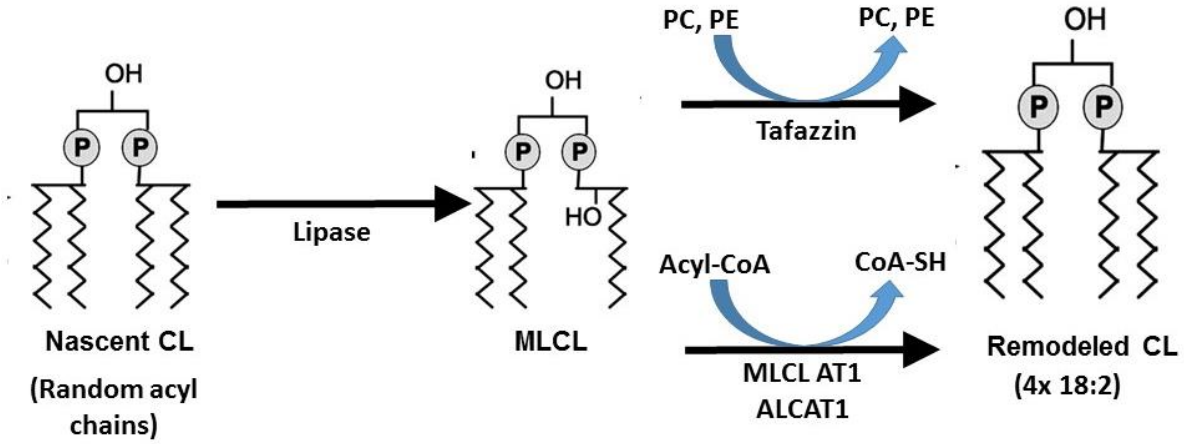

Figure 1.4. Cardiolipin remodeling in mammalian cells. After synthesis, CL contains shorter, more saturated fatty acids than are found in mature CL. To remodel CL, a lipase cleaves an acyl chain to form MLCL. Tafazzin can then transacylate CL using a different phospholipid as an acyl-chain donor. An acyl-CoA can be directly added to MLCL by MLCL AT-1 or ALCAT1. After several cycles, cardiac CL contains four linoleates (18:2). Abbreviations: CL- cardiolipin; MLCL- monolyso-cardiolipin; PC- phosphatidylcholine; PE- phosphatidylethanolamine; MLCL AT1- MLCL acyltransferase 1; ALCAT1- lysocardiolipin acyltransferase 1**.** Adapted from (208).

Table 1.2. Evidence for partitioning from loss of function studies Published in (1).

Gene	Tissue	FA partitioning information	Phenotype	Ref.
Acsl1 KO	Liver-specific	Decreased FA incorporation into TAG & oxidation	none	(86)
	Adipose-specific	Decreased FA oxidation	Increased adipose mass; defective thermogenesis	(105)
	Multi-tissue- heart	Decreased FA oxidation	none	(87)
	Heart-specific	Decreased FA oxidation	none	(87)
	Macrophage-specific	Altered 20:4 metabolism and PGE2	Protects macrophages against diabetes-mediated inflammation	(122)
	Endothelial cell-specific	No information	none	(126)
Acsl3 KD	Rat hepatocytes	Glycerolipid synthesis on lipid droplets? Regulation of transcription factors	__	(209)
Acsl4 KD	Cultured cells, various	Altered eicosanoid metabolism	Human X-linked mental retardation	(210, 211)
Acsl5 KD Acsl5 KO	Primary hepatocytes Total KO	Decreased FA incorporation into glycerolipids and cholesterol esters No information	Decreased lipid droplet formation none	(212) (213)
Acsl6 KD	Neuroblastoma cells	22:6ω3 metabolism?	Inhibited neurite outgrowth	(214)
Fatp1/ Acsvl4 KO	Skeletal muscle, BAT, L6E9 cells Retina	Decreased FA oxidation ? Decreased FA oxidation	Defective thermogenesis Accelerated retinal ageing	(215) (216)
Fatp2/Acsvl1 KO	Total KO	? Decreased oxidation of 24:0	none	(217)
Fatp3/Acsvl3 KD	Glioma	No information	Decreased anchorage-dependent growth	(218)
Fatp4/Acsvl5 KO	Human mutation Keratinocytes	Decreased type II diester wax in the sebum Decreased long-chain ceramides	Ichthyosis prematurity syndrome Postnatal restrictive skin	(219) (220)
Fatp5/Acsvl6 KO	Gall bladder bile	Decreased conjugated bile acids	Low weight gain on a high fat diet	(76)
Fatp6/Acsvl2	---	No information	---	---
AcsBg1 KD KO	Neuro2a cells Various tissues	Decreased β-oxidation Increased amounts of some long-chain fatty acids	--- none	(221) (222, 223)
AcsBg2	---	No information	---	---

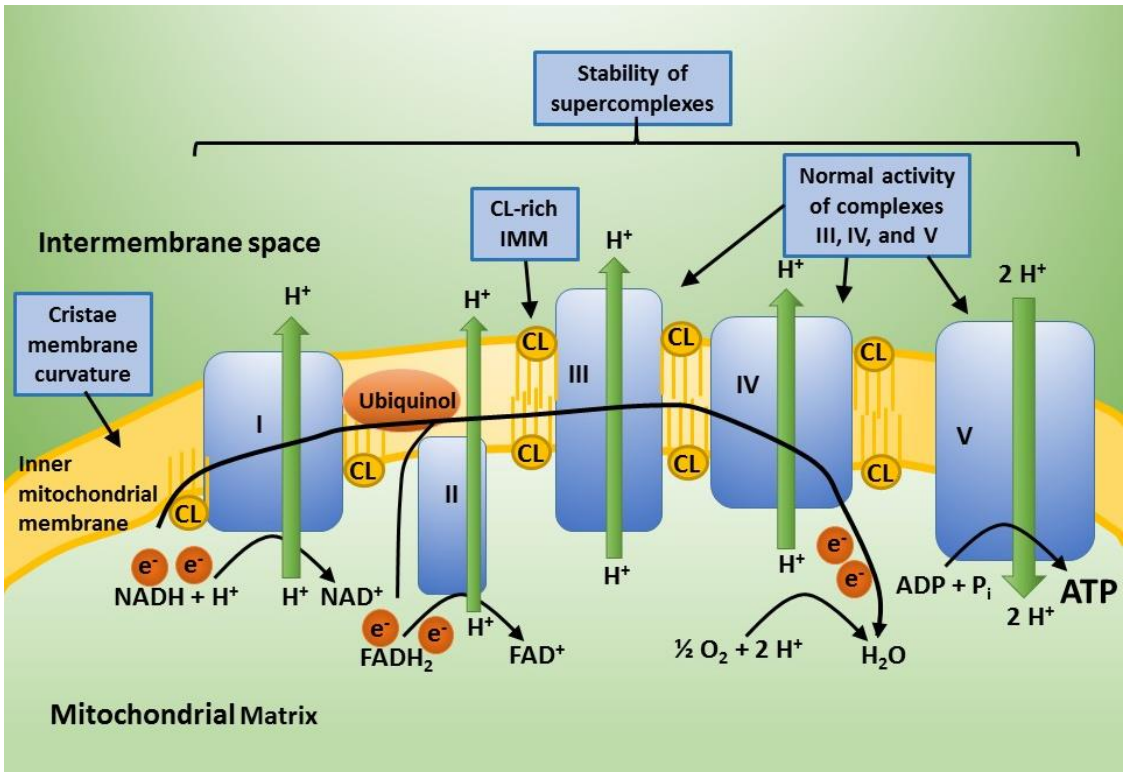

Figure 1.5 Cardiolipin in ETC function. Cardiolipin is necessary for normal curvature of the cristae of the inner mitochondrial membrane. The complexes of the ETC are found in CL-rich areas of the inner mitochondrial membrane, and CL binding is necessary for normal function of complexes III, IV, and V. CL also stabilizes supercomplexes, which are important for normal mitochondrial respiration. Abbreviations: IMM- inner mitochondrial membrane; CL- cardiolipin. Adapted from (189,224).

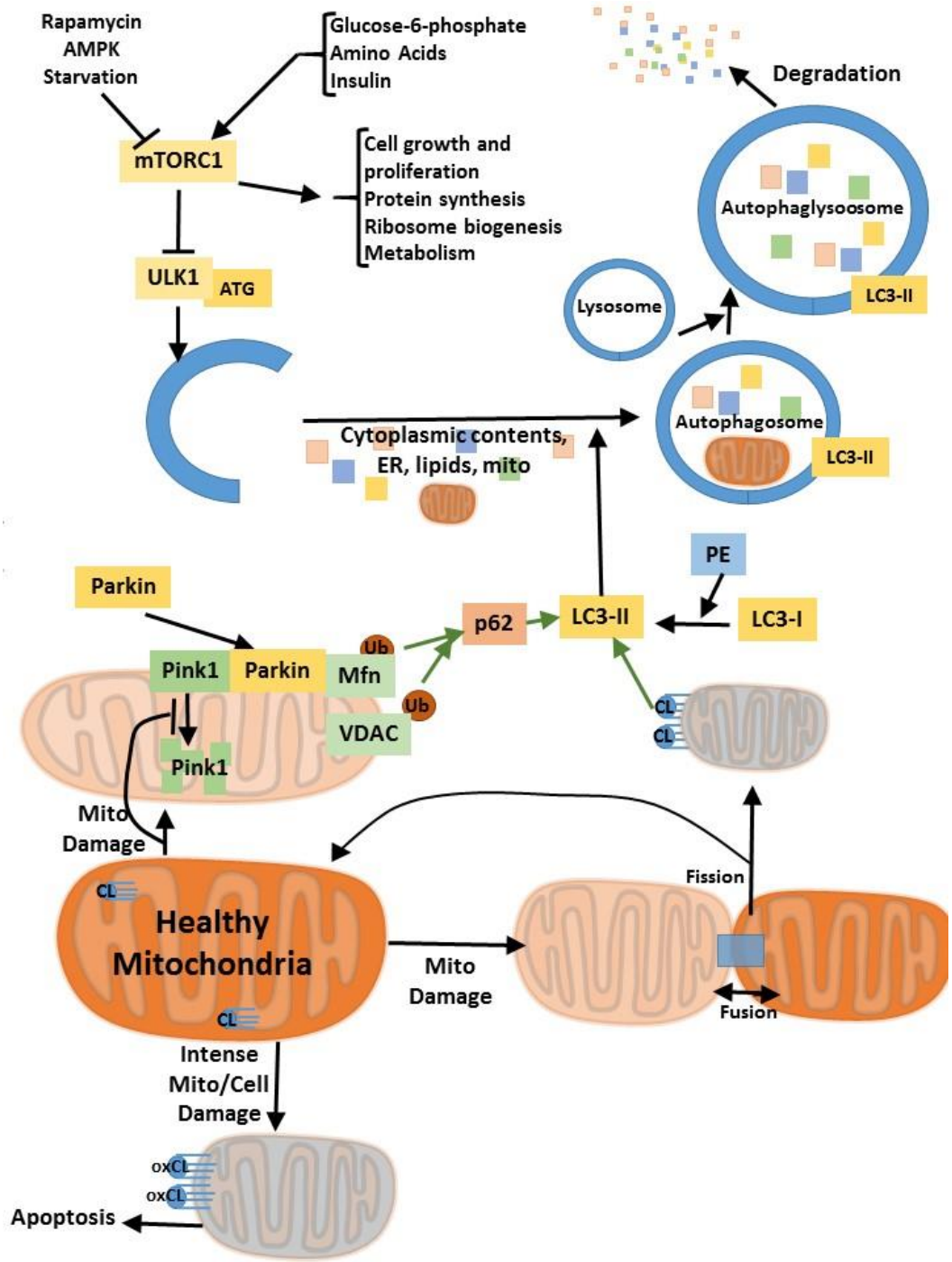

Figure 1.6. Mitochondrial quality control through fission and fusion, autophagy, or apoptosis. Damaged mitochondria are cleared by general autophagy, controlled by mTORC1 or by mitophagy controlled by the Pink/Parkin pathway or by CL externalization. Abbreviations: mTORC1- mechanistic target of rapamycin complex 1; CL- cardiolipin; oxCL- oxidized CL; PE- phosphatidylethanolamine; ATG- autophagosome proteins. Adapted from (204,207)

Specific Aims

Mitochondria produce up to 95% of ATP made in cardiomyocytes, making these critical organelles to heart health. Loss of mitochondrial respiratory function is seen in many cardiac diseases, such as heart failure, Barth syndrome, and aging (225,226), which could render these hearts less able to respond to stressors such as low energy availability or exercise. Understanding the causes and consequences of cardiac mitochondrial dysfunction can have a large impact on how heart disease is treated.

Long chain acyl-CoA synthetases (ACSLs) catalyze the addition of coenzyme A (CoA) to long chain fatty acids, the predominant dietary fatty acids, thereby activating and enabling them to enter into pathways of either oxidation or incorporation into complex lipids. ACSL1 is the major ACSL isoform in heart, contributing 90% of total ACSL activity. Loss of ACSL1 has profound effects on cardiac metabolism. In heart, loss of ACSL1 causes an 80-90% loss of fatty acid oxidation and an 8-fold increase in glucose use (105,227,228). With loss of 90% of ACSL activity, which is required for glycerolipids synthesis, hearts lacking ACSL1 may also have altered phospholipid and TAG synthesis. Alterations in saturation and chain length of fatty acids incorporated into membrane lipids can change membrane dynamics, movement of substrates and solutes across membranes, and lipid raft composition (229-231) . Loss of ACSL1 also causes activation of mTORC1, which can increase growth and inhibit autophagy (87). These changes to substrate use, membrane composition, cell growth, and autophagy can all affect mitochondrial function.

Preliminary experiments using transmission electron microscopy of hearts from multi-tissue Acsl1 knockouts (*Acsl1*$^{T-/-}$) showed many swollen and vacuolated mitochondria with disrupted cristae. Compared to floxed littermate controls, the oxygen consumption response of *Acsl1*$^{T-/-}$ heart mitochondria to ADP-stimulation was diminished (47-60% lower respiratory control ratio (RCR) with pyruvate/malate and 56% lower with palmitoyl-carnitine), indicating that loss of ACSL1 caused an impaired ability to respond to a stimulus of low energy. *Acsl1*$^{T-/-}$ heart mitochondria also took up 34% less calcium than controls before the permeability transition, potentially causing increased

susceptibility to apoptosis. Therefore, loss of ACSL1 causes mitochondrial dysfunction, which could predispose *Acsl1*$^{T-/-}$ hearts to failure if stressed.

Overall aim: Determine why loss of ACSL1 in heart causes mitochondrial dysfunction.

Aim 1. Determine if loss of ACSL1 alters cardiac phospholipids.

1a. Determine whether ACSL1 determines acyl-chain composition of membrane phospholipids, specifically focusing on mitochondrial cardiolipin.

1b. Determine whether alterations to mitochondrial phospholipids alters mitochondrial function.

Aim 2. Determine if activation of mTOR in *Acsl1*$^{T-/-}$ hearts impairs mitochondrial function.

2a. Determine whether activation of mTORC1 in *Acsl1*$^{T-/-}$ hearts prevents clearance of damaged mitochondria through inhibition of autophagy.

2b. Determine whether mTORC1 activation in *Acsl1*$^{T-/-}$ hearts impairs mitochondrial function.

CHAPTER 2: ACYL-COA SYNTHETASE 1 DEFICIENCY ALTERS CARDIOLIPIN SPECIES AND IMPAIRS MITOCHONDRIAL FUNCTION

Trisha J. Grevengoed[1], Sarah A. Martin[2], Lalage Katunga[3], Daniel E. Cooper[1], Ethan J. Anderson[3], Robert C. Murphy[2], Rosalind A. Coleman[1]

Summary

Long-chain acyl-CoA synthetase 1 (ACSL1) contributes more than 90% of total cardiac ACSL activity, but its role in phospholipid synthesis has not been determined. Mice with an inducible knockout of ACSL1 (*Acsl1*$^{T-/-}$) have impaired cardiac fatty acid oxidation and rely on glucose for ATP production. In *Acsl1*$^{T-/-}$ mice, cardiac mitochondria were dysfunctional. Because ACSL1 exhibited a strong substrate preference for linoleate, we investigated the composition of heart phospholipids. *Acsl1*$^{T-/-}$ hearts contained 83% less tetralinoleoyl-cardiolipin (CL), the major form present in control hearts. A stable knockdown of ACSL1 in H9c2 rat cardiomyocytes resulted in low incorporation of linoleate into CL, as well as diminished incorporation of palmitate and oleate into other phospholipids. Overexpression of ACSL1 in both H9c2 and HEK-293 cells increased incorporation of linoleate into CL and other phospholipids. To determine whether increasing the content of linoleate in CL would improve mitochondrial respiratory function, control and *Acsl1*$^{T-/-}$ mice were fed a high linoleate diet; this normalized the amount of tetralinoleoyl-CL, but did not improve respiratory function. Thus, ACSL1 is required for the normal composition of several phospholipid species in heart. Although ACSL1 determines the acyl-chain composition of heart CL, a high tetralinoleoyl-CL content may not be required for normal function.

[1] Department of Nutrition, University of North Carolina at Chapel Hill, NC 27599
[2] Department of Pharmacology, University of Colorado, Anschutz Medical Campus, Aurora, CO 80045
[3] Department of Pharmacology and Toxicology, East Carolina University, Greenville, NC 27858

Introduction

In order to metabolize long-chain fatty acids in pathways of β-oxidation or the synthesis of complex lipids, they must first be activated to acyl-CoAs by long-chain acyl-CoA synthetases (ACSL). Five mammalian ACSL isoforms have been identified, each with a specific substrate preference, subcellular location, and tissue distribution (232). In the heart, the ACSL1 isoform predominates, such that with deficiency, total ACSL specific activity and fatty acid oxidation decrease by more than 90% (87). Because ACSL activity is required for the incorporation of fatty acids into phospholipids, we asked whether the ACSL1 isoform is also required for the synthesis and remodeling of cardiac phospholipids, particularly cardiolipin (CL).

The mitochondrial phospholipid CL contributes to many aspects of mitochondrial function, including energy production through oxidative phosphorylation (233,234), mitochondrial fission and fusion (235,236), and cellular apoptosis (237). Tetralinoleoyl-CL is the predominant CL species in the mammalian heart (238), but the mechanism by which this species is formed is unclear. Because the enzymes of CL synthesis lack acyl-chain specificity, nascent CL contains a mixture of acyl chain lengths and degrees of unsaturation (58). To obtain mature CL, most remodeling occurs within the mitochondria by sequentially removing each acyl chain to form monolyso-CL (MLCL) and then replacing the missing fatty acid with linoleate (18:2), added by the transacylation from a donor phospholipid (239) or by direct incorporation of a linoleoyl-CoA (62,240).

Tafazzin is the enzyme believed to be responsible for the transacylase pathway of cardiolipin remodeling. Mutations in tafazzin cause Barth syndrome, an X-linked cardiomyopathy characterized by skeletal muscle weakness and heart failure in childhood (59). Hearts with tafazzin loss-of-function mutations contain low levels of tetralinoleoyl-CL and have a high ratio of MLCL to CL. Because tafazzin does not have a substrate preference for linoleate, it has been proposed that the linoleate enrichment must be caused by either an alteration in the physical shape of CL or by the action of an additional enzyme (239).

Here we show that ACSL1, which has a distinct preference for linoleate, significantly contributes to CL remodeling. Because fatty acids must be converted to acyl-CoAs, both to be available for the initial steps in the synthesis of phospholipids, as well as to enter the mitochondrial matrix where CL remodeling occurs, we asked whether ACSL1 might be responsible for activating linoleate destined to be incorporated into CL. We found that hearts lacking ACSL1 are deficient in tetralinoleoyl-CL, but that normalizing the CL species cannot ameliorate the mitochondrial dysfunction in these hearts. These findings call into question the idea that the acyl-chains of CL are important for cardiac and mitochondrial respiratory function.

Methods

Animal care and diets: All protocols were approved by the Institutional Animal Care and Use Committee at University of North Carolina at Chapel Hill. Mice were housed under a 12 h light/dark cycle with free access to food and water. Unless otherwise specified, mice were fed a purified low-fat diet (Research Diets, DB12451B). A multi-tissue knockout of ACSL1 was achieved by mating mice with loxP sequences flanking exon one of the *Acsl1* gene to animals expressing a tamoxifen-inducible Cre driven by a ubiquitous promoter enhancer (87). Between six and eight weeks of age, $Acsl1^{T-/-}$ and littermate control $Acsl1^{flox/flox}$ (control) mice were injected intraperitoneally on four consecutive days with 20 mg/mL (75 μg/g body weight) tamoxifen dissolved in corn oil. All studies were performed 20 weeks after tamoxifen was injected, unless otherwise specified. Cardiac echocardiography was performed (blinded to mouse type) on conscious mice using a VisualSonics Vevo 770 or Vevo 2100 ultrasound biomicroscopy system (VisualSonics, Inc.). A model 707B (30 MHz) or model MS-550D (22-55 MHz) scan head was used on the Vevo 770 and Vevo 2100, respectively, as previously described (241). Two-dimensional guided M-mode echocardiography was performed in the parasternal long-axis view at the level of the papillary muscle on loosely restrained conscious mice. Wall thickness was then determined by measurements of epicardial to endocardial leading edges. For the diet study, mice were

fed a high-linoleate safflower oil diet (Research Diets, D02062104, 45% kcal fat (75% linoleate)) for 4 weeks.

ACSL activity assay: ACSL specific activity was measured in heart membranes and cell homogenates (87). Briefly, homogenized tissues were centrifuged at 100,000 x *g* for 1 h at 4°C to isolate total membrane fractions. Between 1 and 6 µg of protein was incubated with 50 µM [1-^{14}C]fatty acid (unless otherwise indicated), 10 mM ATP, 250 µM CoA, 5 mM dithiothreitol, and 8 mM $MgCl_2$ in 175 mM Tris, pH 7.4 at RT° for 10 min. The enzyme reaction was stopped with 1 mL of Dole's solution (heptane:isopropanol:1M H_2SO_4; 80:20:1; v/v). Two mL of heptane and 0.5 ml of water were added to separate phases. Radioactivity of the acyl-CoAs in the aqueous phase was measured using a liquid scintillation counter.

Mitochondrial function studies: Mitochondrial function was measured in permeabilized myofibers and in isolated mitochondria prepared from portions of the left ventricle and septum. After dissection, muscle samples were placed in ice-cold (4°C) Buffer X containing (in mM): 7.23 K_2EGTA, 2.77 CaK_2EGTA, 20 imidazole, 20 taurine, 5.7 ATP, 14.3 phosphocreatine, 6.56 $MgCl_2$-$6H_2O$ and 50 MES (pH 7.1, 295 mOsm). Fibers were delicately separated in ice-cold Buffer X using fine forceps under a dissecting scope. Cardiac fibers were then permeabilized in Buffer X with 50 µg/mL saponin for 30 min, then washed in ice-cold wash buffer Z (110 mM K-MES, 35 mM KCl, 1 mM EGTA, 5 mM K_2HPO_4, 3 mM $MgCl_2 \cdot 6H_2O$, 5 mg/ml bovine serum albumin, pH 7.1, 295 mOsm) to remove endogenous substrates. To prevent Ca^{2+} independent contraction of the permeabilized fibers, 20 µM blebbistatin was added to Buffer Z during wash and experiments. All mitochondrial O_2 consumption (JO_2) measurements were performed at 30°C using the Oroboros O_2K Oxygraph system (Oroboros Instruments). The H_2O_2 and Ca^{2+} uptake measurements were performed in a spectrofluorometer (Photon Technology Instruments or Horiba Jobin Yvon), equipped with a thermo-jacketed cuvette chamber. All mitochondrial experiments were performed in Buffer Z plus 5 mg/mL bovine serum albumin. O_2 consumption was measured with either 5 mM pyruvate plus 2 mM malate or 125 µM

palmitoyl-carnitine plus 2 mM malate. State 3 respiration was induced by adding ADP as indicated in the Figure Legends.

The rate of ATP production within the permeabilized myofibers was continuously recorded alongside the O_2 consumption in real time, by monitoring the increasing fluorescence in the respiration chamber coming from NADPH (340ex/460em) with a spectrofluorometer, as described (242). To maintain this reaction, 2.5 U/mL of glucose-6-phosphate dehydrogenase (Roche), 2.5 U/mL yeast hexokinase (Roche), 5 mM nicotinamide adenine dinucleotide phosphate ($NADP^+$) (Sigma-Aldrich), and 5 mM D-glucose (Sigma-Aldrich) were added to the assay media. P1,P5-Di(adenosine-5')pentaphosphate (Ap5A) (Sigma-Aldrich) was included in the respiration medium to inhibit adenylate kinase and to ensure that ATP production was solely due to mitochondrial oxidative phosphorylation. An absolute amount of ATP generated across a given time frame was then calculated using a standard curve of fixed concentrations of ATP added to the saturating amounts of hexokinase, glucose, G6PDH, and $NADP^+$. Mitochondrial H_2O_2 emission was detected using Amplex UltraRed reagent (Invitrogen) in the presence of 1 U/mL horseradish peroxidase and 25 U/mL superoxide dismutase. The rate of H_2O_2 produced from the mitochondrial electron transport system supported by 125 µM palmitoyl-L-carnitine, 5 mM glutamate, and 5 mM succinate oxidation was determined in permeabilized fibers with 100 µM ADP, 5 mM glucose, and 1 U/mL hexokinase present to maintain the mitochondria in a permanent, submaximal phosphorylating state.

To isolate mitochondria, hearts were minced in 0.125 mg/mL trypsin in homogenization buffer (0.25 M sucrose, 10 mM HEPES, 1 mM EDTA, pH 7.4). Soybean trypsin inhibitor (0.65 mg/mL) was added, and tissues were homogenized and centrifuged at 500 x *g* for 5 min to remove nuclei and unbroken cells. Mitochondria were isolated by centrifuging at 10,000 x *g* for 15 min and washed twice with homogenization buffer. Calcium uptake was measured in Buffer Z, using 1 µM Calcium Green 5-N with 1 µM thapsigargin (Sigma-Aldrich) added to inhibit SERCA, a calcium transport ATPase. In separate experiments, the function of isolated mitochondria was assessed using a Seahorse XF24

Analyzer. Mitochondria (15 µg protein) were stimulated sequentially with 100 µM ADP, 1.26 µM oligomycin, 4 µM FCCP, and 4 µm antimycin A (Sigma-Aldrich).

Phosphate quantification: Lipids were extracted from approximately 15 mg of ventricular myocardium, and phospholipids were separated by thin-layer chromatography on LK5D silica gel 150 Å plates (Whatman) in chloroform:ethanol:water:triethylamine (30:35:7:35; v/v) with authentic standards (243). Phosphate was quantified in the scraped silica regions for each phospholipid. The reaction was initiated by adding 30 µL 10% $Mg(NO_3)_2$ in ethanol to each sample and heating over an open flame (244). After adding 300 µL 0.5 N HCl, samples were boiled for 15 min. Then, 700 µL of a solution of 1.43% ascorbic acid and 0.36% ammonium molybdate in 0.86 N sulfuric acid was added, and the mixture was incubated at 45°C for 20 min. The absorbance of samples and a standard curve of sodium phosphate was measured at 605 nm.

Sample preparation for mass spectrometry: Samples of left ventricle were homogenized on ice using a Dounce homogenizer in 50 mM phosphate buffer pH 7.2, 0.1 M NaCl, 2 mM EDTA, 1 mM dithiothreitol, and protease inhibitors (Roche). Protein was determined by the bicinchoninic acid method (Pierce Biotechnology). Preparations of heart mitochondria (180 µg protein) or total left ventricle (300 µg protein) were diluted with 50 mM PBS to a total volume of 200 µl. An internal standard mixture was made in 100% methanol containing: 1-dodecanoyl-2-tridecanoyl-*sn*-glycero-3-phosphate (PA-12:0/13:0), 1-dodecanoyl-2-tridecanoyl-*sn*-glycero-3-phosphocholine (PC-12:0/13:0), 1-dodecanoyl-2-tridecanoyl-*sn*-glycero-3-phosphoethanolamine (PE-12:0/13:0), 1-dodecanoyl-2-tridecanoyl-*sn*-glycero-3-phosphoglycerol (PG-12:0/13:0), 1-dodecanoyl-2-tridecanoyl-*sn*-glycero-3-phosphoinositol (PI-12:0/13:0), 1-dodecanoyl-2-tridecanoyl-*sn*-glycero-3-phosphoserine (PS-12:0/13:0), and 1'–[1,2-di-(9*Z*-tetradecenoyl)-*sn*-glycero-3-phospho], 3'–[1-(9*Z*-tetradecenoyl), 2-(10*Z*-pentadecenoyl)-*sn*-glycero-3-phospho]-*sn*-glycero (CL- (14:1) x3/15:1). Then 750 µl of methanol:chloroform (2:1; v/v) and an internal standard mixture (for mitochondrial preparations and left ventricles on low-fat diet, 50 ng of each phospholipid class and 100 ng of CL; for left ventricles on safflower oil diet, 25 ng of each phospholipid class and 100 ng of CL) was added, and products were

extracted (245). The samples were dried under a stream of nitrogen and were then resuspended in 100 µl of 75% solvent A (isopropanol:hexanes; 4:3; v/v) and 25% solvent B (isopropanol:hexanes:water; 4:3:0.7; v/v, containing 5 mM $C_2H_3O_2NH_4$). Samples were analyzed by liquid chromatography coupled to tandem mass spectrometry (LC/MS/MS) as described below.

Liquid chromatography/mass spectrometry: For normal phase separation, samples were injected onto an Ascentis-Si HPLC column (150 x 2.1 mm, 5 µm; Supelco) at a flow rate of 0.2 ml/min with 25% solvent B and 75% solvent A. Solvent B was maintained at 25% for 5 min, increased to 60% over 10 min, and then to 95% over 5 min. The system was held at 95% Solvent B for 20 min before re-equilibration at 25% for 14 min. Phospholipids were measured using an API3200 triple quadrupole mass spectrometer (AB Sciex). Positive ion mode was used to detect phosphatidylcholine (PC) and phosphatidylethanolamine (PE) lipids with quadrupole 1 scanning a *m/z* range from 250 to 1100 in 0.1 Da increments over 2 sec. Negative ion mode was used to detect CL, phosphatidic acid, phosphatidylinositol (PI), phosphatidylglycerol, and phosphatidylserine with quadrupole 1 scanning an *m/z* range from 150 to 1600 in 0.1 Da increments over 4 sec. Quantitation was performed using AB Sciex MultiQuant software and using the internal standards for each phospholipid analyzed. Quantified data were corrected for isotope abundance. Fragmentation of endogenous lipids of *m/z* 818.5, 842.6, 844.6, 846.5, 864.5, and 890.5 (PC), 742.5, 738.5, 790.5, 762.5 (PE), 885.5 (PI), and 1448.0 (CL) was performed as described above, except for the following details. In the MS/MS experiment, the parent ions listed above were selected in quadrupole 1, subjected to collision-induced decomposition using N_2 gas, and quadrupole 2 was allowed to scan the product ions in the *m/z* range from 150 to 900 (*m/z* 818.5, 842.6, 844.6, 846.5, 864.5, 890.5, 742.5, 738.5, 790.5, 762.5, 885.5) or 150 to 1450 (*m/z* 1448.0). After each of these specific phospholipid molecular species was identified, the number of acyl carbons and double bonds present in the set of fragment molecule was confirmed. From these data, the other phospholipids were converted from mass-to-charge to number of acyl carbons and double bonds.

Preparation and Analysis of Tissue for Matrix Assisted Laser Desorption Ionization/Imaging Mass Spectrometry (MALDI-IMS): A modified optimal cutting medium

(mOCT) was made by heating a 10% solution of Mowiol 6-98 in MilliQ H_2O. Once in solution, 8% Poly (propylene glycol) average MW 2000 was added until mixed thoroughly. A heart from a control animal and an *Acsl1*$^{T-/-}$ animal was placed in the mOCT mixture and stored overnight at -20°C. Hearts were sectioned at -17°C at 20 μm, placed on glass cover slips, and stored at -20°C until used. DHAP (2' 5'-dihydroxyacetophenone) matrix (150 mg) was sublimated onto the tissue. In brief detail, an AB-Sciex qTOF XL using a solid state laser (355 nm) at and energy of 7.6 μJ and a pulse rate of 500 Hz in negative ion mode was used to capture the MALDI/IMS data. The laser was moved in a horizontal pattern with a resolution of approximately 50 μm. At each point, the negative ion spectrum from 600 – 1700 m/z was captured. The data set was analyzed using TissueView software (AB-Sciex).

Generation of stable ACSL1-knockdown H9c2 cells: *Acsl1* rat shRNA or *scrambled* control shRNA constructs in pGFP-C-shLenti vector (Origene) were co-transfected with pHR-CMV-Δ8.2 and pCMB-VSV-G vectors in HEK293T cells to generate lentivirus. H9c2 cells (rat cardiomyocytes; ATCC) were incubated with media containing lentivirus for *Acsl1* shRNA or *scrambled* shRNA for 24 h. Cells were treated with 1 μM puromycin for 7 d to select cells that contained the shRNA. Knockdown of ACSL1 was confirmed by mRNA, protein, and ACSL enzyme activity.

Cellular phospholipid incorporation: H9c2 cells were cultured to confluence in 25 mM glucose DMEM with 10% fetal bovine serum. Cells were differentiated for 4 d in 5 mM glucose DMEM with 1% horse serum. For overexpression experiments, cells were infected with adenovirus containing either *GFP* or *Acsl1-FLAG* (multiplicity of infection of 150) for 24 h. Cells were incubated with 0.5 μCi [1-^{14}C]palmitate, [1-^{14}C]oleate, or [1-^{14}C]linoleate for 6 h and then washed twice with 1% bovine serum albumin. For etomoxir studies, cells were preincubated with 40 μM etomoxir for 1 h before incubating with 40 μM etomoxir and [1-^{14}C]linoleate for 6 h. HEK-293 cells were grown to 50% confluence in 25 mM glucose DMEM with 10% fetal bovine serum and then infected with adenovirus containing either *GFP* or *Acsl1-FLAG* (multiplicity of infection of 2.5) for 24 h. Cells were then incubated with a mixture of 30 μM oleate, 15 μM palmitate, and 5 μM linoleate with 0.5 μCi [1-^{14}C]palmitate, [1-^{14}C]oleate, or [1-^{14}C]linoleate for an additional 24 h. For oxidation measurements,

0.4 mL media was collected in a tube containing 20 µL 15% bovine serum albumin and then incubated with 100 µL 20% perchloric acid overnight at 4°C. The acidified media was centrifuged at 20,000 rpm for 5 min, and radioactivity in the supernatant was counted to determine acid soluble metabolites (ASM). For pulse-chase experiments, H9c2 cells were incubated with 0.5 µCi [1-^{14}C]linoleate for 2 h and then either collected (pulse) or washed and incubated with 10 µM unlabeled linoleate (chase). Cellular lipids were extracted and phospholipids were separated by thin layer chromatography as described above.

Microscopy: H9c2 cells grown on glass coverslips were incubated with MitoTracker CMXRos (Life Technologies; 200 nM) for 30 min, fixed with 3.7% paraformaldehyde, and permeabilized with 0.2% Triton X-100. Cells were incubated with primary antibody (FLAG (Sigma) and/or Grp78 (Novus Biologicals)) for 2 h, then secondary antibody (Alexafluor 488 or 568; Life Technologies) for 1 h. Cells were then incubated with DAPI (Life Technologies) for 5 min, mounted on glass slides with Prolong Gold (Life Technologies), and then visualized with a Zeiss 710 confocal microscope.

Statistics: Data are presented as the mean ± SE for each group. Differences between genotypes were evaluated by Student's t-test. For experiments with multiple treatments or diets, differences between groups were evaluated by two-way ANOVA with Tukey multiple-comparison posttests. Differences between means with $p < 0.05$ were considered statistically significant.

Results:

ACSL1 was located on cardiac mitochondria and preferred to activate linoleate. Cardiac ACSL1 protein and ACSL specific activity were enriched in the mitochondrial fraction, compared to whole tissue (**Fig. 2.1A, B**). Purified recombinant ACSL1 from rat liver shows a broad fatty acid substrate preference with varying chain lengths and degrees of unsaturation (246). To determine the fatty acid substrate preference in mouse heart, long-chain acyl-CoA synthetase (ACSL) activity was assayed with different fatty acid substrates in total membrane preparations from control and *Acsl1*$^{T-/-}$ hearts. Control hearts exhibited the highest ACSL activity with linoleate (18:2) (**Fig. 2.1C**). This clear

substrate preference was lost in *Acsl1*$^{T-/-}$ hearts, which lack more than 90% of total ACSL activity with all fatty acids (**Fig. 2.1D**), indicating that the preferential activation of linoleate was due to ACSL1 activity.

Loss of ACSL1 caused mitochondrial dysfunction. *Acsl1*$^{T-/-}$ and littermate control mice were injected with tamoxifen at 6-8 week to produce ACSL1 deficiency. Ten weeks after tamoxifen injection, Acsl1T$^{-/-}$ hearts were enlarged but had normal systolic function (87). To determine whether function worsened with time, echocardiography was performed 20 weeks after initiating the ACSL1 knockout. *Acsl1*$^{T-/-}$ hearts remained hypertrophied with no impairment in contractile function (**Fig. 2.2A, B, C**). To determine whether loss of ACSL1 caused mitochondrial dysfunction, O_2 consumption in saponin-permeabilized cardiac muscle fibers was measured using palmitoyl-carnitine and malate (**Fig. 2.2D**) or pyruvate and malate (**Fig. 2.2E**) with increasing concentrations of ADP or succinate. Basal O_2 consumption rate was normal in *Acsl1*$^{T-/-}$ mitochondria, but compared to controls, the mitochondrial response to ADP stimulation was 56% lower. In addition to impaired ADP-stimulated oxygen consumption, *Acsl1*$^{T-/-}$ mitochondria produced less ATP for each O_2 molecule consumed, indicative of inefficient energy production (**Fig. 2.2F**). Many models of mitochondrial dysfunction produce increased amounts of H_2O_2, but *Acsl1*$^{T-/-}$ mitochondria did not, possibly due to their lower metabolic rate (**Fig. 2.2G**). Isolated *Acsl1*$^{T-/-}$ mitochondria took up less calcium than controls before reaching the permeability transition (**Fig. 2.2H**), suggesting that *Acsl1*$^{T-/-}$ mitochondria may be more susceptible to stress and apoptosis. Calcium uptake into mitochondria increases oxygen consumption and NADH production, but once calcium uptake exceeds the permeability transition, mitochondria are more likely to become disrupted, release cytochrome c into the cytosol, and undergo apoptosis (247). Despite severely impaired respiratory function, *Acsl1*$^{T-/-}$ hearts do not develop failure under unstressed conditions.

Loss of ACSL1 altered the acyl-chain composition of mitochondrial cardiolipin and phospholipids. Cardiolipin associates closely with complexes of the electron transport chain and is highly important for mitochondrial function (233,234). Cardiac cardiolipin normally contains a high

amount of linoleate (238). Because ACSL1 has a distinct preference for linoleate, we questioned whether the loss of ACSL1 would affect the composition of cardiolipin and other phospholipids in cardiac mitochondria. The content of individual phospholipid species in cardiac ventricles did not differ between genotypes (**Fig. 2.3A**); however, mass spectrometry analysis revealed that loss of ACSL1 caused large changes in the acyl-chain composition of the major phospholipid species. As has been reported previously (238), the major cardiolipin (CL) species in control mouse hearts contained four linoleate acyl-chains (tetralinoleoyl-CL; 72:8-CL) (**Fig. 2.3B**). In the *Acsl1*$^{T-/-}$ mitochondria, however, this species was 83% lower and compared to controls, the CL species containing 2 linoleate and 2 arachidonate acyl chains (76:12-CL) was 80% lower (**Fig. 2.3B**). *Acsl1*$^{T-/-}$ heart mitochondria contained larger amounts of CL species containing stearate (18:0) and oleate (18:1), indicating either impaired remodeling of the CL or decreased availability of linoleate.

To determine whether the loss of ACSL1 impaired linoleate incorporation into other phospholipids, several species were fragmented to identify the acyl chains present. Linoleate-containing species of PC and PE (36:3-PC, 36:2-PC, and 36:2-PE) were approximately 2- to 4-fold higher in *Acsl1*$^{T-/-}$ hearts than in controls (**Fig. 2.3C, D, E; Table 2.1**). Excess linoleate in these species suggests that ACSL1, which is primarily located on the mitochondrial outer membrane, normally plays a role in the initial synthetic reactions which occur on the endoplasmic reticulum, but that its absence alters the availability of acyl-CoA species at this site. Furthermore, the excess linoleate could indicate impaired transacylation between CL and donor phospholipids, such as PC and PE. Compared to controls, the expression of the transacylase tafazzin was 31% lower in *Acsl1*$^{T-/-}$ hearts (**Fig. 2.3F**). Loss of tafazzin impairs tetralinoleoyl-CL formation (37). Thyroxine treatment lowers *tafazzin* expression (248), but increases total CL without favoring tetralinoleoyl-CL formation (249). Heart failure diminishes both *tafazzin* expression (250) and tetralinoleoyl-CL content (251), demonstrating a physiological relationship between *tafazzin* expression and CL species. The excess linoleate in PC and PE together with the decrease in tafazzin suggests that impaired remodeling of CL through tafazzin-mediated transacylation may have resulted in diminished tetralinoleoyl-CL.

Loss of ACSL1 altered other mitochondrial phosphatidylinositol (PI), PC, and PE species (**Fig. 2.3C, D, E**), but no differences were seen in phosphatidylglycerol or phosphatidylserine (data not shown). In control mitochondria the most abundant mitochondrial PI was 18:0, 20:4-PI. This species was 64% lower in the *Acsl1*$^{T-/-}$ hearts, and was compensated for by higher content of multiple minor PI species, so that the total content of PI was unchanged in the two genotypes. For PC, the major species in control hearts contained docosahexaenoic acid (DHA; 22:6) together with either palmitate (38:6-PC) or stearate (40:6-PC). These species were 53% and 48% lower, respectively, in *Acsl1*$^{T-/-}$ hearts. PC species that contained DHA were replaced with oleate in the *Acsl1*$^{T-/-}$ mitochondria so that 16:0-18:1-PC (34:1-PC) was 2-fold higher and 18:0-18:1-PC (36:1-PC) was 3-fold higher than in control hearts. The major PE species in control hearts also contained DHA and stearate (40:6-PE) and was approximately 30% lower in the *Acsl1*$^{T-/-}$ hearts. Impaired activation of α-linolenate due to loss of ACSL1 at the peroxisomal membrane may result in decreased uptake into peroxisomes where DHA synthesis occurs (252). The compositions of PC and PE in isolated mitochondria from control and *Acsl1*$^{T-/-}$ ventricles were similar to those in total membranes (data not shown), suggesting that ACSL1 influences phospholipid synthesis in the endoplasmic reticulum where these phospholipids are synthesized and remodeled (253).

Knockdown of *Acsl1* in H9c2 cardiomyocytes impaired both the oxidation of fatty acid and its incorporation into complex lipids. To further investigate how loss of ACSL1 affects phospholipid formation, we made a stable knockdown of *Acsl1* in H9c2 cells, a rat cardiomyocyte cell line. The knockdown caused a 67% loss of *Acsl1* mRNA, a 55% reduction of ACSL1 protein, and a 26% decrease in total ACSL activity (**Fig. 2.4A, B**, **C**). To avoid high concentrations of fatty acid which drive triacylglycerol synthesis, cells were incubated with trace amounts of individual [1-^{14}C]fatty acids (palmitate, oleate, or linoleate) to measure their incorporation into phospholipids. As measured by acid soluble metabolites (ASM) in the media, the oxidation of these fatty acids was 80% lower in the *Acsl1* knockdown cells than in controls (**Fig. 2.4D**), consistent with the requirement for ACSL1 in

channeling long-chain fatty acids into the pathway of β-oxidation (87). Decreased ACSL1 also caused approximately 40% lower incorporation of fatty acids into total glycerolipids (**Fig. 2.4E**).

ACSL1 knockdown greatly diminished incorporation of fatty acids into neutral lipids and PC (**Fig. 2.4F, H**). The incorporation of linoleate into CL was 32% lower in *Acsl1* knockdown cells (**Fig 2.4G),** which is consistent with the low content of tetralinoleoyl-CL in the *Acsl1*$^{T-/-}$ hearts. Compared to control cells, the incorporation of palmitate into PC, PE, PS, and CL was lower by 43%, 34%, 17%, and 46%, respectively (**Fig. 2.4H**). In contrast to highly oxidative cardiomyocytes *in vivo*, cultured cells rely minimally on fatty acid oxidation for energy. Thus, in cultured cells, ACSL1 may activate more palmitate destined for esterification into phospholipids, unlike heart, in which palmitate is more readily oxidized. Other than PC in which 37% less oleate was incorporated, no differences in the incorporation of oleate into phospholipids were observed between control and *Acsl1* knockdown cells. Therefore, in cultured cardiomyocytes, as in liver (86), loss of ACSL1 impaired activation of fatty acids for both neutral and phospholipid synthesis, with the largest effects found with palmitate and linoleate.

Overexpressed ACSL1 increased linoleate metabolism. To confirm that ACSL1 preferentially activates linoleate that is incorporated into CL, ACSL1 was overexpressed in H9c2 cardiomyocytes (**Fig. 2.5A**). As in heart, ACSL1-FLAG localized primarily to mitochondria (**Fig. 2.5B**), and *Ad-Acsl1* infection increased ACSL specific activity 3.3-fold (**Fig. 2.5C**). After a 6 h incubation with trace amounts of each of the [1-^{14}C]fatty acids, overexpressed ACSL1 increased the oxidation of linoleate by 28%, but not palmitate or oleate (**Fig. 2.5D**). ACSL1 overexpression increased both palmitate and linoleate incorporation into total lipids by 17% and 26%, respectively (**Fig. 2.5E**). ACSL1 overexpression increased linoleate incorporation into neutral lipid by 48%, cardiolipin by 28%, PC by 28%, and phosphatidylserine by 22% (**Fig. 2.5F, G, H**). Palmitate incorporation was less influenced by overexpressed ACSL1; its incorporation into PC, PI, and phosphatidylserine increased 17-18%, similar to the increase seen in total lipid incorporation of 17% (**Fig. 2.5F**). In heart and skeletal muscle which both contain high proportions of tetralinoleoyl-CL (86,87), the predominance of the ACSL1 isoform may underlie their enrichment in tetralinoleoyl- CL.

To determine whether the source of the linoleate in CL occurred via esterification of acyl-CoAs or from transacylation from donor phospholipids, we conducted a pulse-chase experiment. Overexpressed ACSL1 did not alter total labeled linoleate incorporation or incorporation into neutral lipids during the 2 h pulse (**Fig. 2.6A, B**). After a 4 h chase with unlabeled linoleate, labeled linoleate in CL in control cells increased 4-fold, suggesting that the majority of the linoleate incorporated into CL came from lipids already present within the cell (**Fig. 2.6C**). In the ACSL1 overexpressing cells, in comparison, 14% less labeled linoleate was incorporated into CL during the 4 h chase. This finding, coupled with the high linoleate incorporation during the 6 h labeling (**Fig. 2.5G**), suggests that more new unlabeled linoleate was being activated to form an acyl-CoA which was then esterified to CL. To determine if entry of linoleoyl-CoA into mitochondria was necessary for ACSL1-mediated increases in CL incorporation, H9c2 cells were incubated with etomoxir, an inhibitor of carnitine palmitoyltransferase-1 (CPT1). As anticipated, etomoxir treatment decreased linoleate oxidation to ASM by more than 80% in both control and ACSL1-overexpressing cells (**Fig. 2.6E**). The diminished entry of linoleoyl-CoA into the mitochondria also resulted in equivalent linoleate incorporation into CL in ACSL1-overexpressing cells and controls (**Fig. 2.6H**). However, overexpression of ACSL1 did not increase the amount of linoleate incorporated in other phospholipids (**Fig. 2.6I**). Without an increase [^{14}C]linoleate incorporation into phospholipids that donate acyl chains to CL, no conclusion about the source of linoleate in CL can be made from this experiment.

ACSL1 overexpression increased linoleate incorporation into CL in HEK-293 cells. To determine whether the ability of ACSL1 to increase linoleate incorporation into CL was specific to cardiomyocytes, we overexpressed ACSL1 in HEK-293 cells, which normally contain little tetralinoleoyl-CL (254). Twenty-four h after the *Ad-Acsl1* infection, ACSL1 protein was present, and total ACSL specific activity increased 9-fold (**Fig. 2.7A, B**). At this time, cells were incubated for an additional 24 h with a mixture of fatty acids to mimic the percentages in a physiological mixture of monounsaturated, saturated, and polyunsaturated fatty acids (30 μM oleate, 15 μM palmitate, and 5 μM linoleate plus the addition of 0.5 μCi [1-^{14}C]-labelled oleate, palmitate, or linoleate). ACSL1

overexpression increased palmitate incorporation into total lipids by 43%, oleate incorporation by 49%, and linoleate incorporation by 75% (**Fig. 2.7C**). The *Ad-Acsl1* infection did not alter the esterification of these fatty acids into neutral lipids (**Fig. 2.7D**), showing that the differences in total lipid incorporation were due to integration into phospholipids. ACSL1 overexpression resulted in 41% and 94% higher incorporation of palmitate and linoleate into CL, respectively, but no difference was seen in oleate incorporation (**Fig. 2.7E**). ACSL1 increased the incorporation of each of the fatty acids into PC, PE, and PI/PS (**Fig. 2.7F**), phospholipids that are synthesized at the endoplasmic reticulum. The high incorporation of labeled fatty acids into these phospholipids is likely due to increased fatty acid uptake and elevated acyl-CoA concentrations in the cytosol. ACSL1 specifically increased linoleate incorporation into CL, which is remodeled within mitochondria, suggesting that the synthesis of linoleoyl-CoA is sufficient for preferential incorporation of linoleate into CL, even in non-cardiomyocytes.

Dietary linoleate enrichment normalized tetralinoleoyl-CL content but did not improve mitochondrial function in *Acsl1*$^{T-/-}$ hearts. The relevance of CL acyl-chain composition to normal oxidative phosphorylation is controversial (195,255). In order to determine whether the impaired respiratory function of mitochondria from *Acsl1*$^{T-/-}$ hearts resulted from the presence of linoleate-deficient mitochondrial CL, we fed control and *Acsl1*$^{T-/-}$ mice a high safflower oil diet, in which 75% of fatty acids are linoleate, for 4 weeks. In spontaneous hypertensive rats, safflower oil feeding normalizes CL species and improves mitochondrial function (256). In our study, safflower oil feeding markedly increased the total amount of linoleate in CL in both control and *Acsl1*$^{T-/-}$ hearts and specifically increased the amount of tetralinoleoyl-CL in *Acsl1*$^{T-/-}$ hearts 4-fold compared to the low-fat diet. Importantly, the tetralinoleoyl-CL content of hearts from *Acsl1*$^{T-/-}$ mice fed safflower oil diet was equal to that of hearts from control mice fed the low fat diet (**Fig. 2.8A**). The normalization of tetralinoleoyl-CL content was not due to increased *tafazzin* expression, as this gene remained 25% lower in the safflower oil-fed *Acsl1*$^{T-/-}$ hearts compared to controls (**Fig. 2.8B**). *Tafazzin* expression was not altered by diet. To determine the effect of normalized tetralinoleoyl-CL content, we measured the

function of the electron transport chain in isolated mitochondria using pyruvate and malate as substrates. Basal O_2 consumption did not differ between groups (**Fig. 2.8C**). Similar to the data from permeabilized cardiac fibers, *Acsl1*$^{T-/-}$ hearts contained functionally defective mitochondria, as shown by impaired responses to ADP and FCCP (**Fig. 2.8D**). In control mitochondria, safflower feeding increased respiration after oligomycin treatment but did not change the response to ADP or FCCP. Despite the normalization of tetralinoleoyl-CL content, safflower oil feeding did not improve the respiratory function of mitochondria from *Acsl1*$^{T-/-}$ hearts, and responses to both ADP and the mitochondrial uncoupler FCCP remained 30-44% lower than controls (**Fig. 2.8D**). Thus, normalizing the content of CL species in *Acsl1*$^{T-/-}$ hearts was not sufficient to improve mitochondrial respiratory function.

Discussion

CL is synthesized and remodeled within the mitochondria, but its precursors, phosphatidic acid and CDP-diacylglycerol, are formed primarily on the endoplasmic reticulum and are imported into the mitochondria where phosphatidylglycerol is synthesized. CL synthase then combines phosphatidylglycerol with the phosphatidyl group from a second CDP-diacylglycerol (60). Because CL synthase lacks a preference for phosphatidylglycerol or CDP-diacylglycerol species that contain linoleate (57,58), the acyl-chains of the nascent CL are more highly saturated than those of mature cardiac CL. CL is remodeled by successive removal of acyl-chains by a phospholipase, followed by replacement via tafazzin-mediated transacylation from donor phospholipids or by acyltransferase-mediated esterification using an acyl-CoA.

Cardiac CL is highly remodeled after synthesis, but the functional significance of the remodeling is, as yet, unknown. In *Saccharomyces cerevisiae* lacking tafazzin, the additional deletion of the CL-specific phospholipase, Cld1, prevents the accumulation of MLCL, inhibits CL remodeling, and rescues the mitochondrial respiratory defect, strongly suggesting that the respiratory defect was due to the accumulation of MLCL and/or the decrease in the mitochondrial content of CL (195). In

mammalian cells, two additional enzymes, lysocardiolipin acyltransferase 1 (ALCAT1) and MLCL acyltransferase 1 (MLCL AT-1), can use acyl-CoAs to esterify MLCL (60). ALCAT1, however, is located on the ER, which would prevent its interaction with most CL (61), but MLCL AT-1 is found in mitochondria (62). Although overexpressing MLCL AT-1 in tafazzin-deficient lymphoblasts increases both linoleate incorporation into CL and total CL content (62), the importance of MLCL AT-1 for normal CL remodeling in heart cells remains unclear.

With its preference for linoleate, ACSL1 appears to be critical in maintaining the abundance of the tetralinoleoyl-CL species in the heart. ACSL1-derived linoleoyl-CoA could be incorporated into donor phospholipids and then transacylated into CL or directly incorporated by an acyltransferase into MLCL. Mitochondrial ACSL1 could increase the concentration of linoleoyl-CoA to be imported into mitochondria for β-oxidation or CL remodeling. Alternatively, because ACSL1 overexpression increased linoleate incorporation into PC, PE, and phosphatidylserine, its enhancement of CL species that contain linoleate could occur via transacylation from these phospholipids to CL or MLCL. Thus, it seems surprising that higher linoleate was also present in PC and PE in *Acsl1*$^{T-/-}$ hearts. We believe that when ACSL1 is absent, linoleate increases within the cell and becomes available for activation by other ACSL isoforms present on the endoplasmic reticulum where the resulting linoleoyl-CoA would be used during the synthesis of PC and PE. Because ACSL1 deficiency also results in a reduced expression of tafazzin mRNA, transacylation may be impaired and result in the diminished tetralinoleoyl-CL observed in the *Acsl1*$^{T-/-}$ hearts. The substrate preference of mitochondria-located ACSL1 for linoleate is therefore important for both the transacylase and the acyltransferase pathways of CL remodeling (**Fig.2.9**).

Because the composition of the major CL species varies in different tissues, it is likely that the CL species formed depends on the fatty acid preference of the ACSL isoforms present. The ER-localized ACSL isoforms would dictate which acyl-CoAs are incorporated into PC and PE, and the ACSL isoforms present on the outer mitochondrial membrane may determine if the acyl-CoA is incorporated directly into CL. For instance, ACSL1 accounts for more than 90% of ACSL activity in

both heart (87) and skeletal muscle (257) in which more than 75% of CL is tetralinoleoyl-CL (238). In contrast, tetralinoleoyl-CL is ~50% of the total CL species in liver (238), a tissue in which ACSL1 is responsible for only about 50% of the total ACSL activity (86). Similarly, ACSL1 is minimally expressed in brain (258) in which the major CL acyl-chains are oleate and arachidonate (259). An analysis of the fatty acid preferences of other ACSL isoforms may explain tissue differences in CL composition.

In contrast to tafazzin-deficient mice, *Acsl1*$^{T-/-}$ hearts do not contain a low total CL content or excess MLCL. Thus the *Acsl1*$^{T-/-}$ model allowed us to study CL remodeling in the presence of a normal CL content, as well as the impact of impaired tetralinoleoyl-CL formation on heart and mitochondrial function. In *Acsl1*$^{T-/-}$ hearts, normalizing the amount of linoleate present in CL did not improve respiratory dysfunction. Similarly in *S. cerevisiae*, CL remodeling was inhibited without impairing basal or ADP-stimulated mitochondrial O_2 consumption (195,255). Thus, in both yeast and *Acsl1*$^{T-/-}$ hearts, when total CL content is normal, mitochondrial function is independent of a specific CL species. In contrast, tafazzin-deficient mice and human hearts contain both an increased content of MLCL and a reduction in total CL (260,261). These CL changes are associated with a dilated cardiomyopathy, cardiac respiratory dysfunction, and heart failure (262). The *Acsl1*$^{T-/-}$ mice do not develop heart failure, suggesting that when total CL abundance is normal, the absence of a high content of tetralinoleoyl-CL does not cause heart failure. Similarly, normalizing tetralinoleoyl-CL in *Acsl1*$^{T-/-}$ hearts was not sufficient to improve mitochondrial respiratory function. Our data, together with the published yeast studies (195,255), suggest that the underlying difficulty in Barth syndrome and tafazzin-deficient mice is a deficiency in CL content and/or the accumulation of MLCL.

Figures

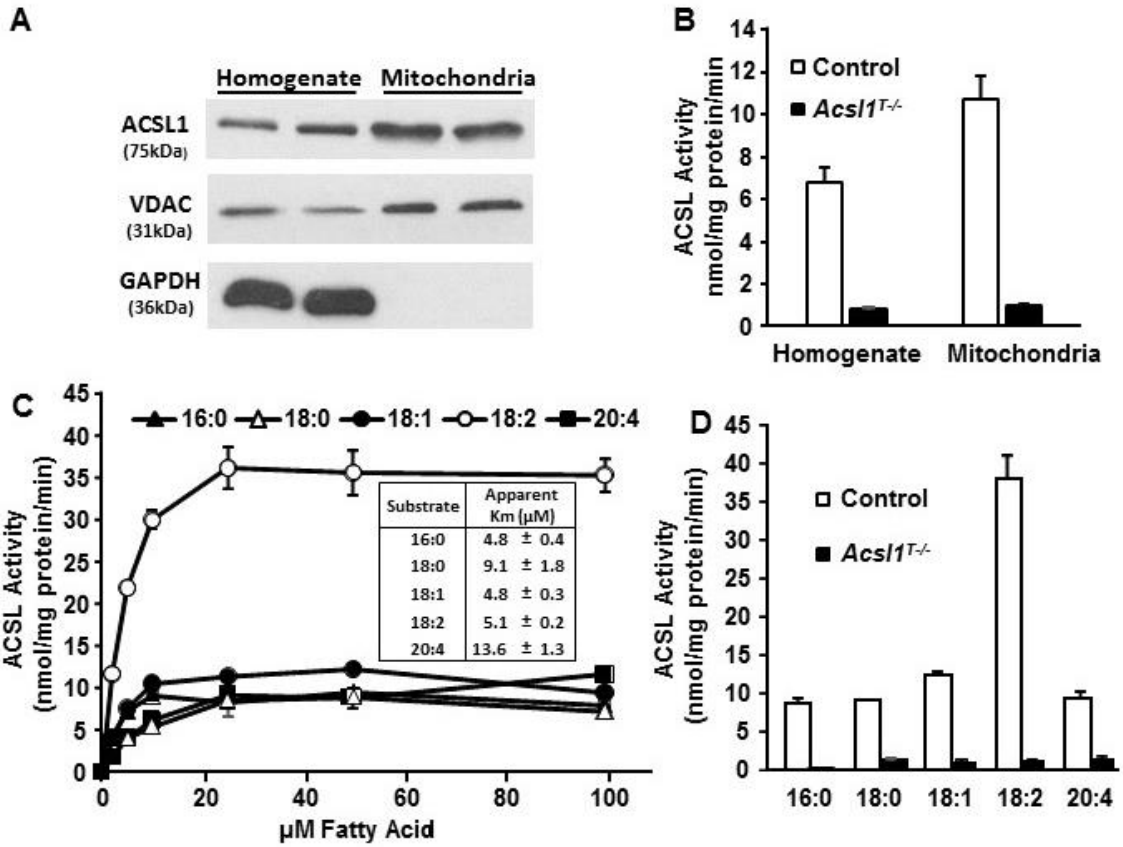

Figure 2.1. ACSL1 is located on cardiac mitochondria and activates linoleate preferentially. **A)** ACSL1 protein from control heart homogenates and isolated mitochondria. **B)** ACSL activity of heart homogenates and mitochondria measured with 50 μM palmitate (n=3). **C)** ACSL activity in total membrane fractions from control hearts measured with 2 μg protein and varying amounts of [^{14}C]-labeled fatty acids (n=3). **D)** ACSL activity in total membrane fractions from control and *Acsl1*$^{T-/-}$ mouse hearts measured with 2 μg protein and 50 μM of [^{14}C]-labeled fatty acids (n=3). *, p-value≤0.05 between control and *Acsl1*$^{T-/-}$.

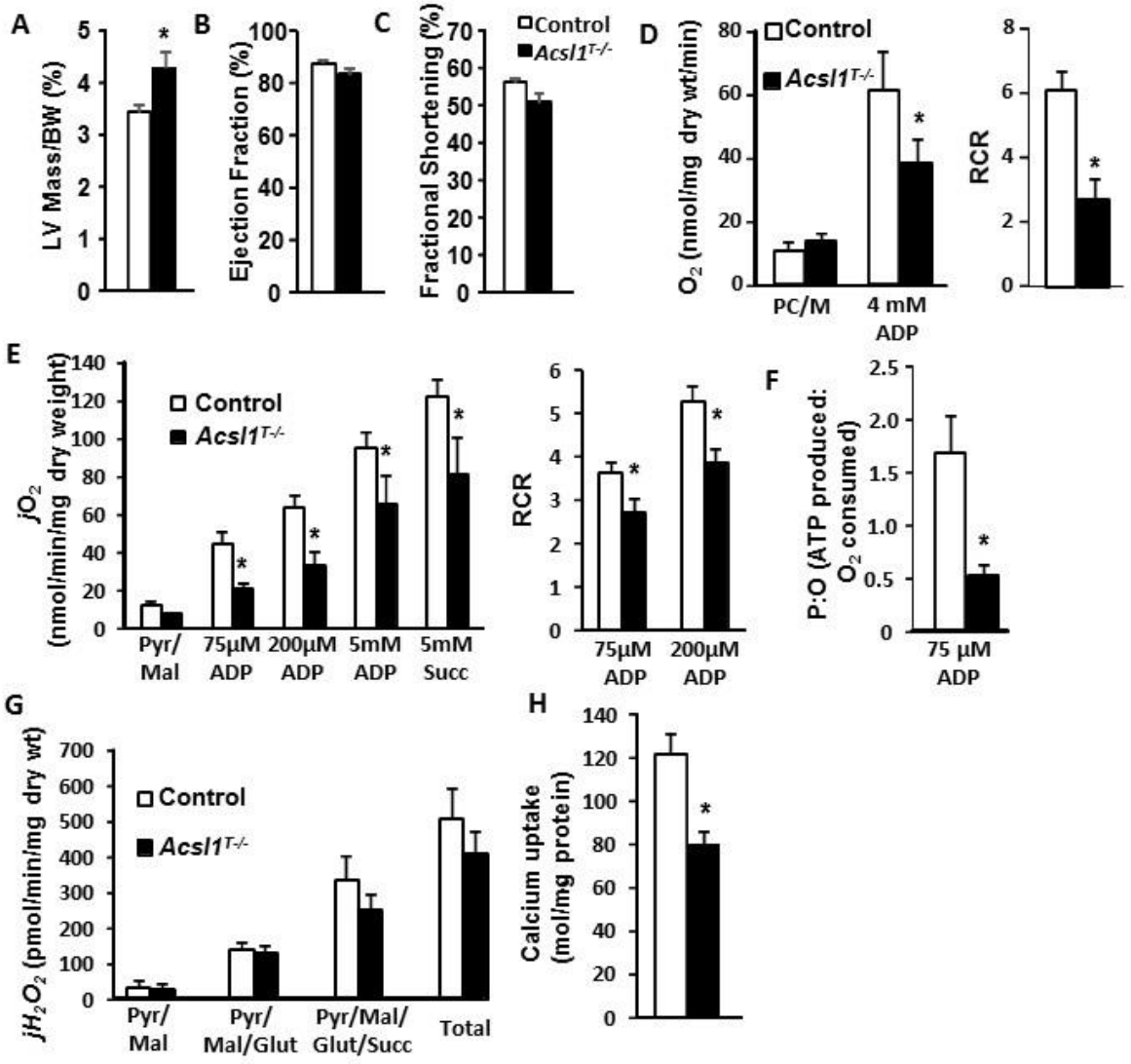

Figure 2.2. Loss of ACSL1 caused mitochondrial dysfunction. A) Left ventricle (LV) mass normalized to body weight (n=4). Ejection fraction **(B)** and fractional shortening **(C)** as measured by echocardiography on conscious mice (n=4). O_2 consumption was measured in saponin-permeabilized cardiac muscle fibers with either **(D)** palmitoyl-carnitine + malate (PC/M) or **(E)** pyruvate + malate (Pyr/Mal) ± ADP and succinate (succ); (Respiratory control ratio: RCR). **F**); ratio of ADP-stimulated O_2 consumption to basal (n=4-6). **G)** Ratio of ATP produced for each O_2 molecule consumed (n=4-5). **E)** Hydrogen peroxide (H_2O_2) production (n=6). **H)** Calcium uptake in isolated cardiac mitochondria before the permeability transition (n=3).

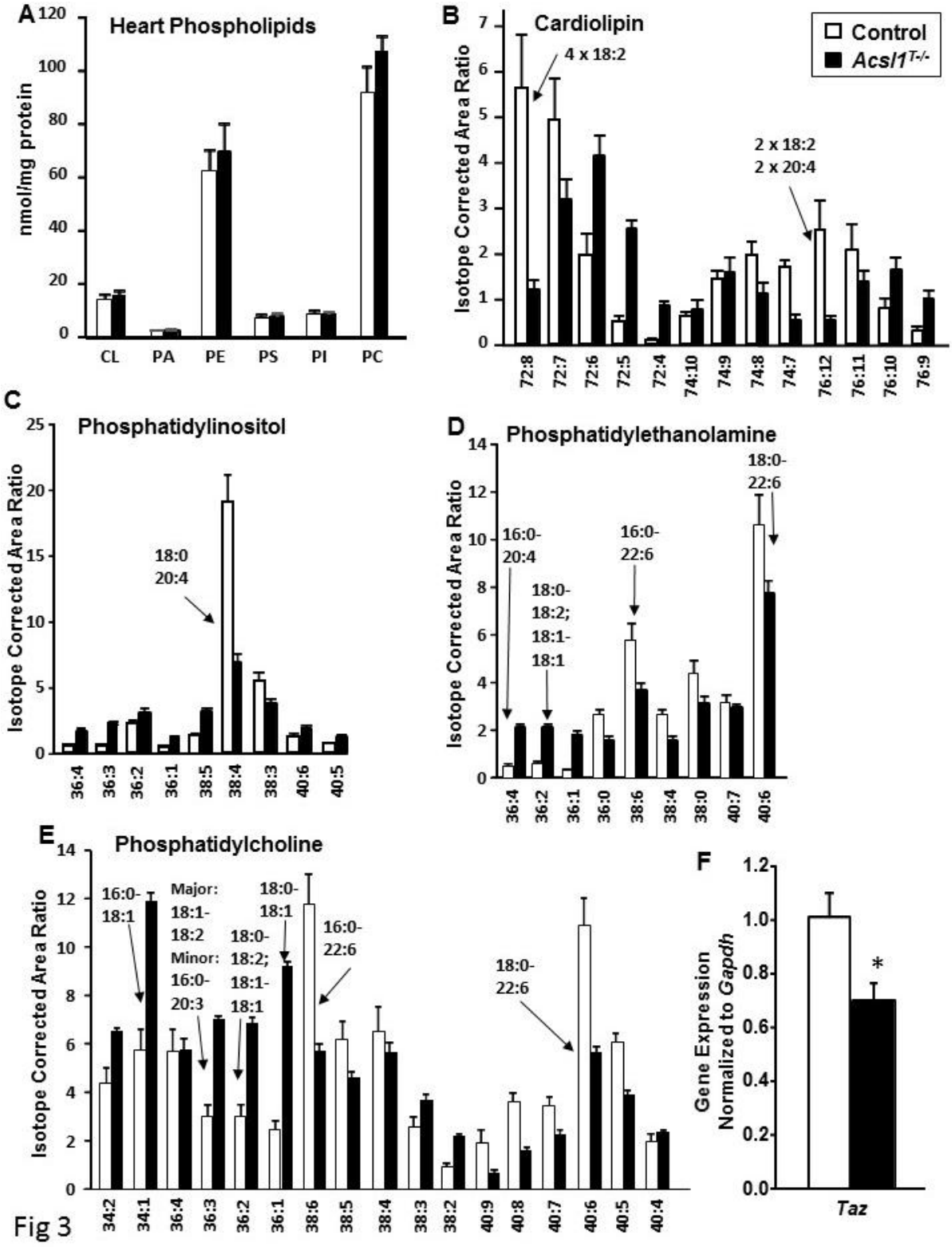
A
Heart Phospholipids
nmol/mg protein
CL
PA
PE
PS
PI
PC
B
Cardiolipin
Control
Acsl1T-/-
4 x 18:2
2 x 18:2
2 x 20:4
Isotope Corrected Area Ratio
C
Phosphatidylinositol
18:0
20:4
D
Phosphatidylethanolamine
16:0-
20:4
18:0-
18:2;
18:1-
18:1
16:0-
22:6
18:0-
22:6
E
Phosphatidylcholine
16:0-
18:1
Major:
18:1-
18:2
Minor:
16:0-
20:3
18:0-
18:2;
18:1-
18:1
18:0-
18:1
16:0-
22:6
18:0-
22:6
F
Gene Expression
Normalized to Gapdh
Taz
*

Fig 3

G

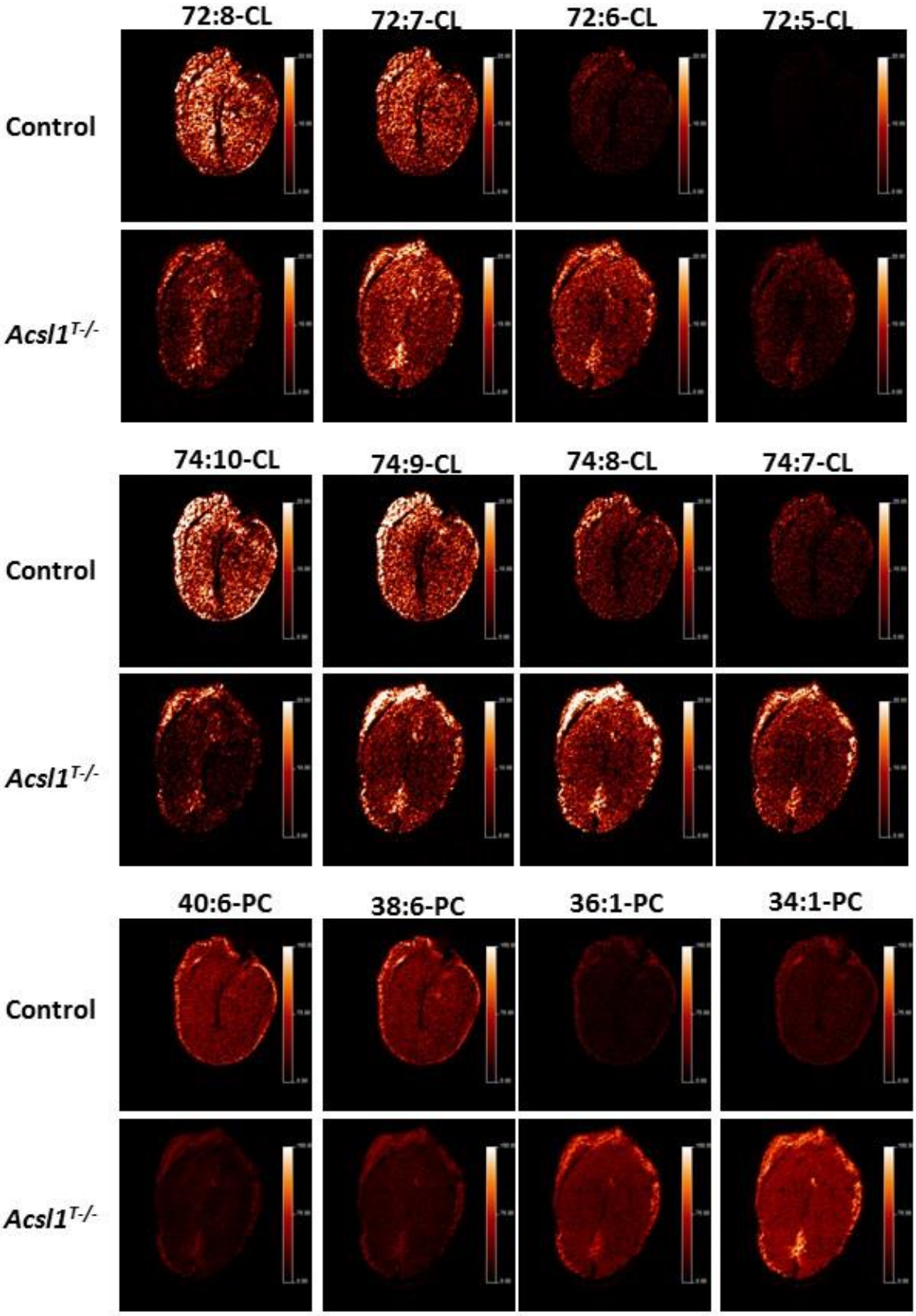
72:8-CL
72:7-CL
72:6-CL
72:5-CL
Control
Acsl1T-/-
74:10-CL
74:9-CL
74:8-CL
74:7-CL
Control
Acsl1T-/-
40:6-PC
38:6-PC
36:1-PC
34:1-PC
Control
Acsl1T-/-

Figure 2.3. Loss of ACSL1 alters acyl-chain composition of mitochondrial phospholipids. **A)** Quantification of phosphate in ventricular phospholipids separated by thin layer chromatography (n=5). **B-E)** LC/MS/MS analysis of phospholipid species in isolated mitochondria (n=5). Phospholipid species are shown as relative amounts normalized to an internal standard for each phospholipid. Species that were fragmented are indicated with arrows and identified acyl-chains. Other species were detected but were omitted from graph if the isotope corrected ratio was lower than 2 and no difference between genotypes was found. **F)** Ventricular tafazzin gene expression (n=4). **G)** Selected phospholipid species analyzed by MALDI-IMS (n=1).

Table 2.1. Phospholipid Species in *Acsl1*$^{T-/-}$ hearts.

PL	m/z	Carbons: double bonds	Percent change	Number of each fatty acid per PL molecule						
				16:0	18:0	18:1	18:2	20:3	20:4	22:6
CL	1448	72:8	-83.4				4			
	1496	76:12	-79.8				2		2	
PC	819	34:1	106.4	1		1				
	843	36:3	131.0			1	1			
				1				1		
	845	36:2	127.2			2				
				1			1			
	847	36:1	272.2		1	1				
	865	38:6	-53.3	1						1
	891	40:6	-48.1		1					1
PI	886	38:4	-64.1		1				1	
PE	739	36:4	337.5	1					1	
	743	36:2	284.6	1			1			
						2				
	763	38:6	-35.0	1						1
	791	40:6	-24.8		1					1

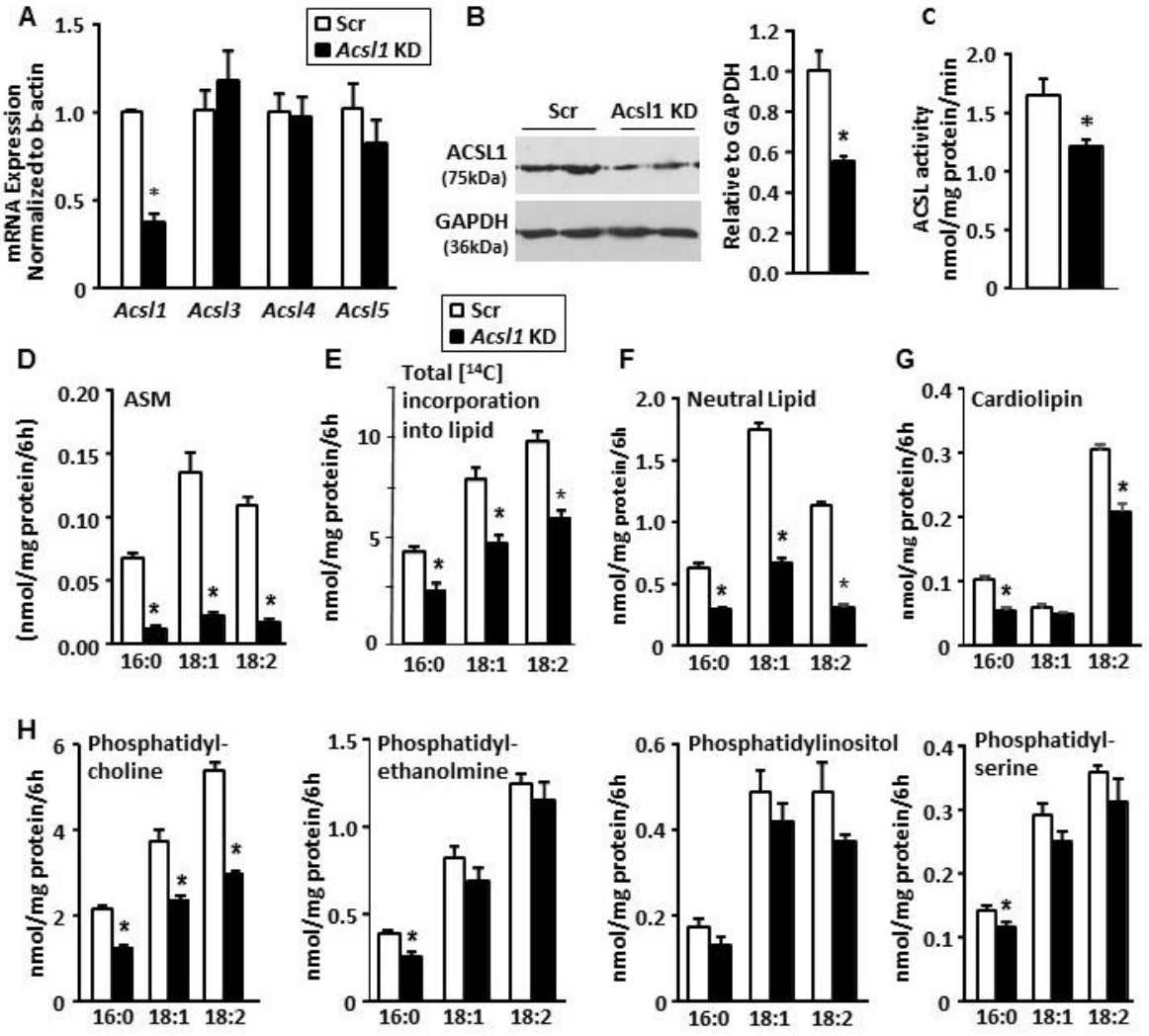

Figure 2.4. Knockdown of ACSL1 impairs fatty acid oxidation and incorporation into lipids. H9c2 cells were infected with lentivirus to stably express shRNA for either *scrambled* control (*Scr*) or *Acsl1* knockdown (KD). **A)** mRNA abundance of *Acsl* isoforms (*Acsl6* was not detected). **B)** ACSL1 protein. **C)** ACSL activity measured with 50 µM palmitate. **D**) Cells were incubated with trace [1-^{14}C]fatty acid (0.5 µCi) for 6 h. Fatty acid oxidation was measured as acid soluble metabolites (ASM, a measure of incomplete fatty acid oxidation) in the media. **E**) Radioactivity in total cellular lipid extract. **F-H)** Lipids were separated by thin layer chromatography, and radioactivity was quantified. (n=3 independent experiments, each performed in triplicate.) *, p-value ≤0.05 between *Scr* and *Acsl1* KD.

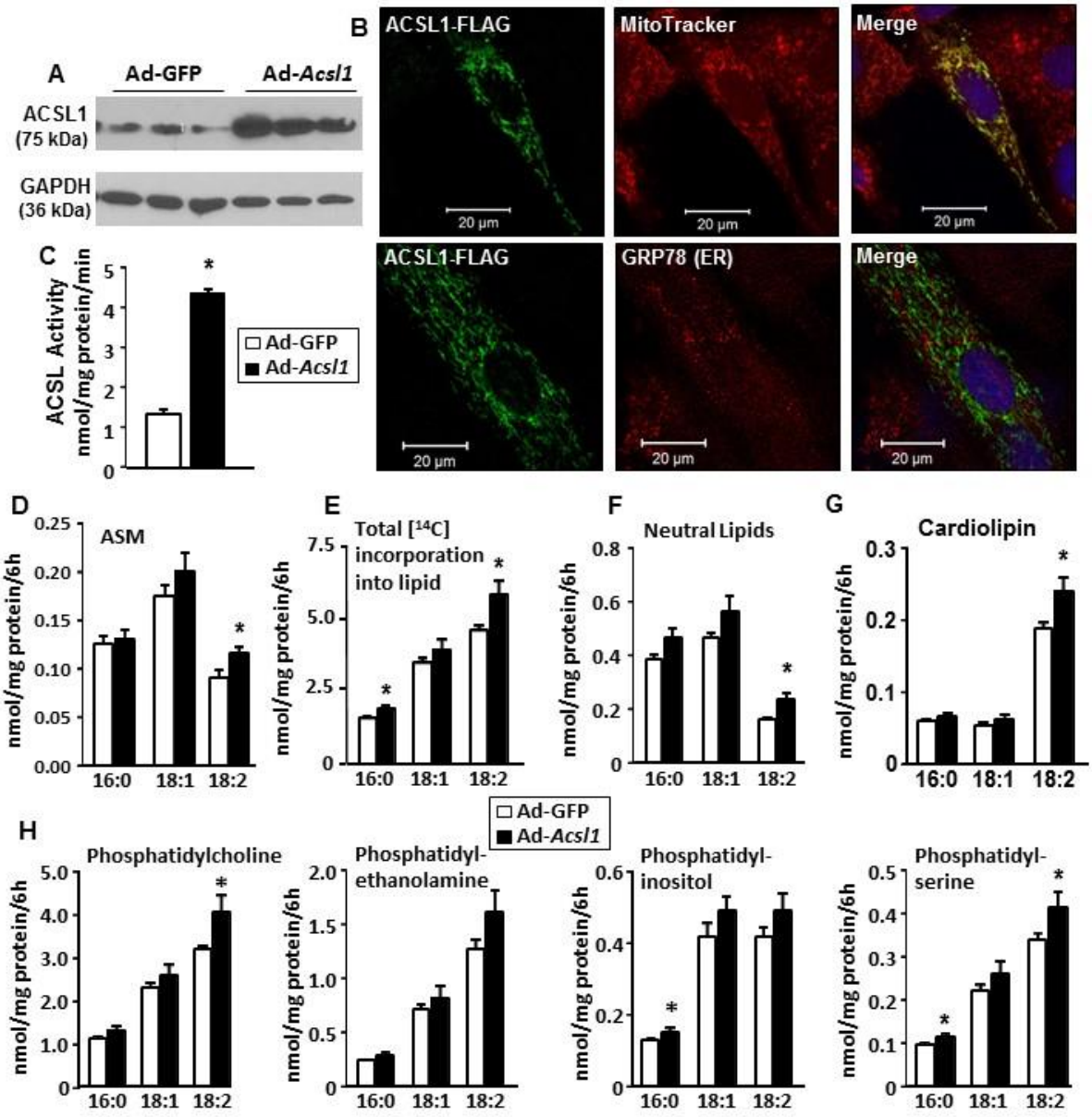

Figure 2.5. Overexpression of ACSL1 increases linoleate metabolism. H9c2 cells were infected with either *Ad-GFP* or *Ad-Acsl1-FLAG*. **A)** ACSL1 protein. **B)** Subcellular localization of ACSL1-FLAG. **C**) ACSL activity measured using 50 μM [1-^{14}C]palmitate. **D**) After a 6 h incubation with trace amounts of [1-^{14}C]fatty acid (0.5 μCi), fatty acid oxidation was measured in acid soluble metabolites (ASM, incomplete fatty acid oxidation) in the media. **E**) Radioactivity in total lipid extract. **F**-**H**) Lipids were separated by thin layer chromatography, and radioactivity in each species was quantified. (n=3 independent experiments, each performed in triplicate) *, p-value≤0.05 between *Ad-GFP* and *Ad-ACSL1-FLAG*.

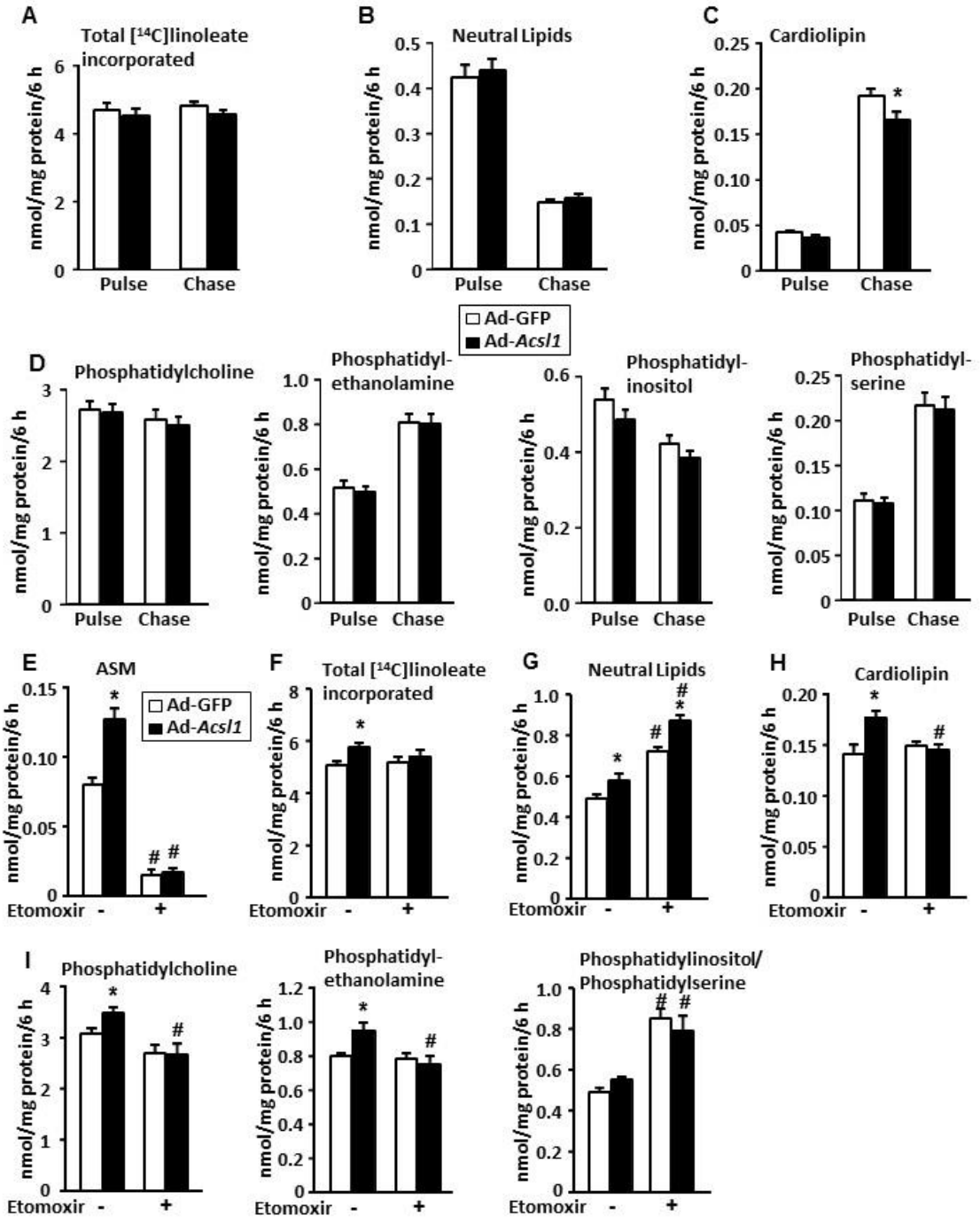

Figure 2.6. Pulse-chase and etomoxir treatment of H9c2 cells overexpressing ACSL1. H9c2 cells infected with *Ad-GFP* or *Ad-Acsl1*. **A-D)** Cells were incubated with [1-^{14}C]linoleate for 2 h (pulse) and then incubated with unlabeled linoleate 4 h (chase). **E-I)** Cells were pre-incubated with or without etomoxir for 1 h, and then with or without etomoxir and [1-^{14}C]linoleate for 6 h.

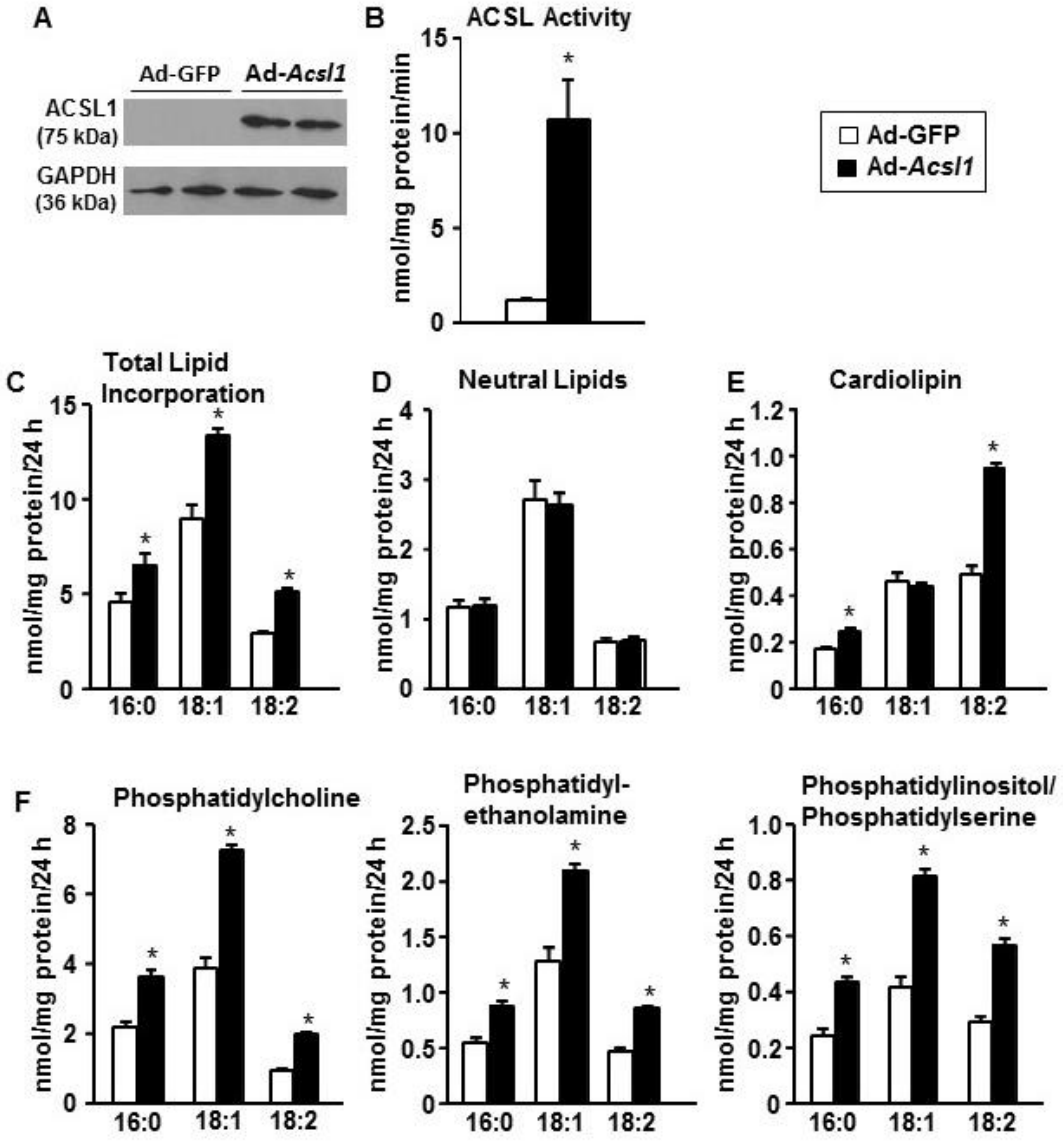

Figure 2.7. ACSL1 overexpression increased linoleate incorporation into CL in HEK-293 cells. HEK-293 cells were infected with either *Ad-GFP* or *Ad-Acsl1-FLAG*. **A)** ACSL1 protein. **B)** ACSL specific activity measured with 50 µM [1-^{14}C]palmitate. **C-F)** Cells were incubated with 30 µM oleate, 15 µM palmitate, and 5 µM linoleate with 0.5 µCi [1-^{14}C]oleate, [1-^{14}C]palmitate or [1-^{14}C]linoleate for 24 h. **C)** Radioactivity in total lipid extract. **D-F)** Lipids were separated by thin layer chromatography, and radioactivity was quantified (n=3 independent experiments, each performed in triplicate). *, p-value ≤0.05 between *Ad-GFP* and *Ad-ACSL1-FLAG*.

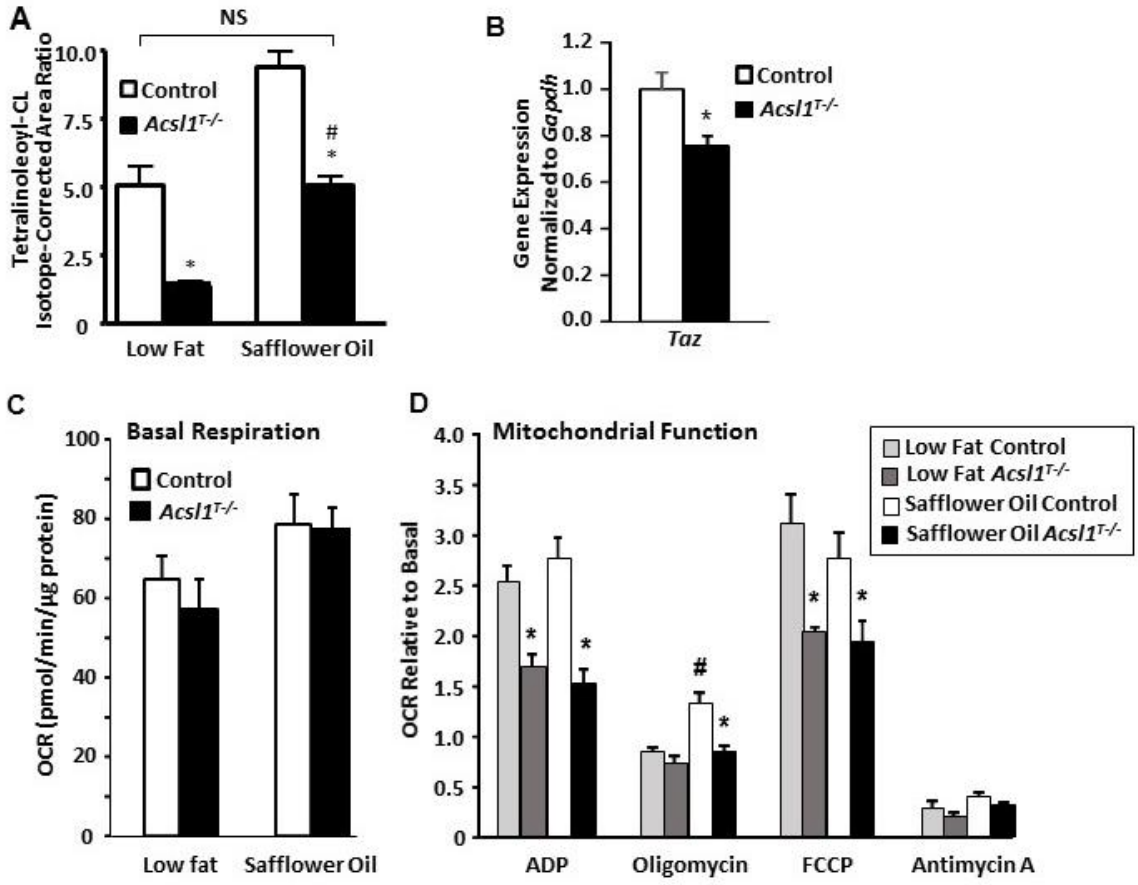

Figure 2.8. High linoleate diet partially normalized CL acyl-chain profile in *Acsl1*$^{T-/-}$ hearts but did not improve mitochondrial respiratory function. For 16 weeks after tamoxifen injections, male mice were fed a low-fat (10% fat) control diet. Mice were then either maintained on the low-fat diet or switched to a high safflower oil diet (Research Diets, D02062104, 45% kcal fat (75% linoleate)) for 4 additional weeks to increase dietary linoleate. **A**) LC/MS/MS analysis of ventricular cardiolipin with low fat and safflower oil diets (n=5). **B)** Ventricular tafazzin gene expression in safflower oil-fed mice (n=5). **C-D)** Mitochondrial respiratory function was measured in isolated mitochondria using a Seahorse XF24 Analyzer, which sequentially injected ADP, oligomycin, FCCP, and antimycin A (n=4-7). O2 consumption rate: OCR. *, p-value ≤0.05 between genotypes within diet. #, p-value ≤0.05 between diets within genotype.

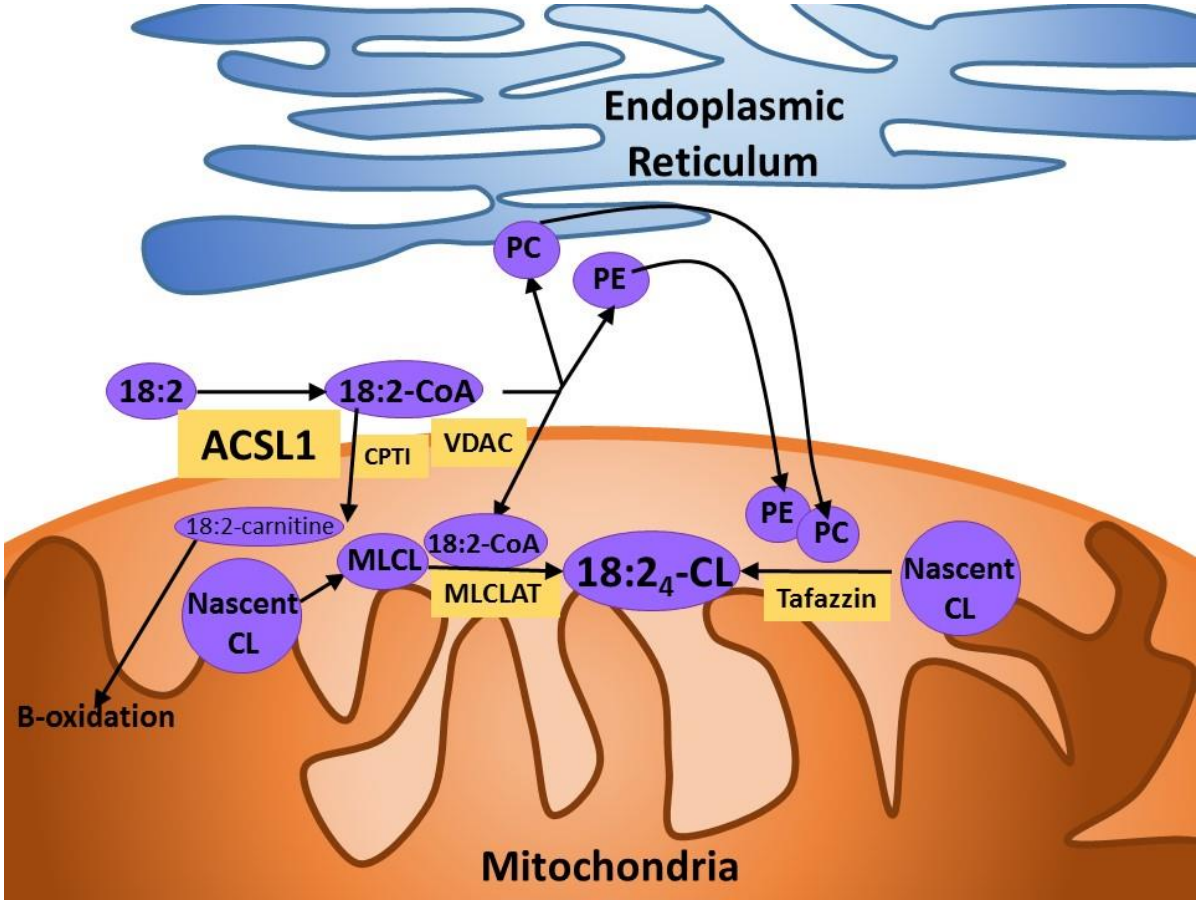

Figure 2.9. Proposed pathway for how ACSL1 increases linoleate incorporation into cardiolipin (CL). After linoleate (18:2) is converted to 18:2-CoA by ACSL1, it can enter 1 of 3 pathways. 1. 18:2-CoA can be converted to 18:2-carnitine by CPT1 and then enter β-oxidation. 2. 18:2-CoA can enter the mitochondria through VDAC and be added to MLCL by MLCL-AT1 to form mature tetralinoleoyl CL (18:2$_4$-CL). 3. 18:2-CoA can be used at the ER to form phospholipids such as PC and PE. These phospholipids are then incorporated into the mitochondrial membrane where tafazzin can transfer acyl chains from PC or PE to CL or MLCL to form tetralinoleoyl-CL.

Rationale for Chapter 3

In Chapter 2, we showed that mitochondria from hearts lacking ACSL1 have impaired respiratory function. A clear role for ACSL1 in activating fatty acids for esterification onto phospholipids was found *in vivo* and *in vitro*. *Acsl1*$^{T-/-}$ hearts display altered acyl chain composition of CL, PC, PE, and PI, and cells deficient in or overexpressing ACSL1 have different incorporation of fatty acids in phospholipids and neutral lipids. However, use of a dietary intervention to normalize the amount of tetralinoleoyl-CL in *Acsl1*$^{T-/-}$ hearts did not improve mitochondrial function. This finding showed that another defect was present in the *Acsl1*$^{T-/-}$ hearts that caused the mitochondrial dysfunction.

In Chapter 3, we explore how alterations to cardiac metabolism, in terms of substrate choice, can impair mitochondrial function. Our lab previously showed that loss of ACSL1 impairs fatty acid oxidation, causing high glucose use. This transition to primarily using glucose for energy causes an accumulation of glucose-6-phosphate, a metabolite of glucose, which can activate mTORC1. mTORC1 then signals for growth of the cell by increasing RNA synthesis, protein translation, and fatty acid use while inhibiting degradation of cellular components. The next chapter examines how the chronic activation of mTORC1 impairs mitochondrial function in *Acsl1*$^{T-/-}$ hearts.

CHAPTER 3: LOSS OF ACSL1 IMPAIRS CARDIAC AUTOPHAGY AND MITOCHONDRIAL STRUCTURE THROUGH MTORC1 ACTIVATION

Trisha J. Grevengoed[1], Daniel E. Cooper[1], Jessica M. Ellis[1], Rosalind A. Coleman[1]

Summary

Because hearts with a temporally-induced knockout of acyl-CoA synthetase 1 (*Acsl1*$^{T-/-}$) are essentially unable to oxidize fatty acids, glucose use increases 8-fold to compensate. This metabolic switch activates mechanistic target of rapamycin complex 1 (mTORC1), which initiates growth by increasing protein and RNA synthesis and fatty acid metabolism while decreasing autophagy. *Acsl1*$^{T-/-}$ hearts contained 3-fold more mitochondria with abnormal structure and displayed 35-43% lower respiratory function. To study the effects of mTORC1 activation on mitochondrial structure and function, mTORC1 was inhibited by treating *Acsl1*$^{T-/-}$ and littermate control mice with rapamycin or vehicle alone for two weeks. Rapamycin treatment normalized mitochondrial structure, number, and the maximal respiration rate in *Acsl1*$^{T-/-}$ hearts but did not improve ADP-stimulated oxygen consumption, which was likely caused by 33-51% lower ATP synthase activity present in both vehicle- and rapamycin-treated *Acsl1*$^{T-/-}$ hearts. The turnover of LC3b in *Acsl1*$^{T-/-}$ hearts was 88% lower than controls, indicating a diminished rate of autophagy. Rapamycin treatment increased autophagy to a rate that was 3.1-fold higher than in controls, allowing clearance of damaged mitochondria. Thus, ACSL1 deficiency in heart activated mTORC1, thereby inhibiting autophagy and increasing the number of damaged mitochondria.

[1] University of North Carolina, Chapel Hill, NC, USA, Dept. of Nutrition

Introduction

The normal heart obtains 60-90% of its energy from fatty acids, but can increase the use of other substrates such as glucose with feeding or hypoxia, or the use of amino acids and ketones with fasting (158). Metabolic flexibility permits the heart to use different substrates to meet its constant high demand for energy (263). Several disease states diminish the metabolic flexibility of the heart and compel the predominate use of a single substrate. For instance, the diabetic heart uses high amounts of fatty acid because glucose uptake is low (164,165). Conversely, glucose use increases with heart failure and pathologic hypertrophy caused by pressure overload (160-163). Because it is unclear whether the switch in substrate use in each of these disease states is compensatory or pathologic, we asked whether predominant glucose use, in the absence of other cardiac dysfunction, would be detrimental.

In the temporally-induced mouse model deficient in long-chain acyl-CoA synthetase isoform-1 (*Acsl1*$^{T-/-}$), the heart's ability to oxidize fatty acids is severely diminished. ACSLs convert fatty acids to acyl-CoAs, which can then be oxidized in the mitochondria to produce energy or incorporated into triacylglycerol (TAG) for storage or into phospholipids for membrane biogenesis. Of the five known mammalian ACSL isoforms, ACSL1 is the major isoform in heart, accounting for 90% of the total ACSL activity. When ACSL1 is temporally knocked out in the adult heart, fatty acid oxidation is diminished by more than 90%, and glucose use increases 8-fold to compensate for this loss (87).

To study the consequences of the switch from fatty acid to glucose use, we focused on the effects of the mechanistic target of rapamycin complex 1 (mTORC1), which is activated by high glucose flux in hearts (264,265). Within ten weeks of inducing the knockout, hearts lacking ACSL1 develop mTORC1-dependent hypertrophy (266). mTORC1 activation has many consequences in cells, including stimulation of growth and protein synthesis (267,268), regulation of lipid metabolism (269,270), and inhibition of autophagy (202). Inhibition of mTOR is associated with longer lifespan

(271), but total loss of mTOR in the heart inhibits mitochondrial respiratory function and causes heart failure (270). Although short-term activation of mTOR increases mitochondrial respiration and biogenesis in cultured cells (272-274), mTORC1 inhibits autophagy, which can allow damaged mitochondria to accumulate. Cardiac mitochondrial DNA and proteins have half-lives of under one week, indicating a high rate of turnover (275,276). Removal of damaged mitochondria is particularly important in cardiomyocytes due to their high demand for energy and the long lifespan of these cells. Impaired removal of damaged mitochondria can exacerbate damage after ischemia (197) or myocardial infarction (198) and cause heart failure (199,200). In the present study we examined the effects of chronic activation of cardiac mTORC1 on mitochondrial number and structure and on the function of the electron transport chain in ACSL1-deficient hearts.

Materials and Methods

Unless otherwise indicated, reagents were obtained from Sigma-Aldrich (St. Louis, MO, USA). Radiolabeled substrates (2-Br-[1-^{14}C]palmitate, [1-^{14}C]palmitate, and [2-^{14}C]pyruvate) were purchased from Perkin-Elmer (Waltham, MA, USA). Trypsin and soybean trypsin inhibitor were from Worthington Biochemical (Lakewood, NJ, USA).

Animal care and diets: All protocols were approved by the Institutional Animal Care and Use Committee at University of North Carolina at Chapel Hill. Mice were housed under a 12 h light/dark cycle with free access to food and water. Unless otherwise specified, mice were fed a purified low-fat diet (Research Diets Inc, New Brunswick, NJ, USA, DB12451B). A multi-tissue knockout of ACSL1 was achieved by mating mice with *LoxP* sequences flanking exon 1 of the *Acsl1* gene to animals expressing a tamoxifen-inducible *Cre* driven by a ubiquitous promoter enhancer (87). Between 6 and 8 weeks of age, $Acsl1^{T-/-}$ and littermate $Acsl1^{flox/flox}$ (control) mice were injected intraperitoneally (i.p.) on 4 consecutive days with tamoxifen (75 μg/g body weight) dissolved in corn oil. All studies were performed with male mice 20 weeks after tamoxifen administration, and tissues were collected after a 4 h fast, unless otherwise specified. The mice were deeply anesthetized with

Avertin and tissues were snap frozen in liquid nitrogen. For mTORC1 inhibition studies, rapamycin (1 mg/kg in phosphate buffered saline, pH 7.4/2% ethanol, 2.5% Tween 20/2.5% PEG-400) or vehicle alone was injected i.p. daily for 7 or 14 d, starting 18 or 19 weeks after tamoxifen treatment. A short rapamycin treatment was chosen to lessen the impaired insulin secretion and glucose tolerance observed with chronic rapamycin treatment (266,277,278). For autophagic flux studies, chloroquine (60 mg/kg in phosphate buffered saline, pH 7.4) was injected i.p. for 7 d.

ACSL activity assay: ACSL specific activity was measured as described (87). Briefly, homogenized tissues were centrifuged at 100,000 x g for 1 h at 4°C to isolate total membrane fractions. Protein (1-6 µg) was incubated with 50 µM [1-^{14}C]palmitate, 10 mM ATP, 250 µM CoA, 5 mM dithiothreitol, and 8 mM $MgCl_2$ in 175 mM Tris, pH 7.4 at RT for 10 min to measure initial rates. The enzyme reaction was stopped with 1 ml of Dole's solution (heptane:isopropanol:1M H_2SO_4; 80:20:1, v/v). Two ml of heptane and 0.5 ml of water were added to separate phases. Radioactivity of the acyl-CoAs in the aqueous phase was measured using a liquid scintillation counter.

Metabolic phenotyping: To quantify fatty acid uptake, 1.5 µCi 2-Br-[1-^{14}C]palmitate complexed to bovine serum albumin was injected retroorbitally. Tail blood was collected 5 min later, and tissues were collected 30 min after injection. Tissues were homogenized in water and radioactivity per mg of tissue was quantified relative to radioactivity in blood. To analyze fatty acid oxidation and TCA cycle activity, respectively, [1-^{14}C]palmitate and [2-^{14}C]pyruvate oxidation were measured in isolated mitochondria as described (87). Ventricle TAG was measured using a colorimetric kit. Tissues for glycogen measurement were collected at 7 am (fed) or after 4 h of fasting and were homogenized in 1 N HCl. A portion was immediately neutralized to measure free glucose. The remaining homogenate was heated to 95°C for 90 min to hydrolyze glycogen, then neutralized with 1 N NaOH and centrifuged at 14,000 x g for 10 min. A colorimetric kit was used to measure glucose in the supernatant (Wako, Richmond, VA, USA).

Electron microscopy: Hearts were first perfused with phosphate buffered saline and then with freshly made 2.5% glutaraldehyde, 2% paraformaldehyde in 0.15 M sodium phosphate buffer, pH 7.4. Left ventricular tissue was prepared for transmission electron microscopy and imaged (279). Mitochondrial area was quantified using ImageJ software in 4 to 7 images, counting at least 1000 mitochondria per animal. Abnormal mitochondria were defined as mitochondria with vacuoles, inclusions, or disrupted cristae.

Mitochondrial function: To isolate mitochondria, hearts were minced in 0.125 mg/ml trypsin in homogenization buffer (0.25 M sucrose, 10 mM HEPES, 1 mM EDTA, pH 7.4). Soybean trypsin inhibitor (0.65 mg/ml) was added, and tissues were homogenized with 10 up-and-down strokes in a Teflon-glass homogenizing vessel and then centrifuged at 500 x g for 5 min to remove nuclei and unbroken cells. Mitochondria were isolated by centrifuging at 10,000 x g for 15 min and washed twice with homogenization buffer. The mitochondrial pellet was resuspended in mitochondrial assay buffer (70 mM sucrose, 220 mM mannitol, 10 mM KH_2PO_4, 5 mM $MgCl_2$, 0.2% bovine serum albumin, 25 mM BES, pH 7.0). The function of isolated mitochondria was assessed using a Seahorse XF24 Analyzer (Seahorse Bioscience, North Billerica, MA, USA) with 5 mM pyruvate and 5 mM malate as substrates. Mitochondria (15 µg of protein) were stimulated in succession with 100 µM ADP, 1 µg/ml oligomycin, 4 µM FCCP, and 4 µm antimycin A. To measure mitochondrial electron transport chain complex formation and complex V activity, mitochondrial proteins were prepared and separated by clear native electrophoresis. ATP hydrolysis activity of complex V was measured as described (280).

Gene expression analysis: Total RNA and DNA were simultaneously isolated from heart ventricles (AllPrep RNA/DNA Mini kit, Qiagen, Valencia, CA, USA). cDNA was synthesized (iScript cDNA Synthesis kit, BioRad, Hercules, CA, USA), and 10 ng of cDNA was added to each qPCR reaction with SYBR Green (iTaq Universal SYBR, BioRad, Hercules, CA, USA) and used to detect amplicons with primers specific to the gene of interest quantified using a qPCR thermocycler

(BioRad, Hercules, CA, USA). Results were normalized to the housekeeping gene *Gapdh* and expressed as arbitrary units of $2^{-\Delta\Delta CT}$ relative to the control group.

Immunoblots: Total protein lysates were isolated in lysis buffer (250 mM sucrose, 20 mM Tris, 1% Triton X-100, 50 mM NaF, 50 mM NaCl, 5 mM $Na_4P_2O_7$, plus protease and phosphatase inhibitor cocktail (Thermo Scientific, Walthan, MA, USA)). Immunoblots were run under standard conditions. Primary antibodies were purchased from the indicated companies: phosphorylated-p70 S6 kinase (Thr389), p70 S6 kinase (S6K), phosphorylated-4E-BP1 (Thr37/46), 4E-BP1, and ACSL1 (Cell Signaling Technology, Danvers, MA, USA), GAPDH (Abcam, Cambridge, MA, USA), LC3B (Sigma-Aldrich, St. Louis, MO, USA), and p62 (Abnova, Taipei City, Taiwan).

Statistics: Data are presented as the mean ± SE for each treatment group. Differences between groups were evaluated by two-way ANOVA with Tukey multiple-comparison posttests. All statistical analyses were performed using GraphPad Prism (GraphPad Software, La Jolla, CA, USA; version 6.0). Differences between means with $p < 0.05$ were considered statistically significant.

Results

Loss of cardiac ACSL1 decreased the use of fatty acids and increased the use of glucose. Hearts lacking ACSL1 were previously characterized 2 and 10 weeks after induction of the knockout with tamoxifen (87); in order to examine long term effects of ACSL1 deficiency, the present study used mice at 20 weeks after tamoxifen. To confirm that the metabolic phenotype persisted, salient points were reexamined. Similar to the previous report, ACSL1 protein and mRNA remained absent from *Acsl1*$^{T-/-}$ hearts 20 weeks after tamoxifen treatment (**Fig. 3.1A, B**). *Acsl3* mRNA expression was 4.5-fold higher and *Acsl6* mRNA was 39% lower in *Acsl1*$^{T-/-}$ hearts (Fig. 1B), and ACSL specific activity was 86% lower in *Acsl1*$^{T-/-}$ ventricles (**Fig. 3.1C**), suggesting that any compensation by other ACSL isoforms had done little to increase ACSL activity. We measured mitochondrial oxidation of [1-^{14}C]palmitate to both CO_2 and acid soluble metabolites (ASM), which are measures of complete and incomplete oxidation, respectively. The diminished activation of fatty acids to acyl-CoAs

resulted in 94% lower [1-^{14}C]palmitate oxidation than in control cardiac mitochondria (**Fig. 3.1D**). In contrast to that of hearts deficient in carnitine palmitoyltransferase 1 (281), the minimal oxidation of fatty acids in *Acsl1*$^{T-/-}$ hearts did not result in cardiac TAG accumulation (**Fig. 3.1E**). The lack of TAG accumulation in *Acsl1*$^{T-/-}$ hearts was likely due to diminished fatty acid uptake. Uptake, as measured using the non-oxidizable fatty acid analogue 2-Br-[1-^{14}C]palmitate, was 76% lower in *Acsl1*$^{T-/-}$ hearts (**Fig. 3.1F**), indicating that conversion of the fatty acid to an acyl-CoA was necessary for fatty acid retention in the cell. Addition of coenzyme A to the fatty acid both traps the fatty acid in the cell and lowers its effective concentration, allowing additional transport into the cell (282). Even though fatty acid oxidation was low in *Acsl1*$^{T-/-}$ hearts compared to controls, phosphorylated (activated) AMPK was reduced in *Acsl1*$^{T-/-}$ hearts, consistent with the production of adequate energy to maintain a low AMP/ATP ratio (**Fig. 3.1G**).

To compensate for low fatty acid oxidation, glucose use was increased in *Acsl1*$^{T-/-}$ hearts. Compared to controls, the oxidation of [2-^{14}C]pyruvate was 2-fold higher in *Acsl1*$^{T-/-}$ cardiac mitochondria, consistent with increased flux through the TCA cycle (**Fig. 3.1H**). *Acsl1*$^{T-/-}$ hearts stored 70% more glycogen than controls during feeding and used the extra glycogen during a 4 h fast. The *Acsl1*$^{T-/-}$ livers, which recover ACSL1 expression (87), contained normal amounts of glycogen with feeding, but after only a 4 h fast, glycogen diminished by 35% (**Fig. 3.1I**), suggesting that the rate of glycogen use was more rapid in *Acsl1*$^{T-/-}$ mice. Together, these observations show that the metabolic changes previously detected in *Acsl1*$^{T-/-}$ hearts persist (87), and that 20 weeks after loss of ACSL1, cardiac metabolism vastly favored glucose metabolism.

Two weeks of rapamycin treatment inhibited mTORC1 activation in *Acsl1*$^{T-/-}$ hearts. mTORC1 is activated in *Acsl1*$^{T-/-}$ 10 weeks after tamoxifen-mediated induction of the knockout (87). We examined phosphorylation of two mTORC1 targets, S6K and 4E-BP1, to confirm that mTORC1 remained activated after an additional 10 weeks. Treatment with the mTORC1 inhibitor rapamycin for 2 weeks repressed mTORC1-mediated phosphorylation of both S6K and 4E-BP1 in *Acsl1*$^{T-/-}$

hearts (**Fig. 3.2A**) and decreased the size of both control and *Acsl1*$^{T-/-}$ hearts (**Fig. 3.2B**). Rapamycin treatment normalized heart size in *Acsl1*$^{T-/-}$ hearts, thereby confirming that the hypertrophy observed in *Acsl1*$^{T-/-}$ hearts had resulted from mTORC1 activation (266).

mTORC1 inhibition improved mitochondrial structure in *Acsl1*$^{T-/-}$ hearts. *Acsl1*$^{T-/-}$ ventricles contained more mitochondria 10 weeks after the knockout was induced with tamoxifen, but no difference in mitochondrial structure was observed at that time point (87). Twenty weeks after tamoxifen, however, electron microscopy of *Acsl1*$^{T-/-}$ ventricles showed the presence of 3-fold more abnormal mitochondria, defined as those containing vacuoles, inclusions, or disrupted cristae (**Fig. 3.3A, B**). Because mTORC1 inhibits autophagy (202), we questioned whether the mitochondria with abnormal structure could be cleared by relieving a block on autophagy. Mitochondrial structure was then examined in mice treated for one and two weeks with rapamycin. One week of rapamycin treatment had no observable effect on mitochondria in control hearts, but dramatically increased the number of autophagic vesicles in *Acsl1*$^{T-/-}$ hearts. After two weeks of rapamycin treatment, most of the autophagic vacuoles had disappeared, and the *Acsl1*$^{T-/-}$ hearts contained significantly fewer abnormal mitochondria containing vacuoles, inclusions, or disrupted cristae (**Fig. 3.3B**). These data strongly suggest that activated mTORC1 had inhibited autophagy, thereby impairing the removal of damaged mitochondria. Quantification of mitochondrial area revealed that, compared to controls, *Acsl1*$^{T-/-}$ hearts contained twice as many very small mitochondria (area <5 AU) and fewer large mitochondria (area of 15-19.9 and 20-24.9 AU) (**Fig. 3.3C**), and rapamycin treatment normalized mitochondrial size in *Acsl1*$^{T-/-}$ hearts. Thus, loss of ACSL1 caused an accumulation of structurally abnormal mitochondria, and inhibition of mTORC1 normalized both the size and appearance of mitochondria.

Rapamycin treatment normalized the high mitochondrial number in *Acsl1*$^{T-/-}$ hearts. Compared to controls, *Acsl1*$^{T-/-}$ hearts contained more mitochondria, as demonstrated by 30% higher mitochondrial DNA content (**Fig. 3.4A**), 18% greater mitochondrial area (**Fig. 3.4B**), and 54% higher mitochondrial number (**Fig. 3.4C**). Rapamycin treatment normalized each of these measures in

Acsl1$^{T-/-}$ hearts, strongly suggesting that mTORC1 activation had caused the increase in mitochondrial number. Although mTORC1 increases mitochondrial biogenesis (283), in the current study expression of the mitochondrial biogenesis genes *Pgc1a* and *Erra* were not altered with genotype or treatment (**Fig. 3.4D**), suggesting that the higher mitochondrial number in *Acsl1*$^{T-/-}$ hearts was not due to the formation of new mitochondria, but instead, to the inhibition of mitochondrial removal.

Inhibition of mTORC1 activated autophagy in *Acsl1*$^{T-/-}$ hearts. mTORC1 lowers the autophagic rate by inhibiting an early step in autophagosome formation (202). To determine whether the normalization of mitochondrial number and structure in *Acsl1*$^{T-/-}$ hearts with rapamycin treatment was due to increased clearance of damaged mitochondria, we examined the rates of autophagy in vehicle- and rapamycin-treated mice. Chloroquine raises the lysosomal pH, thereby inhibiting the degradation of the autophagolysosomes (284). LC3b-I, a protein found on the outer membrane of the autophagosome, is activated by cleavage and lipidation with phosphatidylethanolamine to form LC3b-II, and then degraded within the autophagosome (285). Because chloroquine inhibits degradation without affecting autophagosome formation or the activation of LC3b-I, comparing the amount of activated LC3b-II in basal and chloroquine-treated hearts indicates how quickly the autophagosome is normally degraded, i.e. autophagic flux. In control hearts, chloroquine caused a 3-fold increase in the accumulation of activated LC3b-II relative to the inactive LC3b-I. The difference in these two ratios displays the rate of autophagy (284,286). Basal activation of LC3b appeared high in *Acsl1*$^{T-/-}$ hearts, but treatment with chloroquine did not cause activated LC3b-II to increase, indicating very low autophagic flux (**Fig 3.5A**). Thus, the large amount of active LC3b-II in *Acsl1*$^{T-/-}$ hearts was likely due to impaired clearance of the autophagosome because of diminished long-term autophagic flux (284). When mice were treated with both rapamycin and chloroquine, the accumulation of LC3b-II was greater in both genotypes. The increase in LC3b-II in rapamycin-treated *Acsl1*$^{T-/-}$ hearts with chloroquine was 3 times greater than controls, indicating a very high rate of autophagy when mTORC1 is inhibited. This high rate of autophagic flux may have occurred to compensate for the low clearance of damaged mitochondria and proteins in the basal state. The p62

(SQSTM1) scaffolding protein that binds to ubiquitin and LC3-II is specifically degraded by autophagy, making it a useful marker for a low autophagic rate (287,288). The accumulation of p62 in *Acsl1*$^{T-/-}$ hearts further demonstrated impaired autophagy. Rapamycin treatment did not alter the amount of p62 in control hearts, but normalized p62 levels in *Acsl1*$^{T-/-}$ hearts (**Fig 3.5B**), showing that autophagy was no longer inhibited by mTORC1. Together with the normalization of mitochondrial number and structure, these data suggest that by inhibiting mTORC1 in *Acsl1*$^{T-/-}$ hearts, the autophagic rate increased, allowing damaged mitochondria to be cleared.

Rapamycin treatment partially normalized mitochondrial function in *Acsl1*$^{T-/-}$ hearts. To determine whether reducing mTORC1 activation and increasing autophagy would enable mitochondrial function to recover, we examined electron transport chain function in control and *Acsl1*$^{T-/-}$ cardiac mitochondria from vehicle- and rapamycin-treated mice. No genotype or treatment difference was found in basal respiration (**Fig. 3.6A**). When stimulated with ADP, *Acsl1*$^{T-/-}$ mitochondria consumed 35% less oxygen than controls, and rapamycin treatment did not improve ADP-stimulated oxygen consumption (**Fig. 3.6B**). In response to the mitochondrial uncoupler FCCP, vehicle-treated *Acsl1*$^{T-/-}$ mitochondria consumed 43% less oxygen than controls. Rapamycin treatment normalized FCCP-stimulated respiration in *Acsl1*$^{T-/-}$ mitochondria, indicating that the mitochondria had regained their capacity for maximal respiration. To determine whether the loss of ACSL1 interfered with ATP synthesis, we examined complex V by measuring the activity and protein amount of ATP synthase in cardiac mitochondria. After separating the mitochondrial complexes, the ATP hydrolysis activity of complex V was lower in both vehicle- and rapamycin-treated *Acsl1*$^{T-/-}$ mitochondria, without loss of total protein (**Fig. 3.6C**). Thus, loss of ATP synthase activity had diminished ADP-stimulated oxygen consumption in *Acsl1*$^{T-/-}$ hearts independent of mTOR activation. Because maximal respiration, as measured in the presence of FCCP, was independent of ATP synthase and was normal in rapamycin-treated *Acsl1*$^{T-/-}$ mitochondria, it appears that short-term rapamycin treatment partially normalized mitochondrial function in *Acsl1*$^{T-/-}$ hearts.

Discussion

The loss of ACSL1 in highly oxidative tissues such as heart results in a severe deficit in fatty acid oxidation and a marked increase in glucose use. It has been questioned whether the substrate used by the heart for energy production is important for heart health. An acute increase in workload causes the heart to preferentially increase carbohydrate metabolism (289), and the failing heart exhibits a low rate of fatty acid oxidation and a high glycolytic rate (163,290,291). An increase in glucose metabolism compensates for the production of energy for contraction and other cellular operations in the absence of oxygen or with inadequate mitochondrial energy production. During pressure overload, overexpression of the glucose transporter GLUT1 prevents the loss of heart and mitochondrial functions, presumably due to increased glucose use (292). In heart, the deficiency of malonyl-CoA decarboxylase impairs fatty acid oxidation and enhances glycolysis and glucose oxidation, and the hearts are protected during ischemia-reperfusion (293). Acute changes in metabolism may protect the heart from injury, but the question remains whether chronic glucose use is detrimental to the heart. When GLUT1-overexpressing mice are fed a high fat diet, their hearts exhibit high oxidative stress and loss of contractile force (294). Reduction of fatty acid oxidation itself can be detrimental to the heart if high amounts of lipids accumulate to cause lipotoxicity, as in hearts deficient in carnitine palmitoyltransferase 1b which are sensitive to heart failure induced by pressure overload (281). Chronic use of glucose seems to be especially detrimental when fatty acids are also highly available (281). Therefore, the lack of fatty acid retention in *Acsl1*$^{T-/-}$ hearts, as evidenced by low uptake of 2-Br-[^{14}C]palmitate, may have protected the hearts from further dysfunction by limiting lipid accumulation.

mTORC1 is activated by signals of high nutrient availability, including insulin and related growth factors, adequate energy levels, and amino acids (295). It is inhibited by signals of low energy status such as activated AMPK. Because *Acsl1*$^{T-/-}$ hearts are unable to oxidize fatty acids, it might be expected that these hearts would fail to produce enough energy to sustain life. However,

Acsl1$^{T-/-}$ hearts increase glucose use to compensate to the point where phosphorylated AMPK was actually lower than that measured in controls. Diminished phospho-AMPK enhances mTORC1 activation, and the markedly increased use of glucose may also contribute. In isolated, perfused working hearts, mTOR is activated when the rate of glucose uptake exceeds oxidation and causes the metabolite glucose-6-phosphate to accumulate (264). Metabolism of glucose to glucose-6-phosphate is also required for insulin-mediated activation of mTORC1 (265), suggesting a mechanism by which cells sense the amount of glucose available to produce energy. Because *Acsl1*$^{T-/-}$ hearts take up 8-fold more 2-deoxyglucose and contain 3 times more glucose-6-phosphate than controls (87), the switch to a high rate of glucose metabolism is likely to underlie to the activation of mTORC1 in *Acsl1*$^{T-/-}$ hearts. Rapamycin treatment does not modify fatty acid or glucose metabolism in hearts lacking ACSL1 (266), indicating that altered substrate metabolism did not contribute to rapamycin-induced normalization of mitochondrial structure and maximal respiration.

In the heart, mTORC1 activation is necessary for growth, and both global and cardiac-specific knockouts of mTOR are embryonic lethal (268,296). A temporal knockout of mTOR in adult heart demonstrated that mTOR is necessary for normal mitochondrial function, fatty acid oxidation, and heart contraction (270). However, the consequences of chronic mTORC1 hyper-activation in adult heart are less well understood. Overexpression of wild-type mTOR (297,298) or a constitutively-active mTOR (299) in the heart activates mTORC1 signaling pathways but does not stimulate heart enlargement, suggesting that another factor such as high pressure or excess energy availability is required for the development of hypertrophy. Pressure overload activates mTORC1, and this activation is necessary for overload-induced cardiac hypertrophy (300,301). Prolonged pressure overload causes heart failure and impaired mitochondrial oxidative phosphorylation (302). Thus, we aimed to determine whether chronic mTORC1 activation in the absence of pressure overload altered mitochondrial structure and function.

Treatment of *Acsl1*$^{T-/-}$ mice with rapamycin normalized mTORC1 signaling and heart size and relieved the block on autophagy. Autophagy is critical for turnover of damaged organelles, proteins, and lipid droplets in non-adipose tissues. This quality control process is indispensable in the heart, as impaired autophagy can trigger cell death during ischemia (303,304), cause a cardiomyopathy (305,306), and exacerbate overload-induced heart failure (307). Conversely, activation of autophagy protects cardiomyocytes from mitochondrial stress induced by antimycin A treatment (308). Regulation of autophagy, therefore, is critical to maintain normal heart function and the ability to adapt to stress. The high rate of autophagy that occurred after treating *Acsl1*$^{T-/-}$ mice with rapamycin suggests that chronically activated mTORC1 in these mice had inhibited autophagy. When mTORC1 activity was diminished for 1 week in *Acsl1*$^{T-/-}$ hearts, large numbers of autophagic vacuoles were observed. After 2 weeks of rapamycin treatment, the number of mitochondria decreased to that of control animals, fewer abnormal mitochondria were observed, and the maximal respiration rate was normalized, indicating that the high autophagic rate after rapamycin treatment cleared the damaged mitochondria.

Whereas mTORC1 inhibition normalized maximal respiration in the *Acsl1*$^{T-/-}$ mitochondria, the improved clearance of damaged mitochondria did not improve ADP-stimulated respiration. This continued impairment is likely due to a deficiency in ATP synthase activity. The ATP synthase complex produces ~ 95% of cellular ATP, using the proton gradient formed by the rest of the electron transport chain (167). The proteins of the ATP synthase complex undergo numerous post-translational modifications that can be altered by energy status or oxidative stress; these modifications can affect both the formation of the complex and its activity (309-312). One recent example is inhibition of ATP synthase by acetylation in the absence of the mitochondrial deacetylase sirtuin 3, which is activated by NAD^+ (310), showing that alterations in energy status can influence ATP synthase activity. Despite low ATP synthase activity in *Acsl1*$^{T-/-}$ hearts, however, AMPK activation is lower than in controls and ATP content is normal (87), suggesting that these hearts are able to

produce sufficient energy. In addition to complete oxidation of glucose, *Acsl1*$^{T-/-}$ hearts may also partially offset the deficit through both enhanced glycolysis and by the use of amino acids to obtain sufficient energy despite impaired mitochondrial function.

In *Acsl1*$^{T-/-}$ hearts, high glucose use caused chronic mTORC1 activation, which inhibits autophagy and is detrimental to mitochondrial structure and maximal respiration capacity, but not to contractile function of the heart (**Fig 3.7**). Low ATP synthase activity coupled with impaired maximal respiration suggests that *Acsl1*$^{T-/-}$ hearts were able to use glycolysis to augment ATP production. Surprisingly, the defect in cardiac respiratory function does not diminish longevity or systolic function in unstressed *Acsl1*$^{T-/-}$ mice (87). Under the stress of pressure overload, however, excessive reliance on glucose could prove to be incompatible with normal systolic function. It will be of interest to determine if inhibiting mTORC1 can improve the response to these stresses in *Acsl1*$^{T-/-}$ hearts.

Figures

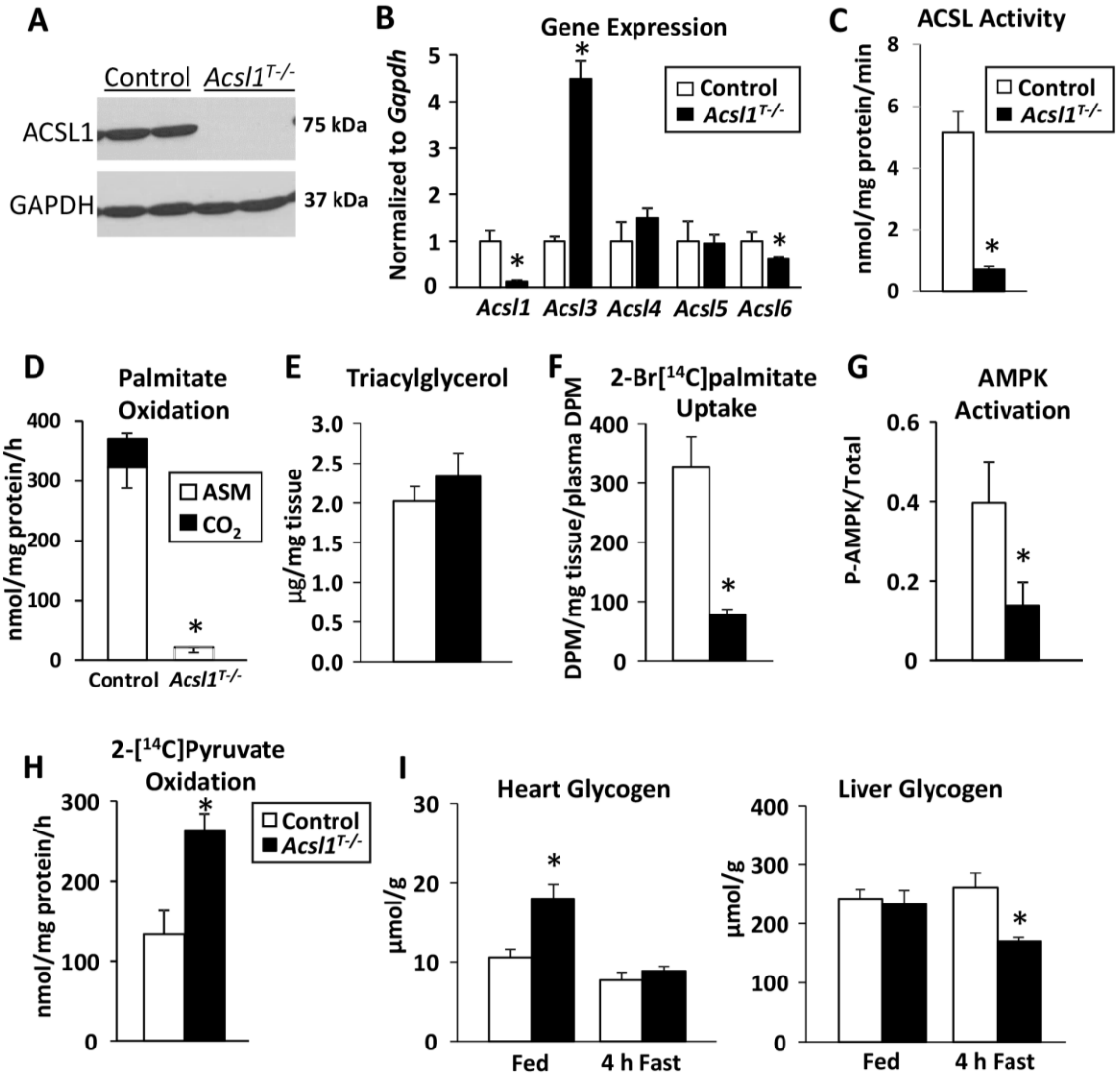

Figure 3.1. Loss of cardiac ACSL1 decreased fatty acid use and increased the use of glucose. **A)** ACSL1 protein in ventricles 20 weeks after tamoxifen-induced knockout of *Acsl1*. **B)** Gene expression in ventricles (n=6). **C)** ACSL specific activity in ventricular membranes (n=3). **D)** [1-^{14}C]palmitate oxidation to CO_2 or acid-soluble metabolites (ASM) in isolated cardiac mitochondria (n=4). **E)** Triacylglycerol content in ventricles (n=5). **F)** *In vivo* 2-Br-[1-^{14}C]palmitate uptake in ventricles (n=5). **G)** Phosphorylated AMPK relative to total AMPK in ventricles (n=4-5). **H)** [2-^{14}C]pyruvate oxidation to CO_2 in isolated cardiac mitochondria (n=5). **I)** Tissues were collected from female mice 10 weeks after tamoxifen at 7 am (fed), or at 11am after 4 h of fasting (fasting). Glucose from glycogen was measured after acid hydrolysis (n=4). *p-value<0.05

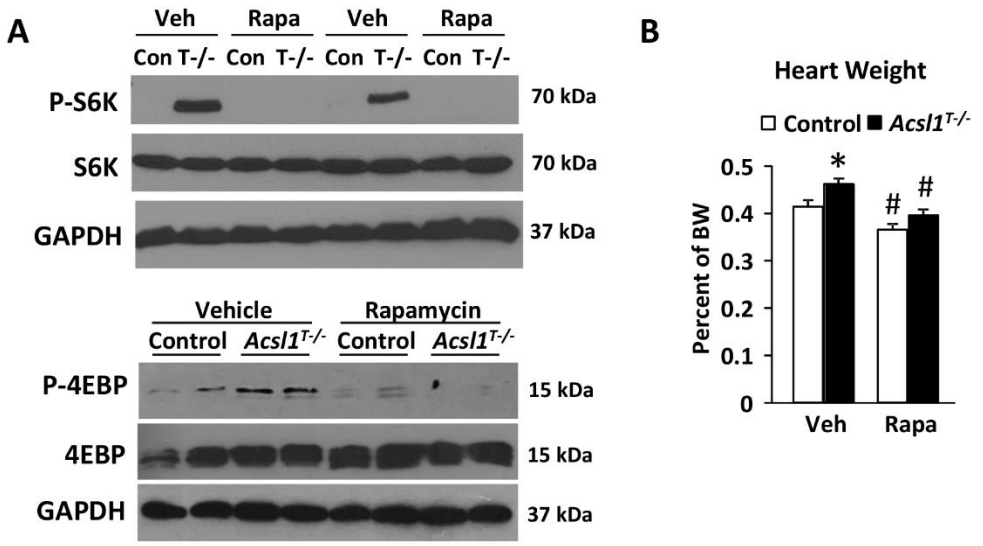

Figure 3.2. Two weeks of rapamycin treatment inhibited mTORC1 activation in *Acsl1*$^{T-/-}$ hearts. Control and *Acsl1*$^{T-/-}$ mice were treated with vehicle or 1 mg/kg rapamycin daily for 2 weeks. **A)** Representative immunoblot of phosphorylation of mTORC1 targets, S6K and 4E-BP1, in ventricles. **B)** Heart weight normalized to body weight (n=5-8). *p-value<0.05 comparing genotype. #p-value<0.05 comparing treatment.

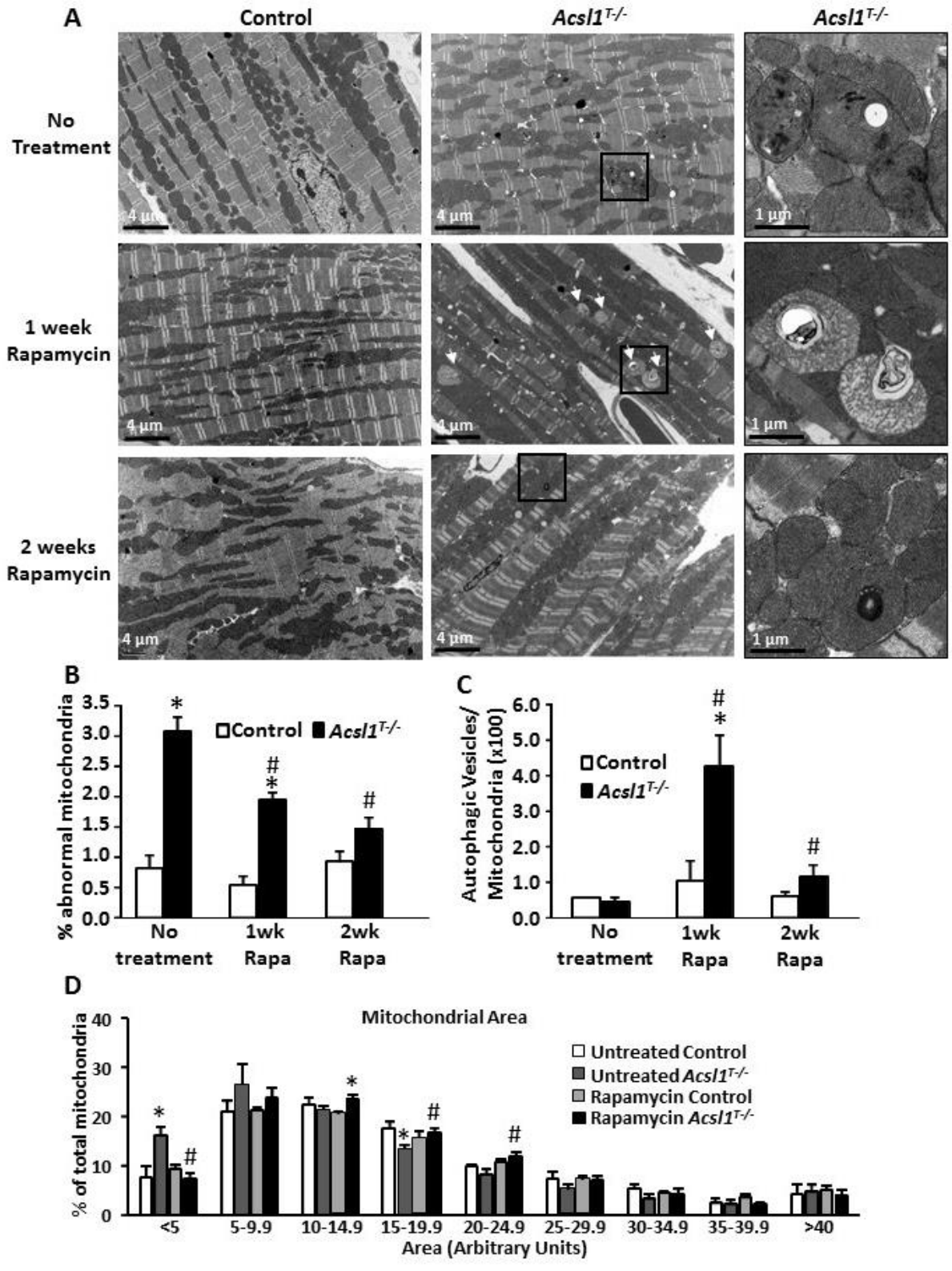
A
Control
Acsl1T-/-
Acsl1T-/-
No Treatment
1 week Rapamycin
2 weeks Rapamycin
4 µm
1 µm
B
% abnormal mitochondria
Control
Acsl1T-/-
No treatment
1wk Rapa
2wk Rapa
C
Autophagic Vesicles/ Mitochondria (x100)
Control
Acsl1T-/-
No treatment
1wk Rapa
2wk Rapa
D
Mitochondrial Area
% of total mitochondria
Untreated Control
Untreated Acsl1T-/-
Rapamycin Control
Rapamycin Acsl1T-/-
<5
5-9.9
10-14.9
15-19.9
20-24.9
25-29.9
30-34.9
35-39.9
>40
Area (Arbitrary Units)

Figure 3.3. mTORC1 inhibition improved mitochondrial structure in *Acsl1*$^{T-/-}$ hearts. A) Representative electron microscopy images of left ventricles for untreated mice and mice treated daily with rapamycin for 1 or 2 weeks. 5000x or 20,000x magnification. White arrows indicate autophagic vesicles. **B)** Abnormal mitochondria in untreated mice or mice treated with rapamycin for 1 or 2 weeks relative to total mitochondria (n=3). Abnormal mitochondria were defined as those containing vacuoles, inclusions, or disrupted cristae. **C)** Number of autophagic vesicles relative to number of mitochondria in untreated mice or mice treated with rapamycin for 1 or 2 weeks (n=3). **D)**Mitochondrial area (n=3).Mitochondrial area was quantified using ImageJ software for at least 1000 mitochondria per heart (4-7 images). *p-value<0.05 comparing genotype. #p-value<0.05 comparing treatment.

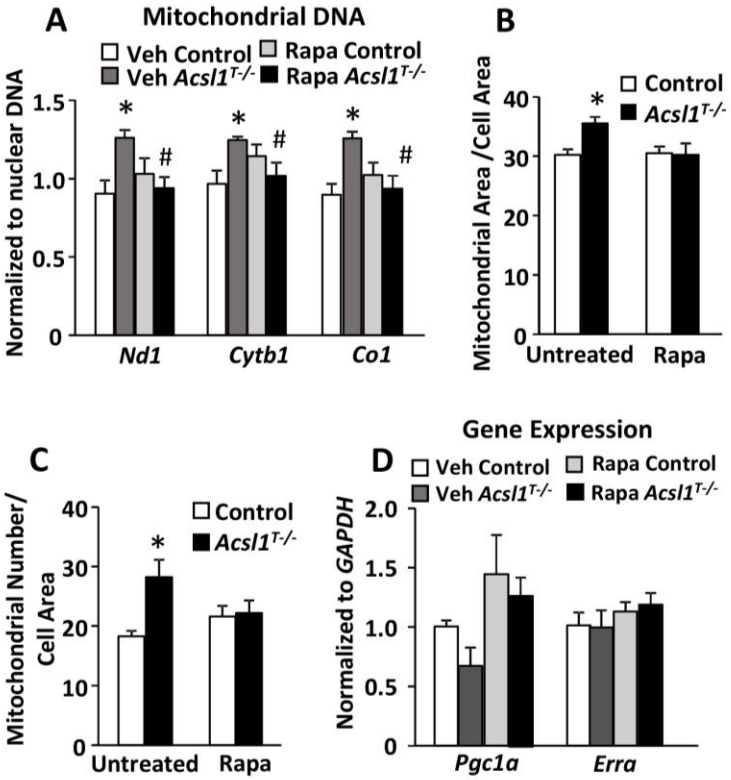

Figure 3.4. Rapamycin treatment normalized high mitochondrial number in *Acsl1*$^{T-/-}$ hearts. Control and *Acsl1*$^{T-/-}$ mice were treated with vehicle or rapamycin daily for 2 weeks. **A)** Mitochondrial DNA normalized to the nuclear gene *H19* (n=8). **B)** Number of mitochondria per cell area (n=3). **C)** Mitochondrial area per cellular area (n=3).Mitochondrial number and area were quantified using ImageJ software for at least 1000 mitochondria per heart (4-7 images). **D)** mRNA expression of genes controlling mitochondrial biogenesis (*Pgc1a, Erra*) (n=4). *p-value<0.05 comparing genotype. #p-value<0.05 comparing treatment.

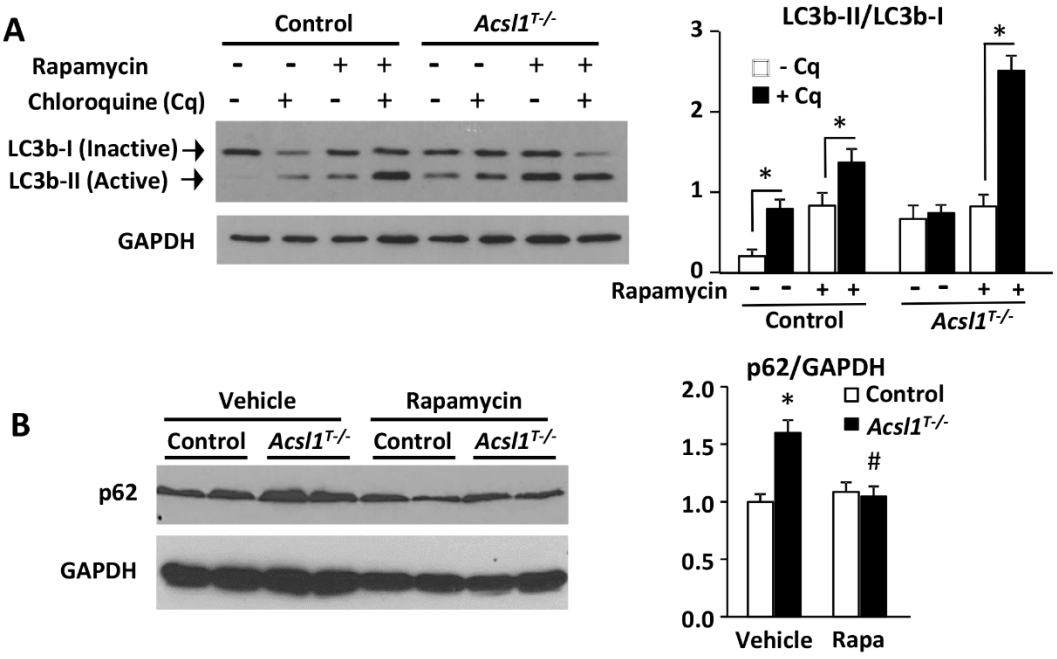

Figure 3.5. Inhibition of mTORC1 activated autophagy in *Acsl1*$^{T-/-}$ hearts. A) Control and *Acsl1*$^{T-/-}$ mice were treated with vehicle or rapamycin for 14 d and vehicle or 60 mg/kg body weight chloroquine, a lysosome inhibitor, for the last 7 d (n=4). Representative immunoblot of LC3b-I and LC3b-II (n=4). **B)** p62 protein in ventricles from mice treated with vehicle or rapamycin for 2 weeks (n=4). *p-value<0.05 comparing genotype. #p-value<0.05 comparing treatment.

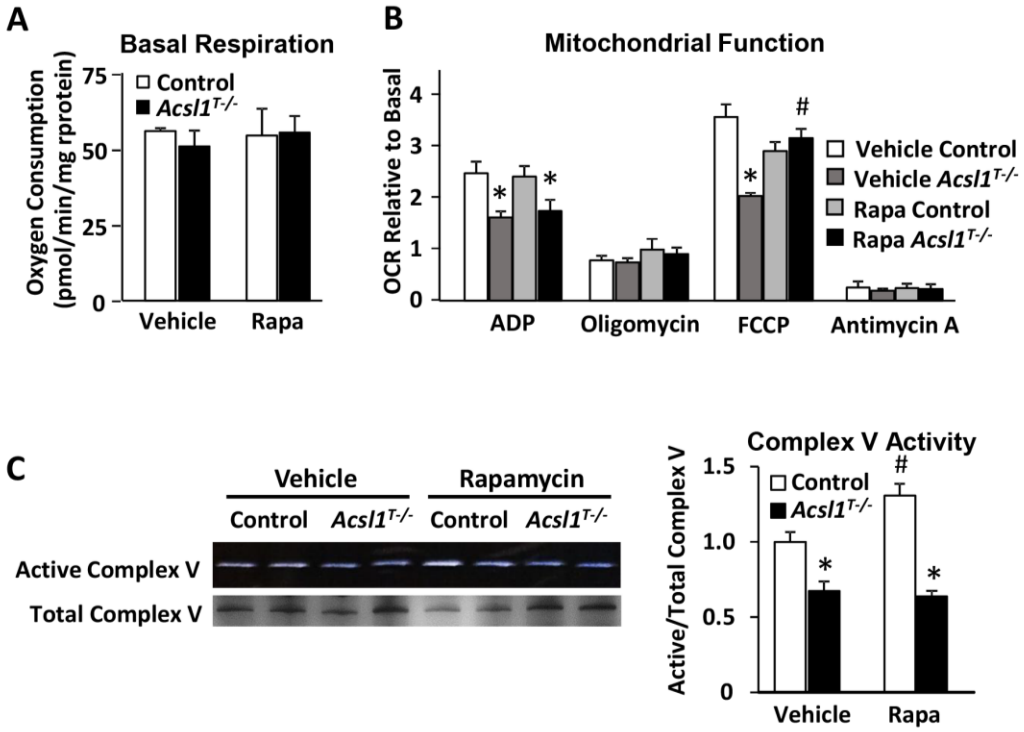

Figure 3.6. Rapamycin treatment partially normalized mitochondrial function in *Acsl1*$^{T-/-}$ hearts. Control and *Acsl1*$^{T-/-}$ mice were treated with vehicle or rapamycin daily for 2 weeks. **A-B)** Mitochondrial function was measured in isolated mitochondria using a Seahorse XF24 Analyzer, which sequentially injected ADP, oligomycin, FCCP, and antimycin A (n=4-5). O_2 consumption rate: OCR. **C)** Mitochondrial complexes were separated by native electrophoresis and stained for either complex V (ATP synthase) activity or total complex V (n=4). *p-value<0.05 comparing genotype. #p-value<0.05 comparing treatment.

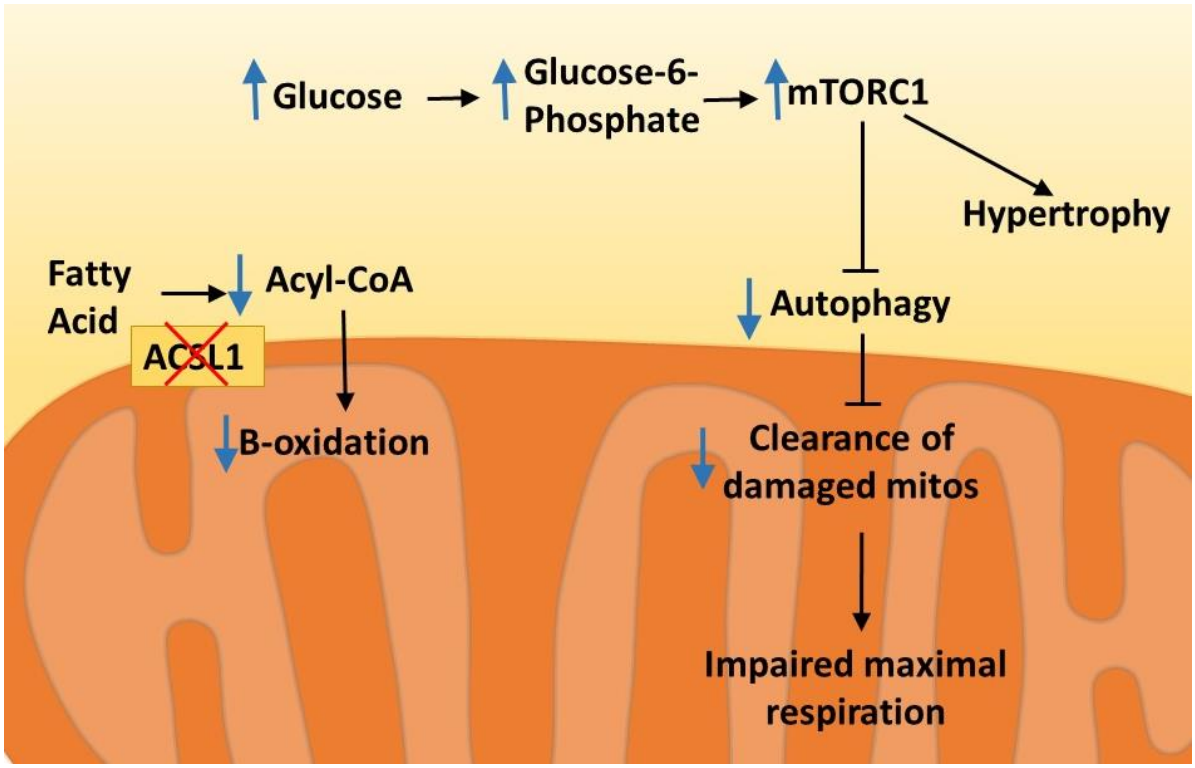

Figure 3.7. Proposed pathway for how loss of ACSL1 causes impaired maximal respiration. Loss of ACSL1 in the heart prevents activation of fatty acids for β-oxidation. Consequently, glucose metabolism increases 8-fold, thus increasing the glucose-6-phosphate concentration in the cell. Glucose-6-phosphate activates mTORC1, causing hypertrophy and inhibiting autophagy. Inhibition of autophagy prevents clearance of damaged mitochondria, thus impairing maximal respiration. ADP-stimulated oxygen consumption was not improved with rapamycin treatment and was likely due to impaired complex V activity. The cause of loss of ATP synthase activity is unknown.

CHAPTER 4: SYNTHESIS

Overview of findings

This dissertation demonstrates the importance of ACSL1 in several aspects of cardiac mitochondrial health, including respiratory function, lipid synthesis and remodeling, and clearance of damaged mitochondria. This work determined that loss of ACSL1 impaired oxygen consumption in cardiac muscle fibers and isolated mitochondria. To define the cause of the respiratory dysfunction, we examined two important factors in mitochondrial health: phospholipids of the membrane and clearance of damaged mitochondria. Loss of ACSL1 caused large changes in the length and degree of unsaturation of the acyl chains of PC, PE, PI, and cardiolipin. Because cardiolipin (CL) is necessary for formation of the electron transport chain complexes and other mitochondrial functions, we focused on this mitochondrial lipid. ACSL1-deficient hearts had a lower amount of the major CL species, which is thought to be important in maintaining heart and mitochondrial functions, but normal total CL amount. Systolic function of the heart was not compromised by reduction in tetralinoleoyl-CL, indicating that this species is not integral to heart function. By altering the expression of ACSL1 in H9c2 and HEK293 cells, we determined that ACSL1 is sufficient to preferentially increase linoleate incorporation into cardiolipin. When *Acsl1*$^{T-/-}$ mice were fed a diet that contained 75% of its fatty acids as linoleate, the amount of linoleate in cardiolipin was normalized, but mitochondrial respiratory function remained impaired. This finding indicated a different cause of the mitochondrial dysfunction found in the ACSL1-deficient hearts.

Because loss of ACSL1 also impaired fatty acid oxidation, we set out to determine how the drastic change in metabolism to force glucose use affected mitochondrial health. Glucose metabolism to glucose-6-phosphate can activate mTORC1, and glucose-6-phosphate is elevated in *Acsl1*$^{T-/-}$ hearts (87). Activation of mTORC1 inhibits formation of the autophagosome, thus impairing mitochondrial

clearance. In *Acsl1*$^{T-/-}$ hearts, low clearance of damaged mitochondria caused an accumulation of mitochondria that were both structurally and functionally abnormal. With pharmacologic inhibition of mTORC1 *in vivo*, the autophagic rate increased greatly, mitochondrial number and structure were normalized, and maximal respiratory capacity was improved. Only ADP-stimulated oxygen consumption was not improved in the *Acsl1*$^{T-/-}$ hearts, and this impairment was likely caused by modification of complex V which inhibited its activity. We concluded that chronic high glucose metabolism activated mTORC1, which inhibited autophagy, preventing clearance of damaged mitochondria. This information points to the importance of maintaining metabolic flexibility in the heart.

Public Health Significance

ACSL1 is highly expressed in many tissues, including heart, skeletal muscle, and adipose tissue in mouse. Highly overexpressing ACSL1 causes heart failure due to lipid accumulation, and loss of ACSL1 impairs fatty acid oxidation, causes hypertrophy, and diminishes exercise capacity. Pharmacologically activating or inhibiting ACSL1 would likely be highly detrimental.

ACSL1 has been implicated in the development of metabolic syndrome because of its role in fatty acid metabolism. A single nucleotide polymorphism (SNP) in the *ACSL1* gene increases the likelihood of developing metabolic syndrome in a middle-aged European population (313). However, the increased risk is diminished by a low fat diet or a diet high in polyunsaturated fatty acids (PUFAs). High ACSL1 expression in adipose tissue from aged Swedish males correlates with decreased risk for insulin resistance markers and is associated with a lower amount of saturated fatty acids stored in adipose tissue (314). A genome-wide association study examining the response to exercise training in a Caucasian and African American population found that an *ACSL1* SNP was positively associated with improved exercise performance (315). Further investigation into how these SNPs affect ACSL1 activity and expression is needed. Effects of these SNPs on heart function should also be determined, as increasing or decreasing ACSL1 expression can have large effects on the

metabolism of the heart. For instance, based on the current work, a SNP that diminished ACSL1 expression or activity in the heart could cause mitochondrial respiratory defects and predispose the hearts to failure.

Analysis of hearts lacking ACSL1 caused us to question the importance of the acyl-chain composition of CL. ACSL1-deficient hearts contain normal total CL, but 83% less tetralinoleoyl-CL, a species that has been thought to be important in mitochondrial function and heart function. *Acsl1*$^{T-/-}$ hearts contract normally, and normalizing the amount of tetralinoleoyl-CL did not improve mitochondrial function. Therefore, research on diseases with low CL, such as Barth syndrome, heart failure, and age-related mitochondrial dysfunction, should focus on increasing the total amount of CL, instead of just the tetralinoleoyl-CL.

The presented research also showed that chronic mTORC1 activation can impair mitochondrial respiratory capacity through diminished clearance of damaged mitochondria. mTORC1 is activated in pathologies, such as hypertension., in which the heart becomes enlarged. Because damaged mitochondria are not efficiently cleared with mTORC1 activation, care needs to be taken in treatment of these patients to prevent excess stress and damage to the mitochondria. This dissertation also showed the importance of maintaining cardiac metabolic flexibility, as chronic glucose use activates mTORC1, which can exacerbate preexisting defects.

Future Directions

Overexpression of ACSL1 in tafazzin- or MLCL AT1- deficient cells

To determine if ACSL1 activates linoleate for direct incorporation into CL or if linoleate must be transacylated from a donor phospholipid, ACSL1 should be overexpressed in cells lacking the transacylase tafazzin or the acyltransferase MLCL AT-1. If ACSL1 is able to increase linoleate incorporation in the tafazzin-deficient cells, but not the MLCL AT-1 deficient cells, we could conclude that ACSL1 is important for the direct incorporation of linoleoyl-CoA into CL. The converse is also possible, which would implicate ACSL1 as important for activating linoleate first for

incorporation into a phospholipid which would then donate it to CL. The experiment could be performed in cell culture, as many stable knockdowns of tafazzin exist, and the knockdown of MLCL AT-1 has been characterized in HeLa cells. These experiments should be performed in a cardiomyocyte or myocyte cell line, such as H9c2 cells or C2C12 cells.

In the tafazzin knockdown heart, mitochondrial ACSL1 is diminished by 68% whereas ACOT13 and ACOT2 are nearly 2-fold higher (316). A preliminary study in our lab, using tissue donated by Matthew Gillum, showed 20% lower ACSL specific activity in tafazzin knockdown hearts (controls: 8.1 ± 0.2 vs tafazzin knockdown: 6.4 ± 0.5 nmol/mg protein/min). Thus, low ACSL activity coupled with high ACOT activity could cause a deficiency of acyl-CoAs that could contribute to impaired CL remodeling seen in the tafazzin-deficient hearts (261). To determine if low acyl-CoA content is partially responsible for the phenotype, tafazzin-knockdown mice could be crossed with mice overexpressing ACSL1 in the heart (159). Using a model of moderate ACSL1 overexpression will prevent lipotoxicity. CL content and species, heart function, and mitochondrial function could be examined to determine if overexpression of ACSL1 can improve these measures in tafazzin-deficient animals.

Effect of loss of ACSL1 on phospholipids in non-cardiac tissues

ACSL1 is the major contributor of acyl-CoA synthetase activity in skeletal muscle, liver, and adipose tissue. Loss of ACSL1 impairs fatty acid oxidation in these tissues, but ACSL1 deficiency may also affect acyl chain composition of the phospholipids in these tissues. It will be especially important to determine if loss of ACSL1 alters the phospholipid species in skeletal muscle. Similar to heart, skeletal muscle normally contains a high proportion of linoleate in CL. If formation of linoleoyl-CoA at the mitochondria determines how much linoleate gets remodeled into CL, then ACSL1-deficient skeletal muscle should also be deficient in tetralinoleoyl-CL. Several caveats exist for this hypothesis, however. In heart, ACSL activity is about 8-fold higher than in skeletal muscle. Despite ACSL1 being the major isoform in both tissues, this disparity in total activity may affect the

rate of activation of fatty acids for phospholipid synthesis and remodeling. Another factor to consider is the age at which ACSL1 is lost from the tissue. In the current studies, we examined hearts in which ACSL1 was lost in fully developed adult heart. Use of a model in which ACSL1 is knocked out in skeletal muscle before birth may provide different results caused by compensation by other ACSL isoforms or in adaptation of the cell to the changes in metabolism. Whereas the heart is constantly beating, the mice used for most studies are sedentary, so the metabolic rate, and thus reactive oxygen species formation and CL damage, are lower. This low metabolic rate may diminish the need for turnover of CL and linoleate acyl chains and minimize a difference between controls and ACSL1-deficient muscle. Analysis of muscle from mice allowed access to running wheels should be considered. Finally, the heart muscle is highly oxidative, whereas skeletal muscle exhibits degrees of oxidative capacity depending on fiber type. Therefore, the role of ACSL1 in these tissues may vary, and the need for linoleate in CL remodeling may also vary. Despite these potential confounders, it will be important to determine if and how ACSL1 affects phospholipid synthesis and remodeling in skeletal muscles. This information could confirm that ACSL1 is important for CL remodeling in non-cardiac tissues, and thus may be important in diseases with impaired CL remodeling, such as Barth syndrome, heart failure, and age-related mitochondrial dysfunction.

Effects of altered phospholipid acyl chains

This dissertation focused on the effect of ACSL1 deficiency on the acyl chains of mitochondrial CL. The effects of altering the saturation and length of acyl chains of other phospholipids should be investigated in mitochondria and other organelles. Alterations in saturation and chain length of fatty acids incorporated into membrane lipids can change membrane dynamics, movement of substrates and solutes across membranes, and lipid raft composition (229-231). Thus, permeability of the plasma membrane and mitochondrial membranes should be investigated. Permeability of the plasma membrane can be measured *in vivo* using Evans Blue dye which will enter cells when the plasma membrane is compromised. Several dyes are available to measure the

mitochondrial permeability transition, such as JC-1 and TMRM, but these would need to be used *in vitro*.

Because large changes were seen in PI species, signaling pathways that use PI-(4,5) bisphosphate (PIP_2) or PI-(3,4,5) triphosphate (PIP_3) should be examined. PIP_2 regulates many membrane proteins, including ion channels, transporters, and receptors, but little is known about the importance of the acyl-chain composition of its major species. The conversion of PIP_2 to PIP_3 activates Akt, which mediates insulin signaling to regulate growth and energy storage. Insulin signaling in ACSL1-deficient hearts should be measured using an *ex vivo* perfusion system, Langendorff perfusion, in which the heart is still beating. Attempting to measure insulin signaling *in vivo* led to variable results, probably because of the stress on the animals. The Langendorff perfusion system eliminates the stress and differences in endogenous insulin or blood metabolites. However, because the $Acsl1^{T-/-}$ hearts exhibit many changes in phospholipids, it may be difficult to tease out the effects of a specific change. Therefore, it will be important to find dietary, chemical, or genetic interventions that can normalize specific phospholipids to eliminate some of the variables and allow more decisive conclusions to be made. For instance, a diet high in DHA may help to normalize PC and PE species in the $Acsl1^{T-/-}$ hearts. Providing DHA to $Acsl1^{T-/-}$ hearts would bypass the need to synthesize DHA from linoleate, which is likely compromised in $Acsl1^{T-/-}$ hearts.

Fatty acid preference in purified ACSL1 vs. tissue ACSL1

This work shows that murine cardiac ACSL1 strongly prefers to activate linoleate. However, no preference for linoleate is found when recombinant rat ACSL1 protein is purified using a bacterial system. One potential cause is that the cardiac ACSL1 is in membranes, whereas purified ACSL1 would be in solution, which may alter the protein's structure in such a way as to alter the fatty acid binding site. Measuring ACSL activity with purified enzyme in the presence of phospholipids or liposomes is one potential way to determine if incorporation of ACSL1 into membranes alters its preference for linoleate. Another possible cause of the discrepancy in fatty acid preference is that

bacteria do not phosphorylate or acetylate ACSL1 in the same way as mammalian cells. ACSL1 has many potential sites of post-translational modifications, and some of these modifications can alter ACSL activity (111). Other modifications could potentially alter fatty acid preference by altering the shape of the fatty acid binding pocket. Modification of these sites to either mimic or prevent post-translational modification would allow the analysis of fatty acid preference.

Complex V activity in Acsl1$^{T-/-}$ hearts

Inhibition of mTORC1 was unable to normalize ADP-stimulated oxygen consumption and complex V activity. The ATP synthase complex has multiple sites for post-translational modifications, such as acetylation and phosphorylation that can be altered by energy status or oxidative stress. These modifications can affect both the formation of the complex and its activity (309-312). Post-translational modifications of complex V can be measured by mass spectrometry after separation of complexes by native electrophoresis. The modifications can be compared between control and *Acsl1*$^{T-/-}$hearts, and then differences can be linked to known modifications of complex V. An example of modifications affecting complex V activity is the inhibition of ATP synthase by acetylation in the absence of the mitochondrial deacetylase sirtuin 3, which is activated by NAD^+ (310). An inhibition of mitochondrial oxidative phosphorylation in the *Acsl1*$^{T-/-}$hearts may cause an accumulation of mitochondrial NADH, as in ischemia (317), causing impaired deacetylase activity (318). Measurement of NADH and NAD^+ in *Acsl1*$^{T-/-}$hearts has previously shown a high amount of variability between animals, so this measurement needs to be repeated with freeze-clamped hearts to prevent loss of NADH. Sirtuin activity could also be measured directly using commercially available kits. Inhibition of sirtuins in the *Acsl1*$^{T-/-}$hearts could predispose the hearts to damage by reactive oxygen species and apoptosis (319).

mTORC1 activation in Acsl1$^{T-/-}$ hearts

Loss of ACSL1 impairs cardiac fatty acid oxidation, causing increased glucose use. Glucose metabolism to glucose-6-phosphate can activate mTORC1, but there are many other activators of

mTORC1, such as insulin, amino acids, and low activation of AMPK. Future studies should confirm that glucose metabolism is the actual activator of mTORC1 in *Acsl1*$^{T-/-}$ hearts. Providing a different substrate, such as medium chain fatty acids, which can be used by *Acsl1*$^{T-/-}$ hearts, may help determine if mTORC1 is activated by high glucose-6-phosphate.

ACSL1 and FA channeling

We have hypothesized that ACSLs are able to channel their acyl-CoA products to specific pathways, such as β-oxidation or glycerolipid synthesis. Previous evidence showed that ACSL1 is necessary for β-oxidation in heart, skeletal muscle, and adipose tissue (87,105,228,320). My dissertation shows that ACSL1 also plays a role in activation of fatty acids for glycerolipid synthesis and remodeling. This information could point to a lack of acyl-CoA channeling by ACSL1, especially because ACSL1 accounts for 90% of total ACSL specific activity. However, ACSL1 is present on multiple organelles, including the ER and mitochondria in liver. It is likely that the localization to multiple organelles is also present in the heart. Thus, ER-localized ACSL1 could interact with enzymes of glycerolipids synthesis and activate fatty acids for incorporation into more complex lipids. Similarly, mitochondrial ACSL1 interacts with VDAC and CPT1a and may activate fatty acids for import into the mitochondria. Independent of protein-protein interactions, ACSL1 may increase the concentration of acyl-CoAs immediately around the organelle in which it is located. Work is currently being performed in our lab to determine which proteins ACSL1 interacts with under conditions to induce either β-oxidation or glycerolipid synthesis. Use of these different conditions will allow us to determine if ACSL1's protein-protein interactions can be altered by energy demands of the cell.

My previous work targeted ACSL1 to the ER or to the mitochondria by replacing the transmembrane domain of the enzyme, because no clear targeting sequence is known. However, these targeted proteins were unable to increase glycerolipid synthesis or β-oxidation to the same extent as wild-type ACSL1, indicating that the targeted proteins were not able to efficiently get the acyl-CoA

product into the downstream pathways. This finding is likely to have occurred because replacing the N-terminus and transmembrane domain altered protein-protein interactions. Future studies should determine the regions of the protein that target the protein to a specific organelle. This information would allow mutation of specific amino acids, instead of removing entire regions of the protein, to target ACSL1 to either the ER or the mitochondria.

ACSL1 in heart maturation

Within days after birth, a number of major metabolic changes occur in the mouse heart. Fatty acid oxidation becomes the dominant source of energy, and membranes change to increase more linoleate and DHA. At this same time, ACSL1 expression increases 2.5-fold. Current models cause loss of ACSL1 in adult hearts. ACSL1 may be necessary for the transition of the heart from fetal metabolism to the adult phenotype. The ability to use fatty acids for energy may be important as the newborn transitions through the early period of starvation after birth. Similarly, if mTORC1 is activated by ACSL1 deficiency, autophagy would be impaired, and this autophagy is necessary for energy production during the early period of starvation. Similarly, the change to more unsaturated acyl chains in the membrane phospholipids maybe important for development. Use of a *Cre* driven by a promoter that is turned on *in utero* would eliminate the *Acsl1* gene before the large increase in its expression after birth. This kind of early knockout would allow the study of viability of the animals as well as heart function when the heart cannot switch from glucose to fatty acid use or remodel membranes to contain unsaturated acyl chains.

Cardiomyocyte differentiation and growth could also be measured in the H9c2 cardiomyocyte-like cells with ACSL1 knocked down. A hallmark of cultured cells and cancer cells is a high use of glucose, suggesting that glucose use is optimal for growth. The studies presented in this dissertation showed an 80% decrease in fatty acid oxidation with ACSL1 deficiency. Examining cell morphology and differentiation markers at several points during differentiation would help to determine if the switch to fatty acid oxidation is necessary for cardiomyocyte differentiation.

LITERATURE CITED

1. Grevengoed, T. J., Klett, E. L., and Coleman, R. A. (2014) Acyl-CoA metabolism and partitioning. *Annu Rev Nutr.* **34**, 1-30

2. Watkins, P. A., Maiguel, D., Jia, Z., and Pevsner, J. (2007) Evidence for 26 distinct acyl-coenzyme A synthetase genes in the human genome. *J. Lipid Res.* **48**, 2736-2750

3. Watkins, P. A. (2008) Very-long-chain acyl-CoA synthetases. *J. Biol. Chem.* **283**, 1773-1777

4. Lerner, E., Shug, A. L., Elson, C., and Shrago, E. (1972) Reversible inhibition of adenine nucleotide translocation by long chain fatty acyl coenzyme A esters in liver mitochondria of diabetic and hibernating animals. *J. Biol. Chem.* **247**, 1513-1519

5. Shug, A., Lerner, E., Elson, C., and Shrago, E. (1971) The inhibition of adenine nucleotide translocase activity by oleoyl CoA and its reversal in rat liver mitochondria. *Biochem Biophys Res Commun.* **43**, 557-563

6. Tippett, P. S., and Neet, K. E. (1982) Specific inhibition of glucokinase by long chain acyl coenzymes A below the critical micelle concentration. *J. Biol. Chem.* **257**, 12839-12845

7. Nikawa, J., Tanabe, T., Ogiwara, H., Shiba, T., and Numa, S. (1979) Inhibitory effects of long-chain acyl coenzyme A analogues on rat liver acetyl coenzyme A carboxylase. *FEBS Lett.* **102**, 223-226

8. Ogiwara, H., Tanabe, T., Nikawa, J., and Numa, S. (1978) Inhibition of rat-liver acetyl-coenzyme-A carboxylase by palmitoyl-coenzyme A. Formation of equimolar enzyme-inhibitor complex. *Eur. J. Biochem.* **89**, 33-41

9. Lehrer, G., Panini, S. R., Rogers, D. H., and Rudney, H. (1981) Modulation of rat liver 3-hydroxy-3-methylglutaryl coenzyme A reductase by lipid inhibitors, substrates, and cytosolic factors. *J. Biol. Chem.* **256**, 5612-5619

10. Jepson, C. A., and Yeaman, S. J. (1992) Inhibition of hormone-sensitive lipase by intermediary lipid metabolites. *FEBS Lett.* **310**, 197-200

11. Newman, C. M., and Magee, A. I. (1993) Posttranslational processing of the ras superfamily of small GTP-binding proteins. *Biochim. Biophys. Acta* **1155**, 79-96

12. Pfanner, N., Glick, B. S., Arden, S. R., and Rothman, J. E. (1990) Fatty acylation promotes fusion of transport vesicles with Golgi cisternae. *J. Cell Biol.* **110**, 955-961

13. Hsu, K. H., and Powell, G. L. (1975) Inhibition of citrate synthase by oleoyl-CoA: a regulatory phenomenon. *Proc. Natl. Acad. Sci. U. S. A.* **72**, 4729-4733

14. Smith, R. H., and Powell, G. L. (1986) The critical micelle concentration of some physiologically important fatty acyl-coenzyme A's as a function of chain length. *Arch. Biochem. Biophys.* **244**, 357-360

15. Constantinides, P. P., and Steim, J. M. (1985) Physical properties of fatty acyl-CoA. Critical micelle concentrations and micellar size and shape. *J Biol Chem.* **260**, 7573-7580

16. Banhegyi, G., Csala, M., Mandl, J., Burchell, A., Burchell, B., Marcolongo, P., Fulceri, R., and Benedetti, A. (1996) Fatty acyl-CoA esters and the permeability of rat liver microsomal vesicles. *Biochem J.* **320 (Pt 1)**, 343-344

17. Soupene, E., and Kuypers, F. A. (2008) Mammalian long-chain acyl-CoA synthetases. *Exp. Biol. Med. (Maywood)* **233**, 507-521

18. Fullekrug, J., Ehehalt, R., and Poppelreuther, M. (2012) Outlook: membrane junctions enable the metabolic trapping of fatty acids by intracellular acyl-CoA synthetases. *Front. Physiol.* **3**, 401

19. Gimeno, R. E. (2007) Fatty acid transport proteins. *Curr Opin Lipidol.* **18**, 271-276

20. Mashek, D. G., and Coleman, R. A. (2006) Cellular fatty acid uptake: the contribution of metabolism. *Curr Opin Lipidol.* **17**, 274-278

21. Black, P. N., and DiRusso, C. C. (2003) Transmembrane movement of exogenous long-chain fatty acids: proteins, enzymes, and vectorial esterification. *Microbiol Mol Biol Rev.* **67**, 454-472

22. Smathers, R. L., and Petersen, D. R. (2011) The human fatty acid-binding protein family: evolutionary divergences and functions. *Hum Genomics.* **5**, 170-191

23. Storch, J., and Thumser, A. E. (2010) Tissue-specific functions in the fatty acid-binding protein family. *J. Biol. Chem.* **285**, 32679-32683

24. Haunerland, N. H., and Spener, F. (2004) Fatty acid-binding proteins--insights from genetic manipulations. *Prog Lipid Res.* **43**, 328-349

25. Rolf, B., Oudenampsen-Kruger, E., Borchers, T., Faergeman, N. J., Knudsen, J., Lezius, A., and Spener, F. (1995) Analysis of the ligand binding properties of recombinant bovine liver-type fatty acid binding protein. *Biochim. Biophys. Acta* **1259**, 245-253

26. Martin, G. G., Danneberg, H., Kumar, L. S., Atshaves, B. P., Erol, E., Bader, M., Schroeder, F., and Binas, B. (2003) Decreased liver fatty acid binding capacity and altered liver lipid distribution in mice lacking the liver fatty acid-binding protein gene. *J. Biol. Chem.* **278**, 21429-21438

27. Newberry, E. P., Xie, Y., Kennedy, S., Han, X., Buhman, K. K., Luo, J., Gross, R. W., and Davidson, N. O. (2003) Decreased hepatic triglyceride accumulation and altered fatty acid uptake in mice with deletion of the liver fatty acid-binding protein gene. *J. Biol. Chem.* **278**, 51664-51672

28. Martin, G. G., Huang, H., Atshaves, B. P., Binas, B., and Schroeder, F. (2003) Ablation of the liver fatty acid binding protein gene decreases fatty acyl CoA binding

capacity and alters fatty acyl CoA pool distribution in mouse liver. *Biochemistry* **42**, 11520-11532

29. Gajda, A. M., Zhou, Y. X., Agellon, L. B., Fried, S. K., Kodukula, S., Fortson, W. M., Patel, K., and Storch, J. (2013) Direct comparison of mice null for liver- or intestinal fatty acid binding proteins reveals highly divergent phenotypic responses to high-fat feeding. *J. Biol. Chem.* **288**, 30330-30344

30. Coe, N. R., and Bernlohr, D. A. (1998) Physiological properties and functions of intracellular fatty acid-binding proteins. *Biochim Biophys Acta.* **1391**, 287-306

31. Makowski, L., and Hotamisligil, G. S. (2005) The role of fatty acid binding proteins in metabolic syndrome and atherosclerosis. *Curr Opin Lipidol.* **16**, 543-548

32. Coe, N. R., Simpson, M. A., and Bernlohr, D. A. (1999) Targeted disruption of the adipocyte lipid-binding protein (aP2 protein) gene impairs fat cell lipolysis and increases cellular fatty acid levels. *J Lipid Res.* **40**, 967-972

33. Hotamisligil, G. S., Johnson, R. S., Distel, R. J., Ellis, R., Papaioannou, V. E., and Spiegelman, B. M. (1996) Uncoupling of obesity from insulin resistance through a targeted mutation in aP2, the adipocyte fatty acid binding protein. *Science* **274**, 1377-1379

34. Daikoku, T., Shinohara, Y., Shima, A., Yamazaki, N., and Terada, H. (1997) Dramatic enhancement of the specific expression of the heart-type fatty acid binding protein in rat brown adipose tissue by cold exposure. *FEBS Lett.* **410**, 383-386

35. Yamashita, H., Wang, Z., Wang, Y., Segawa, M., Kusudo, T., and Kontani, Y. (2008) Induction of fatty acid-binding protein 3 in brown adipose tissue correlates with increased demand for adaptive thermogenesis in rodents. *Biochem Biophys Res Commun.* **377**, 632-635

36. Nakamura, Y., Sato, T., Shiimura, Y., Miura, Y., and Kojima, M. (2013) FABP3 and brown adipocyte-characteristic mitochondrial fatty acid oxidation enzymes are induced in beige cells in a different pathway from UCP1. *Biochem Biophys Res Commun.* **441**, 42-46

37. Erol, E., Cline, G. W., Kim, J. K., Taegtmeyer, H., and Binas, B. (2004) Nonacute effects of H-FABP deficiency on skeletal muscle glucose uptake in vitro. *Am J Physiol Endocrinol Metab.* **287**, E977-982

38. Shearer, J., Fueger, P. T., Bracy, D. P., Wasserman, D. H., and Rottman, J. N. (2005) Partial gene deletion of heart-type fatty acid-binding protein limits the severity of dietary-induced insulin resistance. *Diabetes* **54**, 3133-3139

39. Vergnes, L., Chin, R., Young, S. G., and Reue, K. (2011) Heart-type fatty acid-binding protein is essential for efficient brown adipose tissue fatty acid oxidation and cold tolerance. *J. Biol. Chem.* **286**, 380-390

40. Rosendal, J., Ertbjerg, P., and Knudsen, J. (1993) Characterization of ligand binding to acyl-CoA-binding protein. *Biochem. J.* **290 (Pt 2)**, 321-326

41. Rasmussen, J. T., Borchers, T., and Knudsen, J. (1990) Comparison of the binding affinities of acyl-CoA-binding protein and fatty-acid-binding protein for long-chain acyl-CoA esters. *Biochem. J.* **265**, 849-855

42. Bovolin, P., Schlichting, J., Miyata, M., Ferrarese, C., Guidotti, A., and Alho, H. (1990) Distribution and characterization of diazepam binding inhibitor (DBI) in peripheral tissues of rat. *Regul Pept.* **29**, 267-281

43. Gaigg, B., Neergaard, T. B., Schneiter, R., Hansen, J. K., Faergeman, N. J., Jensen, N. A., Andersen, J. R., Friis, J., Sandhoff, R., Schroder, H. D., and Knudsen, J. (2001) Depletion of acyl-coenzyme A-binding protein affects sphingolipid synthesis and causes vesicle accumulation and membrane defects in Saccharomyces cerevisiae. *Mol. Biol. Cell* **12**, 1147-1160

44. Landrock, D., Atshaves, B. P., McIntosh, A. L., Landrock, K. K., Schroeder, F., and Kier, A. B. (2010) Acyl-CoA binding protein gene ablation induces pre-implantation embryonic lethality in mice. *Lipids* **45**, 567-580

45. Bloksgaard, M., Bek, S., Marcher, A. B., Neess, D., Brewer, J., Hannibal-Bach, H. K., Helledie, T., Fenger, C., Due, M., Berzina, Z., Neubert, R., Chemnitz, J., Finsen, B., Clemmensen, A., Wilbertz, J., Saxtorph, H., Knudsen, J., Bagatolli, L., and Mandrup, S. (2012) The acyl-CoA binding protein is required for normal epidermal barrier function in mice. *J Lipid Res.* **53**, 2162-2174

46. Neess, D., Bloksgaard, M., Bek, S., Marcher, A. B., Elle, I. C., Helledie, T., Due, M., Pagmantidis, V., Finsen, B., Wilbertz, J., Kruhoffer, M., Faergeman, N., and Mandrup, S. (2011) Disruption of the acyl-CoA-binding protein gene delays hepatic adaptation to metabolic changes at weaning. *J. Biol. Chem.* **286**, 3460-3472

47. Færgeman, N. J., and Knudsen, J. (1997) Role of long-chain fatty acyl-CoA esters in the regulation of metabolism and in cell signalling. *Biochem J.* **323**, 1-12

48. Simpson, A. E. (1997) The cytochrome P450 4 (CYP4) family. *Gen Pharmacol.* **28**, 351-359

49. Okita, R. T., and Okita, J. R. (2001) Cytochrome P450 4A fatty acid omega hydroxylases. *Curr Drug Metab.* **2**, 265-281

50. Bell, R. M., and Coleman, R. A. (1980) Enzymes of glycerolipid synthesis in eukaryotes. *Ann Rev Biochem.* **49**, 459-487

51. Wendel, A. A., Lewin, T. M., and Coleman, R. A. (2009) Glycerol-3-phosphate acyltransferases: rate limiting enzymes of triacylglycerol biosynthesis. *Biochim. Biophys. Acta* **1791**, 501-506

52. Lewin, T. M., Wang, S., Nagle, C. A., Van Horn, C. G., and Coleman, R. A. (2005) Mitochondrial glycerol-3-phosphate acyltransferase-1 directs the metabolic fate of exogenous fatty acids in hepatocytes. *Am. J. Physiol. Endocrinol. Metab.* **288**, E835-E844

53. Nagle, C. A., An, J., Shiota, M., Torres, T. P., Cline, G. W., Liu, Z.-X., Wang, S., Catlin, R. L., Shulman, G. I., Newgard, C. B., and Coleman, R. A. (2007) Hepatic overexpression of glycerol-sn-3-phosphate acyltransferase 1 in rats causes insulin resistance. *J. Biol. Chem.* **282**, 14807-14815

54. Wendel, A. A., Cooper, D. E., Ilkayeva, O. R., Muoio, D. M., and Coleman, R. A. (2013) Glycerol-3-phosphate acyltransferase (GPAT)-1, but not GPAT4, incorporates newly synthesized fatty acids into triacylglycerol and diminishes fatty acid oxidation. *J. Biol. Chem.* **288**, 27299-27306

55. Muoio, D. M., Seefeld, K., Witters, L. A., and Coleman, R. A. (1999) AMP-activated kinase reciprocally regulates triacylglycerol synthesis and fatty acid oxidation in liver and muscle: evidence that sn-glycerol-3-phosphate acyltransferase is a novel target. *Biochem. J.* **338 (Pt 3)**, 783-791

56. Fagone, P., and Jackowski, S. (2009) Membrane phospholipid synthesis and endoplasmic reticulum function. *J Lipid Res.* **50 Suppl**, S311-316

57. Houtkooper, R. H., Akbari, H., van Lenthe, H., Kulik, W., Wanders, R. J., Frentzen, M., and Vaz, F. M. (2006) Identification and characterization of human cardiolipin synthase. *FEBS Lett.* **580**, 3059-3064

58. Hostetler, K. Y., Galesloot, J. M., Boer, P., and Van Den Bosch, H. (1975) Further studies on the formation of cardiolipin and phosphatidylglycerol in rat liver mitochondria. Effect of divalent cations and the fatty acid composition of CDP-diglyceride. *Biochim Biophys Acta.* **380**, 382-389

59. Vreken, P., Valianpour, F., Nijtmans, L. G., Grivell, L. A., Plecko, B., Wanders, R. J., and Barth, P. G. (2000) Defective remodeling of cardiolipin and phosphatidylglycerol in Barth syndrome. *Biochem Biophys Res Commun.* **279**, 378-382

60. Ye, C., Shen, Z., and Greenberg, M. L. (2014) Cardiolipin remodeling: a regulatory hub for modulating cardiolipin metabolism and function. *J. Bioenerg. Biomembr.*

61. Zhao, Y., Chen, Y. Q., Li, S., Konrad, R. J., and Cao, G. (2009) The microsomal cardiolipin remodeling enzyme acyl-CoA lysocardiolipin acyltransferase is an acyltransferase of multiple anionic lysophospholipids. *J. Lipid Res.* **50**, 945-956

62. Taylor, W. A., and Hatch, G. M. (2009) Identification of the human mitochondrial linoleoyl-coenzyme A monolysocardiolipin acyltransferase (MLCL AT-1). *J. Biol. Chem.* **284**, 30360-30371

63. Hunt, M. C., Siponen, M. I., and Alexson, S. E. (2012) The emerging role of acyl-CoA thioesterases and acyltransferases in regulating peroxisomal lipid metabolism. *Biochim. Biophys. Acta* **1822**, 1397-1410

64. Farrell, S. O., Fiol, C. J., Reddy, J. K., and Bieber, L. L. (1984) Properties of purified carnitine acyltransferases of mouse liver peroxisomes. *J Biol Chem.* **259**, 13089-13095

65. Brocker, C., Carpenter, C., Nebert, D. W., and Vasiliou, V. (2010) Evolutionary divergence and functions of the human acyl-CoA thioesterase gene (ACOT) family. *Hum Genomics* **4**, 411-420

66. Kirkby, B., Roman, N., Kobe, B., Kellie, S., and Forwood, J. K. (2010) Functional and structural properties of mammalian acyl-coenzyme A thioesterases. *Prog. Lipid Res.* **49**, 366-377

67. Westin, M. A., Alexson, S. E., and Hunt, M. C. (2004) Molecular cloning and characterization of two mouse peroxisome proliferator-activated receptor alpha (PPARalpha)-regulated peroxisomal acyl-CoA thioesterases. *J. Biol. Chem.* **279**, 21841-21848

68. Hunt, M. C., Solaas, K., Kase, B. F., and Alexson, S. E. (2002) Characterization of an acyl-coA thioesterase that functions as a major regulator of peroxisomal lipid metabolism. *J. Biol. Chem.* **277**, 1128-1138

69. Kang, H. W., Niepel, M. W., Han, S., Kawano, Y., and Cohen, D. E. (2012) Thioesterase superfamily member 2/acyl-CoA thioesterase 13 (Them2/Acot13) regulates hepatic lipid and glucose metabolism. *FASEB. J.* **26**, 2209-2221

70. Capdevila, J. H., Falck, J. R., and Harris, R. C. (2000) Cytochrome P450 and arachidonic acid bioactivation. Molecular and functional properties of the arachidonate monooxygenase. *J Lipid Res.* **41**, 163-181

71. Hisanaga, Y., Ago, H., Nakagawa, N., Hamada, K., Ida, K., Yamamoto, M., Hori, T., Arii, Y., Sugahara, M., Kuramitsu, S., Yokoyama, S., and Miyano, M. (2004) Structural basis of the substrate-specific two-step catalysis of long chain fatty acyl-CoA synthetase dimer. *J. Biol. Chem.* **279**, 31717-31726

72. Gulick, A. M., Starai, V. J., Horswill, A. R., Homick, K. M., and Escalante-Semerena, J. C. (2003) The 1.75 A crystal structure of acetyl-CoA synthetase bound to adenosine-5'-propylphosphate and coenzyme A. *Biochemistry* **42**, 2866-2873

73. Jogl, G., Hsiao, Y. S., and Tong, L. (2005) Crystal structure of mouse carnitine octanoyltransferase and molecular determinants of substrate selectivity. *J. Biol. Chem.* **280**, 738-744

74. Fraisl, P., Tanaka, H., Forss-Petter, S., Lassmann, H., Nishimune, Y., and Berger, J. (2006) A novel mammalian bubblegum-related acyl-CoA synthetase restricted to testes and possibly involved in spermatogenesis. *Archives of biochemistry and biophysics* **451**, 23-33

75. Stinnett, L., Lewin, T. M., and Coleman, R. A. (2007) Mutagenesis of rat acyl-CoA synthetase 4 indicates amino acids that contribute to fatty acid binding. *Biochim. Biophys. Acta* **1771**, 119-125

76. Hubbard, B., Doege, H., Punreddy, S., Wu, H., Huang, X., Kaushik, V. K., Mozell, R. L., Byrnes, J. J., Stricker-Krongrad, A., Chou, C. J., Tartaglia, L. A., Lodish, H. F., Stahl, A., and Gimeno, R. E. (2006) Mice deleted for fatty acid transport protein 5

have defective bile acid conjugation and are protected from obesity. *Gastroenterology* **130**, 1259-1269

77. Steinberg, S. J., Mihalik, S. J., Kim, D. G., Cuebas, D. A., and Watkins, P. A. (2000) The human liver-specific homolog of very long-chain acyl-CoA synthetase is cholate: CoA ligase. *J. Biol. Chem.* **275**, 15605-15608

78. Mihalik, S. J., Steinberg, S. J., Pei, Z., Park, J. H., Kim, D. G., Heinzer, A. K., Dacremont, G., Wanders, R. J., Cuebas, D. A., Smith, K. D., and Watkins, P. A. (2002) Participation of two members of the very long-chain acyl-CoA synthetase family in bile acid synthesis and recycling. *J. Biol. Chem.* **277**, 24771-24779

79. Sleeman, M. W., Donegan, N. P., Heller-Harrison, R., Lane, W. S., and Czech, M. P. (1998) Association of acyl-CoA synthetase-1 with GLUT4-containing vesicles. *J. Biol. Chem.* **273**, 3132-3135

80. Fujimoto, Y., Itabe, H., Kinoshita, T., Homma, K. J., Onoduka, J., Mori, M., Yamaguchi, S., Makita, M., Higashi, Y., Yamashita, A., and Takano, T. (2007) Involvement of ACSL in local synthesis of neutral lipids in cytoplasmic lipid droplets in human hepatocyte HuH7. *J Lipid Res.* **48**, 1280-1292

81. Gargiulo, C. E., Stuhlsatz-Krouper, S. M., and Schaffer, J. E. (1999) Localization of adipocyte long-chain fatty acyl-CA synthetase at the plasma membrane. *J. Lipid. Res.* **40**, 881-892

82. Lewin, T. M., Kim, J. H., Granger, D. A., Vance, J. E., and Coleman, R. A. (2001) Acyl-CoA synthetase isoforms 1, 4, and 5 are present in different subcellular membranes in rat liver and can be inhibited independently. *J. Biol. Chem.* **276**, 24674-24679

83. Bousette, N., Kislinger, T., Fong, V., Isserlin, R., Hewel, J. A., Emil, A., and Gramolini, A. O. (2009) Large-scale characterization and analysis of the murine cardiac proteome. *J Proteome Res.* **8**, 1887-1901

84. Kislinger, T., and Gramolini, A. O. (2010) Proteome analysis of mouse model systems: A tool to model human disease and for the investigation of tissue-specific biology. *J. Proteomics* **73**, 2205-2218

85. Wu, Q., Ortegon, A. M., Tsang, B., Doege, H., Feingold, K. R., and Stahl, A. (2006) FATP1 is an insulin-sensitive fatty acid transporter involved in diet-induced obesity. *Mol. Cell. Biol.* **26**, 3455-3467

86. Li, L. O., Ellis, J. M., Paich, H. A., Wang, S., Gong, N., Altshuller, G., Thresher, R. J., Koves, T. R., Watkins, S. M., Muoio, D. M., Cline, G. W., Shulman, G. I., and Coleman, R. A. (2009) Liver-specific loss of long chain acyl-CoA synthetase-1 decreases triacylglycerol synthesis and beta-oxidation and alters phospholipid fatty acid composition. *J. Biol. Chem.* **284**, 27816-27826

87. Ellis, J. M., Mentock, S. M., Depetrillo, M. A., Koves, T. R., Sen, S., Watkins, S. M., Muoio, D. M., Cline, G. W., Taegtmeyer, H., Shulman, G. I., Willis, M. S., and Coleman, R. A. (2011) Mouse cardiac acyl coenzyme a synthetase 1 deficiency

impairs fatty acid oxidation and induces cardiac hypertrophy. *Mol. Cell. Biol.* **31**, 1252-1262

88. Poppelreuther, M., Rudolph, B., Du, C., Grossmann, R., Becker, M., Thiele, C., Ehehalt, R., and Fullekrug, J. (2012) The N-terminal region of acyl-CoA synthetase 3 is essential for both the localization on lipid droplets and the function in fatty acid uptake. *J. Lipid Res.* **53**, 888-900

89. Brasaemle, D. L., Dolios, G., Shapiro, L., and Wang, R. (2004) Proteomic analysis of proteins associated with lipid droplets of basal and lipolytically stimulated 3T3-L1 adipocytes. *J Biol Chem.* **279**, 46835-46842

90. Milger, K., Herrmann, T., Becker, C., Gotthardt, D., Zickwolf, J., Ehehalt, R., Watkins, P. A., Stremmel, W., and Fullekrug, J. (2006) Cellular uptake of fatty acids driven by the ER-localized acyl-CoA synthetase FATP4. *J. Cell Sci.* **119**, 4678-4688

91. Lewin, T. M., Van Horn, C. G., Krisans, S. K., and Coleman, R. A. (2002) Rat liver acyl-CoA synthetase 4 is a peripheral-membrane protein located in two distinct subcellular organelles, peroxisomes, and mitochondrial-associated membrane. *Arch. Biochem. Biophys.* **404**, 263-270

92. Zhan, T., Poppelreuther, M., Ehehalt, R., and Fullekrug, J. (2012) Overexpressed FATP1, ACSVL4/FATP4 and ACSL1 increase the cellular fatty acid uptake of 3T3-L1 adipocytes but are localized on intracellular membranes. *PloS one* **7**, e45087

93. Srere, P. A. (1987) Complexes of sequential metabolic enzymes. *Methods Enzymol.* **56**, 89-124

94. Lee, K., Kerner, J., and Hoppel, C. L. (2011) Mitochondrial carnitine palmitoyltransferase 1a (CPT1a) is part of an outer membrane fatty acid transfer complex. *J. Biol. Chem.* **286**, 25655-25662

95. McGarry, J. D., and Brown, N. F. (1997) The mitochondrial carnitine palmitoyltransferase system. From concept to molecular analysis. *Eur. J. Biochem.* **244**, 1-14

96. Coleman, R. A., and Haynes, E. B. (1983) Selective changes in microsomal enzymes of triacylglycerol and phosphatidylcholine synthesis in fetal and postnatal rat liver. Induction of microsomal sn-glycerol 3-phosphate and dihydroxyacetonephosphate acyltransferase activities. *J Biol Chem.* **258**, 450-456

97. Mashek, D. G., Li, L. O., and Coleman, R. A. (2006) Rat long chain acyl-CoA synthetase mRNA, protein and activity vary in tissue distribution and in response to diet. *J. Lipid Res.* **47**, 2004-2010

98. Suzuki, H., Kawarabayasi, Y., Kondo, J., Abe, T., Nishikawa, K., Kimura, S., Hashimoto, T., and Yamamoto, T. (1990) Structure and regulation of rat long-chain acyl-CoA synthetase. *J. Biol. Chem.* **265**, 8681-8685

99. Oikawa, E., Iijima, H., Suzuki, T., Sasano, H., Sato, H., Kamataki, A., Nagura, H., Kang, M.-J., Fujino, T., Suzuki, H., and Yamamoto, T. T. (1998) A novel acyl-CoA

synthetase, ACS5, expressed in intestinal epithelial cells and proliferating preadipocytes. *J. Biochem.* **124**, 679-685

100. Dong, B., Kan, C. F., Singh, A. B., and Liu, J. (2013) High-fructose diet downregulates long-chain acyl-CoA synthetase 3 expression in liver of hamsters via impairing LXR/RXR signaling pathway. *J. Lipid Res.* **54**, 1241-1254

101. Wu, M., Liu, H., Chen, W., Fujimoto, Y., and Liu, J. (2009) Hepatic expression of long-chain acyl-CoA synthetase 3 is upregulated in hyperlipidemic hamsters. *Lipids* **44**, 989-998

102. Shimomura, I., Tokunaga, K., Kotani, K., Keno, Y., Yansase-Fujiwara, M., Kanosue, K., Jiao, S., Funahashi, T., Kobatake, T., Yamamoto, T., and Matsuzawa, Y. (1993) Marked reduction of acyl-CoA synthetase activity and mRNA in intra-abdominal visceral fat by physical exercise. *Am. J. Physiol.* **265**, E44 - 50

103. Hall, M., and Saggerson, E. D. (1985) Reversible inactivation by noradrenaline of long-chain fatty acyl-CoA synthetase in rat adipocytes. *Biochem. J.* **226**, 275-282

104. Martin, G., Schoonjans, K., Lefebvre, A. M., Staels, B., and Auwerx, J. (1997) Coordinate regulation of the expression of the fatty acid transport protein and acyl-CoA synthetase genes by PPARalpha and PPARgamma activators. *J. Biol. Chem.* **272**, 28210-28217

105. Ellis, J. M., Li, L. O., Wu, P. C., Koves, T. R., Ilkayeva, O., Stevens, R. D., Watkins, S. M., Muoio, D. M., and Coleman, R. A. (2010) Adipose acyl-CoA synthetase-1 directs fatty acids toward beta-oxidation and is required for cold thermogenesis. *Cell Metab.* **12**, 53-64

106. Kansara, M. S., Mehra, A. K., Von Hagen, J., Kabotyansky, E., and Smith, P. J. (1996) Physiological concentrations of insulin and T3 stimulate 3T3-L1 adipocyte acyl-CoA synthetase gene transcription. *Am J Physiol.* **270**, E873-E881

107. Durgan, D. J., Smith, J. K., Hotze, M. A., Egbejimi, O., Cuthbert, K. D., Zaha, V. G., Dyck, J. R., Abel, E. D., and Young, M. E. (2006) Distinct transcriptional regulation of long-chain acyl-CoA synthetase isoforms and cytosolic thioesterase 1 in the rodent heart by fatty acids and insulin. *Am J Physiol Heart Circ Physiol.* **290**, H2480-2497

108. de Jong, H., Neal, A. C., Coleman, R. A., and Lewin, T. M. (2007) Ontogeny of mRNA expression and activity of long-chain acyl-CoA synthetase (ACSL) isoforms in Mus musculus heart. *Biochim Biophys Acta.* **1771**, 75-82

109. Nchoutmboube, J. A., Viktorova, E. G., Scott, A. J., Ford, L. A., Pei, Z., Watkins, P. A., Ernst, R. K., and Belov, G. A. (2013) Increased long chain acyl-Coa synthetase activity and fatty acid import is linked to membrane synthesis for development of picornavirus replication organelles. *PLoS pathogens* **9**, e1003401

110. Chang, Y. S., Tsai, C. T., Huangfu, C. A., Huang, W. Y., Lei, H. Y., Lin, C. F., Su, I. J., Chang, W. T., Wu, P. H., Chen, Y. T., Hung, J. H., Young, K. C., and Lai, M. D. (2011) ACSL3 and GSK-3beta are essential for lipid upregulation induced by endoplasmic reticulum stress in liver cells. *J Cell Biochem.* **112**, 881-893

111. Frahm, J. L., Li, L. O., Grevengoed, T. J., and Coleman, R. A. (2011) Phosphorylation and acetylation of acyl-CoA synthetase- I. *J Proteomics Bioinform.* **4**, 129-137

112. Grimsrud, P. A., Carson, J. J., Hebert, A. S., Hubler, S. L., Niemi, N. M., Bailey, D. J., Jochem, A., Stapleton, D. S., Keller, M. P., Westphall, M. S., Yandell, B. S., Attie, A. D., Coon, J. J., and Pagliarini, D. J. (2012) A quantitative map of the liver mitochondrial phosphoproteome reveals posttranslational control of ketogenesis. *Cell Metab.* **16**, 672-683

113. Johnson, D. R., Knoll, J. J., Rowley, N., and Gordon, J. L. (1994) Genetic analysis of the role of *Saccharomyces cerevisiae* acyl-CoA synthetase genes in regulating protein N-myristoylation. *J. Biol. Chem.* **269**, 18037-18046

114. Tong, F., Black, P. N., Coleman, R. A., and DiRusso, C. C. (2006) Fatty acid transport by vectorial acylation in mammals: roles played by different isoforms of rat long-chain acyl-CoA synthetases. *Arch. Biochem. Biophys.* **447**, 46-52

115. DiRusso, C. C., Li, H., Darwis, D., Watkins, P. A., Berger, J., and Black, P. N. (2005) Comparative biochemical studies of the murine fatty acid transport proteins (FATP) expressed in yeast. *J Biol Chem.* **280**, 16829-16837

116. Caviglia, J. M., Li, L. O., Wang, S., DiRusso, C. C., Coleman, R. A., and Lewin, T. M. (2004) Rat long chain acyl-CoA synthetase 5, but not 1, 2, 3, or 4, complements *Escherichia coli* fadD. *J Biol Chem.* **279**, 11163-11169

117. Muoio, D. M., Lewin, T. M., Wiedmer, P., and Coleman, R. A. (2000) Acyl-CoAs are functionally channeled in liver: potential role of acyl-CoA synthetase. *Am. J. Physiol. Endocrinol. Metab.* **279**, E1366-1373

118. Igal, R. A., Wang, P., and Coleman, R. A. (1997) Triacsin C blocks de novo synthesis of glycerolipids and cholesterol esters but not recycling of fatty acid into phospholipid: evidence for functionally separate pools of acyl-CoA. *Biochem. J.* **324**, 529-534

119. Tomoda, H., Igarashi, K., and Omura, S. (1987) Inhibition of acyl-CoA synthetase by triacsins. *Biochim. Biophys. Acta* **921**, 595-598

120. Van Horn, C. G., Caviglia, J. M., Li, L. O., Wang, S., Granger, D. A., and Coleman, R. A. (2005) Characterization of recombinant long-chain rat acyl-CoA synthetase isoforms 3 and 6: identification of a novel variant of isoform 6. *Biochemistry* **44**, 1635-1642

121. Lobo, S., Wiczer, B. M., and Bernlohr, D. A. (2009) Functional analysis of long-chain acyl-coa synthetase 1 in 3T3-L1 adipocytes. *J. Biol. Chem.* **284**, 18347-18356.

122. Kanter, J. E., Kramer, F., Barnhart, S., Averill, M. M., Vivekanandan-Giri, A., Vickery, T., Li, L. O., Becker, L., Yuan, W., Chait, A., Braun, K. R., Potter-Perigos, S., Sanda, S., Witght, T. N., Pennathur, S., Serhan, C. N., Heinecke, J. W., Coleman, R. A., and Bornfeldt, K. E. (2011) Diabetes promotes an inflammatory macrophage phenotype and atherosclerosis via acyl-CoA synthetase 1 *Proc. Natl. Acad. Sci. U.S.A.*

123. Kanter, J. E., and Bornfeldt, K. E. (2013) Inflammation and diabetes-accelerated atherosclerosis: myeloid cell mediators. *Trends Endocrinol Metab.* **24**, 137-144

124. Kanter, J. E., Tang, C., Oram, J. F., and Bornfeldt, K. E. (2012) Acyl-CoA synthetase 1 is required for oleate and linoleate mediated inhibition of cholesterol efflux through ATP-binding cassette transporter A1 in macrophages. *Biochim. Biophys. Acta* **1821**, 358-364

125. Rubinow, K. B., Wall, V. Z., Nelson, J., Mar, D., Bomsztyk, K., Askari, B., Lai, M. A., Smith, K. D., Han, M. S., Vivekanandan-Giri, A., Pennathur, S., Albert, C. J., Ford, D. A., Davis, R. J., and Bornfeldt, K. E. (2013) Acyl-CoA synthetase 1 is induced by Gram-negative bacteria and lipopolysaccharide and is required for phospholipid turnover in stimulated macrophages. *J. Biol. Chem.* **288**, 9957-9970

126. Li, X., Gonzalez, O., Shen, X., Barnhart, S., Kramer, F., Kanter, J. E., Vivekanandan-Giri, A., Tsuchiya, K., Handa, P., Pennathur, S., Kim, F., Coleman, R. A., Schaffer, J. E., and Bornfeldt, K. E. (2013) Endothelial acyl-CoA synthetase 1 is not required for inflammatory and apoptotic effects of a saturated fatty acid-rich environment. *Arterioscler Thromb Vasc Biol.* **33**, 232-240

127. Chiu, H. C., Kovacs, A., Ford, D. A., Hsu, F. F., Garcia, R., Herrero, P., Saffitz, J. E., and Schaffer, J. E. (2001) A novel mouse model of lipotoxic cardiomyopathy. *J. Clin. Invest.* **107**, 813-822

128. Chiu, H. C., Kovacs, A., Blanton, R. M., Han, X., Courtois, M., Weinheimer, C. J., Yamada, K. A., Brunet, S., Xu, H., Nerbonne, J. M., Welch, M. J., Fettig, N. M., Sharp, T. L., Sambandam, N., Olson, K. M., Ory, D. S., and Schaffer, J. E. (2005) Transgenic expression of fatty acid transport protein 1 in the heart causes lipotoxic cardiomyopathy. *Circ Res.* **96**, 225-233

129. Liu, L., Shi, X., Bharadwaj, K. G., Ikeda, S., Yamashita, H., Yagyu, H., Schaffer, J. E., Yu, Y. H., and Goldberg, I. J. (2009) DGAT1 expression increases heart triglyceride content but ameliorates lipotoxicity. *J. Biol. Chem.* **284**, 36312-36323

130. Hatch, G. M., Smith, A. J., Xu, F. Y., Hall, A. M., and Bernlohr, D. A. (2002) FATP1 channels exogenous FA into 1,2,3-triacyl-sn-glycerol and down-regulates sphingomyelin and cholesterol metabolism in growing 293 cells. *J. Lipid Res.* **43**, 1380-1389

131. Garcia-Martinez, C., Marotta, M., Moore-Carrasco, R., Guitart, M., Camps, M., Busquets, S., Montell, E., and Gomez-Foix, A. M. (2005) Impact on fatty acid metabolism and differential localization of FATP1 and FAT/CD36 proteins delivered in cultured human muscle cells. *Am J Physiol Cell Physiol.* **288**, C1264-1272

132. Mashek, D. G., Li, L. O., and Coleman, R. A. (2007) Long-chain acyl-CoA synthetases and fatty acid channeling. *Future Lipidol.* **2**, 465-476

133. Menendez, J. A., and Lupu, R. (2007) Fatty acid synthase and the lipogenic phenotype in cancer pathogenesis. *Nature reviews. Cancer* **7**, 763-777

134. Currie, E., Schulze, A., Zechner, R., Walther, T. C., and Farese, R. V., Jr. (2013) Cellular fatty acid metabolism and cancer. *Cell Metab.* **18**, 153-161

135. Cao, Y., Dave, K. B., Doan, T. P., and Prescott, S. M. (2001) Fatty acid CoA ligase 4 is up-regulated in colon adenocarcinoma. *Cancer Res.* **61**, 8429-8434

136. Sung, Y. K., Hwang, S. Y., Park, M. K., Bae, H. I., Kim, W. H., Kim, J. C., and Kim, M. (2003) Fatty acid-CoA ligase 4 is overexpressed in human hepatocellular carcinoma. *Cancer Sci.* **94**, 421-424

137. Monaco, M. E., Creighton, C. J., Lee, P., Zou, X., Topham, M. K., and Stafforini, D. M. (2010) Expression of long-chain fatty acyl-CoA synthetase 4 in breast and prostate cancers Is associated with sex steroid hormone receptor negativity. *Transl. Oncol.* **3**, 91-98

138. Maloberti, P. M., Duarte, A. B., Orlando, U. D., Pasqualini, M. E., Solano, A. R., Lopez-Otin, C., and Podesta, E. J. (2010) Functional interaction between acyl-CoA synthetase 4, lipooxygenases and cyclooxygenase-2 in the aggressive phenotype of breast cancer cells. *PloS one* **5**, e15540

139. Kang, M. J., Fujino, T., Sasano, H., Minekura, H., Yabuki, N., Nagura, H., Iijima, H., and Yamamoto, T. T. (1997) A novel arachidonate-preferring acyl-CoA synthetase is present in steroidogenic cells of the rat adrenal, ovary, and testis. *Proc Natl Acad Sci. U.S.A.* **94**, 2880-2884

140. Cao, Y., Pearman, A. T., Zimmerman, G. A., McIntyre, T. M., and Prescott, S. M. (2000) Intracellular unesterified arachidonic acid signals apoptosis. *Proc Natl Acad Sci U.S.A.* **97**, 11280-11285

141. Sung, Y. K., Park, M. K., Hong, S. H., Hwang, S. Y., Kwack, M. H., Kim, J. C., and Kim, M. K. (2007) Regulation of cell growth by fatty acid-CoA ligase 4 in human hepatocellular carcinoma cells. *Exp. Mol. Med.* **39**, 477-482

142. Hertz, R., Magenheim, J., Berman, I., and Bar-Tana, J. (1998) Fatty acyl-CoA thioesters are ligands of hepatic nuclear factor-4alpha. *Nature* **392**, 512-516

143. Ning, B. F., Ding, J., Yin, C., Zhong, W., Wu, K., Zeng, X., Yang, W., Chen, Y. X., Zhang, J. P., Zhang, X., Wang, H. Y., and Xie, W. F. (2010) Hepatocyte nuclear factor 4 alpha suppresses the development of hepatocellular carcinoma. *Cancer Res.* **70**, 7640-7651

144. Mashima, T., Oh-hara, T., Sato, S., Mochizuki, M., Sugimoto, Y., Yamazaki, K., Hamada, J., Tada, M., Moriuchi, T., Ishikawa, Y., Kato, Y., Tomoda, H., Yamori, T., and Tsuruo, T. (2005) p53-defective tumors with a functional apoptosome-mediated pathway: a new therapeutic target. *J Natl Cancer Inst.* **97**, 765-777

145. McGarry, J. D., and Foster, D. W. (1979) In support of the roles of malonyl-CoA and carnitine acyltransferase I in the regulation of hepatic fatty acid oxidation and ketogenesis. *J. Biol. Chem.* **254**, 8163-8168

146. McGarry, J. D., and Foster, D. W. (1980) Regulation of hepatic fatty acid oxidation and ketone body production. *Annu. Rev. Biochem.* **49**, 395-420

147. Prentki, M., and Corkey, B. E. (1996) Are the β-Cell signaling molecules malonyl-CoA and cytosolic long-chain acyl-CoA implicated in multiple tissue defects of obesity and NIDDM. *Diabetes* **45**, 273-283

148. Prentki, M., and Corkey, B. E. (1996) Are the beta-cell signaling molecules malonyl-CoA and cystolic long-chain acyl-CoA implicated in multiple tissue defects of obesity and NIDDM? *Diabetes* **45**, 273-283

149. Prentki, M., Joly, E., El-Assaad, W., and Roduit, R. (2002) Malonyl-CoA signaling, lipid partitioning, and glucolipotoxicity: role in beta-cell adaptation and failure in the etiology of diabetes. *Diabetes* **51 Suppl 3.**, S405-413

150. Liang, Y., and Matschinsky, F. M. (1991) Content of CoA-esters in perifused rat islets stimulated by glucose and other fuels. *Diabetes* **40**, 327-333

151. Chen, S., Ogawa, A., Ohneda, M., Unger, R. H., Foster, D. W., and McGarry, J. D. (1994) More direct evidence for a malonyl-CoA-carnitine palmitoyltransferase I interaction as a key event in pancreatic beta-cell signaling. *Diabetes* **43**, 878-883

152. Shanik, M. H., Xu, Y., Skrha, J., Dankner, R., Zick, Y., and Roth, J. (2008) Insulin resistance and hyperinsulinemia: is hyperinsulinemia the cart or the horse? *Diabetes care* **31 Suppl 2**, S262-268

153. Kim, J. K., Fillmore, J. J., Sunshine, M. J., Albrecht, B., Higashimori, T., Kim, D. W., Liu, Z. X., Soos, T. J., Cline, G. W., O'Brien, W. R., Littman, D. R., and Shulman, G. I. (2004) PKC-theta knockout mice are protected from fat-induced insulin resistance. *J. Clin. Invest.* **114**, 823-827

154. Chen, M. T., Kaufman, L. N., Spennetta, T., and Shrago, E. (1992) Effects of high fat-feeding to rats on the interrelationship of body weight, plasma insulin, and fatty acyl-coenzyme A esters in liver and skeletal muscle. *Metabolism: clinical and experimental* **41**, 564-569

155. Neschen, S., Morino, K., Hammond, L. E., Zhang, D., Liu, Z. X., Romanelli, A. J., Cline, G. W., Pongratz, R. L., Zhang, X. M., Choi, C. S., Coleman, R. A., and Shulman, G. I. (2005) Prevention of hepatic steatosis and hepatic insulin resistance in mitochondrial acyl-CoA:glycerol-sn-3-phosphate acyltransferase 1 knock out mice. *Cell Metab.* **2**, 55-65

156. Ellis, B. A., Poynten, A., Lowy, A. J., Furler, S. M., Chisholm, D. J., Kraegen, E. W., and Cooney, G. J. (2000) Long-chain acyl-CoA esters as indicators of lipid metabolism and insulin sensitivity in rat and human muscle. *Am J Physiol Endocrinol Metab.* **279**, E554-560

157. Houmard, J. A., Tanner, C. J., Yu, C., Cunningham, P. G., Pories, W. J., MacDonald, K. G., and Shulman, G. I. (2002) Effect of weight loss on insulin sensitivity and intramuscular long-chain fatty acyl-CoAs in morbidly obese subjects. *Diabetes* **51**, 2959-2963

158. Doenst, T., Nguyen, T. D., and Abel, E. D. (2013) Cardiac metabolism in heart failure: implications beyond ATP production. *Circ. Res.* **113**, 709-724

159. Chiu, H. C., Kovacs, A., Ford, D. A., Hsu, F. F., Garcia, R., Herrero, P., Saffitz, J. E., and Schaffer, J. E. (2001) A novel mouse model of lipotoxic cardiomyopathy. *J Clin Invest.* **107**, 813-822

160. Allard, M. F., Henning, S. L., Wambolt, R. B., Granleese, S. R., English, D. R., and Lopaschuk, G. D. (1997) Glycogen metabolism in the aerobic hypertrophied rat heart. *Circulation.* **96**, 676-682

161. Barger, P. M., and Kelly, D. P. (1999) Fatty acid utilization in the hypertrophied and failing heart: molecular regulatory mechanisms. *Am J.Med Sci.* **318**, 36-42

162. Tian, R. (2003) Transcriptional regulation of energy substrate metabolism in normal and hypertrophied heart. *Current hypertension reports* **5**, 454-458

163. Davila-Roman, V. G., Vedala, G., Herrero, P., de las Fuentes, L., Rogers, J. G., Kelly, D. P., and Gropler, R. J. (2002) Altered myocardial fatty acid and glucose metabolism in idiopathic dilated cardiomyopathy. *J. Am. Coll. Cardiol.* **40**, 271-277

164. Belke, D. D., Larsen, T. S., Gibbs, E. M., and Severson, D. L. (2000) Altered metabolism causes cardiac dysfunction in perfused hearts from diabetic (db/db) mice. *Am J Physiol Endocrinol Metab.* **279**, E1104-1113

165. Mazumder, P. K., O'Neill, B. T., Roberts, M. W., Buchanan, J., Yun, U. J., Cooksey, R. C., Boudina, S., and Abel, E. D. (2004) Impaired cardiac efficiency and increased fatty acid oxidation in insulin-resistant ob/ob mouse hearts. *Diabetes* **53**, 2366-2374

166. Westermeier, F., Navarro-Marquez, M., Lopez-Crisosto, C., Bravo-Sagua, R., Quiroga, C., Bustamante, M., Verdejo, H. E., Zalaquett, R., Ibacache, M., Parra, V., Castro, P. F., Rothermel, B. A., Hill, J. A., and Lavandero, S. (2015) Defective insulin signaling and mitochondrial dynamics in diabetic cardiomyopathy. *Biochim Biophys Acta.* **1853**, 1113-1118

167. Kane, L. A., and Van Eyk, J. E. (2009) Post-translational modifications of ATP synthase in the heart: biology and function. *J. Bioenerg. Biomembr.* **41**, 145-150

168. Rimessi, A., Giorgi, C., Pinton, P., and Rizzuto, R. (2008) The versatility of mitochondrial calcium signals: from stimulation of cell metabolism to induction of cell death. *Biochim Biophys Acta.* **1777**, 808-816

169. Fassone, E., and Rahman, S. (2012) Complex I deficiency: clinical features, biochemistry and molecular genetics. *J Med Genet.* **49**, 578-590

170. Alston, C. L., Davison, J. E., Meloni, F., van der Westhuizen, F. H., He, L., Hornig-Do, H. T., Peet, A. C., Gissen, P., Goffrini, P., Ferrero, I., Wassmer, E., McFarland, R., and Taylor, R. W. (2012) Recessive germline SDHA and SDHB mutations causing leukodystrophy and isolated mitochondrial complex II deficiency. *J Med Genet.* **49**, 569-577

171. Marin-Buera, L., Garcia-Bartolome, A., Moran, M., Lopez-Bernardo, E., Cadenas, S., Hidalgo, B., Sanchez, R., Seneca, S., Arenas, J., Martin, M. A., and Ugalde, C. (2015) Differential proteomic profiling unveils new molecular mechanisms associated with mitochondrial complex III deficiency. *J Proteomics.* **113**, 38-56

172. Olahova, M., Haack, T. B., Alston, C. L., Houghton, J. A., He, L., Morris, A. A., Brown, G. K., McFarland, R., Chrzanowska-Lightowlers, Z. M., Lightowlers, R. N., Prokisch, H., and Taylor, R. W. (2014) A truncating PET100 variant causing fatal infantile lactic acidosis and isolated cytochrome c oxidase deficiency. *Eur J Hum Genet.*

173. Jonckheere, A. I., Smeitink, J. A., and Rodenburg, R. J. (2012) Mitochondrial ATP synthase: architecture, function and pathology. *J Inherit Metab Dis.* **35**, 211-225

174. Rodenburg, R. J. (2011) Biochemical diagnosis of mitochondrial disorders. *J Inherit Metab Dis.* **34**, 283-292

175. Abramovitch, D. A., Marsh, D., and Powell, G. L. (1990) Activation of beef-heart cytochrome c oxidase by cardiolipin and analogues of cardiolipin. *Biochim Biophys Acta.* **1020**, 34-42

176. Paradies, G., Ruggiero, F. M., Dinoi, P., Petrosillo, G., and Quagliariello, E. (1993) Decreased cytochrome oxidase activity and changes in phospholipids in heart mitochondria from hypothyroid rats. *Arch Biochem Biophys.* **307**, 91-95

177. Fry, M., Blondin, G. A., and Green, D. E. (1980) The localization of tightly bound cardiolipin in cytochrome oxidase. *J Biol Chem.* **255**, 9967-9970

178. Paradies, G., Ruggiero, F. M., Petrosillo, G., and Quagliariello, E. (1998) Peroxidative damage to cardiac mitochondria: cytochrome oxidase and cardiolipin alterations. *FEBS Lett.* **424**, 155-158

179. Paradies, G., Petrosillo, G., Pistolese, M., Di Venosa, N., Serena, D., and Ruggiero, F. M. (1999) Lipid peroxidation and alterations to oxidative metabolism in mitochondria isolated from rat heart subjected to ischemia and reperfusion. *Free Radic Biol Med.* **27**, 42-50

180. Acehan, D., Malhotra, A., Xu, Y., Ren, M., Stokes, D. L., and Schlame, M. (2011) Cardiolipin affects the supramolecular organization of ATP synthase in mitochondria. *Biophys J.* **100**, 2184-2192

181. Eble, K. S., Coleman, W. B., Hantgan, R. R., and Cunningham, C. C. (1990) Tightly associated cardiolipin in the bovine heart mitochondrial ATP synthase as analyzed by 31P nuclear magnetic resonance spectroscopy. *J Biol Chem.* **265**, 19434-19440

182. Schafer, E., Dencher, N. A., Vonck, J., and Parcej, D. N. (2007) Three-dimensional structure of the respiratory chain supercomplex I1III2IV1 from bovine heart mitochondria. *Biochemistry.* **46**, 12579-12585

183. van Raam, B. J., Sluiter, W., de Wit, E., Roos, D., Verhoeven, A. J., and Kuijpers, T. W. (2008) Mitochondrial membrane potential in human neutrophils is maintained by

complex III activity in the absence of supercomplex organisation. *PLoS One.* **3**, e2013

184. Beyer, K., and Klingenberg, M. (1985) ADP/ATP carrier protein from beef heart mitochondria has high amounts of tightly bound cardiolipin, as revealed by 31P nuclear magnetic resonance. *Biochemistry.* **24**, 3821-3826

185. Power, G. W., Yaqoob, P., Harvey, D. J., Newsholme, E. A., and Calder, P. C. (1994) The effect of dietary lipid manipulation on hepatic mitochondrial phospholipid fatty acid composition and carnitine palmitoyltransferase I activity. *Biochem Mol Biol Int.* **34**, 671-684

186. Kaplan, R. S., Pratt, R. D., and Pedersen, P. L. (1986) Purification and characterization of the reconstitutively active phosphate transporter from rat liver mitochondria. *J Biol Chem.* **261**, 12767-12773

187. Noel, H., and Pande, S. V. (1986) An essential requirement of cardiolipin for mitochondrial carnitine acylcarnitine translocase activity. Lipid requirement of carnitine acylcarnitine translocase. *Eur J Biochem.* **155**, 99-102

188. Trivedi, A., Fantin, D. J., and Tustanoff, E. R. (1986) Role of phospholipid fatty acids on the kinetics of high and low affinity sites of cytochrome c oxidase. *Biochem Cell Biol.* **64**, 1195-1210

189. Sparagna, G. C., and Lesnefsky, E. J. (2009) Cardiolipin remodeling in the heart. *J Cardiovasc Pharmacol.* **53**, 290-301

190. Kagan, V. E., Tyurin, V. A., Jiang, J., Tyurina, Y. Y., Ritov, V. B., Amoscato, A. A., Osipov, A. N., Belikova, N. A., Kapralov, A. A., Kini, V., Vlasova, II, Zhao, Q., Zou, M., Di, P., Svistunenko, D. A., Kurnikov, I. V., and Borisenko, G. G. (2005) Cytochrome c acts as a cardiolipin oxygenase required for release of proapoptotic factors. *Nat Chem Biol.* **1**, 223-232

191. Sevanian, A., Wratten, M. L., McLeod, L. L., and Kim, E. (1988) Lipid peroxidation and phospholipase A2 activity in liposomes composed of unsaturated phospholipids: a structural basis for enzyme activation. *Biochim Biophys Acta.* **961**, 316-327

192. Vasdev, S. C., Biro, G. P., Narbaitz, R., and Kako, K. J. (1980) Membrane changes induced by early myocardial ischemia in the dog. *Can J Biochem.* **58**, 1112-1119

193. Sparagna, G. C., Chicco, A. J., Murphy, R. C., Bristow, M. R., Johnson, C. A., Rees, M. L., Maxey, M. L., McCune, S. A., and Moore, R. L. (2007) Loss of cardiac tetralinoleoyl cardiolipin in human and experimental heart failure. *J Lipid Res.* **48**, 1559-1570

194. Heyen, J. R., Blasi, E. R., Nikula, K., Rocha, R., Daust, H. A., Frierdich, G., Van Vleet, J. F., De Ciechi, P., McMahon, E. G., and Rudolph, A. E. (2002) Structural, functional, and molecular characterization of the SHHF model of heart failure. *Am J Physiol Heart Circ Physiol.* **283**, H1775-1784

195. Baile, M. G., Sathappa, M., Lu, Y. W., Pryce, E., Whited, K., McCaffery, J. M., Han, X., Alder, N. N., and Claypool, S. M. (2014) Unremodeled and remodeled cardiolipin are functionally indistinguishable in yeast. *J Biol Chem.* **289**, 1768-1778

196. Ye, C., Lou, W., Li, Y., Chatzispyrou, I. A., Huttemann, M., Lee, I., Houtkooper, R. H., Vaz, F. M., Chen, S., and Greenberg, M. L. (2014) Deletion of the cardiolipin-specific phospholipase Cld1 rescues growth and life span defects in the tafazzin mutant: implications for Barth syndrome. *J Biol Chem.* **289**, 3114-3125

197. Hoshino, A., Matoba, S., Iwai-Kanai, E., Nakamura, H., Kimata, M., Nakaoka, M., Katamura, M., Okawa, Y., Ariyoshi, M., Mita, Y., Ikeda, K., Ueyama, T., Okigaki, M., and Matsubara, H. (2012) p53-TIGAR axis attenuates mitophagy to exacerbate cardiac damage after ischemia. *J. Mol. Cell. Cardiol.* **52**, 175-184

198. Kubli, D. A., Zhang, X., Lee, Y., Hanna, R. A., Quinsay, M. N., Nguyen, C. K., Jimenez, R., Petrosyan, S., Murphy, A. N., and Gustafsson, A. B. (2013) Parkin protein deficiency exacerbates cardiac injury and reduces survival following myocardial infarction. *J. Biol. Chem.* **288**, 915-926

199. Thomas, R. L., Roberts, D. J., Kubli, D. A., Lee, Y., Quinsay, M. N., Owens, J. B., Fischer, K. M., Sussman, M. A., Miyamoto, S., and Gustafsson, A. B. (2013) Loss of MCL-1 leads to impaired autophagy and rapid development of heart failure. *Genes Dev.* **27**, 1365-1377

200. Oka, T., Hikoso, S., Yamaguchi, O., Taneike, M., Takeda, T., Tamai, T., Oyabu, J., Murakawa, T., Nakayama, H., Nishida, K., Akira, S., Yamamoto, A., Komuro, I., and Otsu, K. (2012) Mitochondrial DNA that escapes from autophagy causes inflammation and heart failure. *Nature.* **485**, 251-255

201. Mei, Y., Thompson, M. D., Cohen, R. A., and Tong, X. (2015) Autophagy and oxidative stress in cardiovascular diseases. *Biochim Biophys Acta.* **1852**, 243-251

202. Jung, C. H., Jun, C. B., Ro, S. H., Kim, Y. M., Otto, N. M., Cao, J., Kundu, M., and Kim, D. H. (2009) ULK-Atg13-FIP200 complexes mediate mTOR signaling to the autophagy machinery. *Mol. Biol. Cell.* **20**, 1992-2003

203. Chu, C. T., Ji, J., Dagda, R. K., Jiang, J. F., Tyurina, Y. Y., Kapralov, A. A., Tyurin, V. A., Yanamala, N., Shrivastava, I. H., Mohammadyani, D., Qiang Wang, K. Z., Zhu, J., Klein-Seetharaman, J., Balasubramanian, K., Amoscato, A. A., Borisenko, G., Huang, Z., Gusdon, A. M., Cheikhi, A., Steer, E. K., Wang, R., Baty, C., Watkins, S., Bahar, I., Bayir, H., and Kagan, V. E. (2013) Cardiolipin externalization to the outer mitochondrial membrane acts as an elimination signal for mitophagy in neuronal cells. *Nat Cell Biol.* **15**, 1197-1205

204. Li, X. X., Tsoi, B., Li, Y. F., Kurihara, H., and He, R. R. (2015) Cardiolipin and its different properties in mitophagy and apoptosis. *J Histochem Cytochem.*

205. Singh, S. B., Ornatowski, W., Vergne, I., Naylor, J., Delgado, M., Roberts, E., Ponpuak, M., Master, S., Pilli, M., White, E., Komatsu, M., and Deretic, V. (2010) Human IRGM regulates autophagy and cell-autonomous immunity functions through mitochondria. *Nat Cell Biol.* **12**, 1154-1165

206. Kuwana, T., Mackey, M. R., Perkins, G., Ellisman, M. H., Latterich, M., Schneiter, R., Green, D. R., and Newmeyer, D. D. (2002) Bid, Bax, and lipids cooperate to form supramolecular openings in the outer mitochondrial membrane. *Cell.* **111**, 331-342

207. Amadoro, G., Corsetti, V., Florenzano, F., Atlante, A., Bobba, A., Nicolin, V., Nori, S. L., and Calissano, P. (2014) Morphological and bioenergetic demands underlying the mitophagy in post-mitotic neurons: the pink-parkin pathway. *Front Aging Neurosci.* **6**, 18

208. Chicco, A. J., and Sparagna, G. C. (2007) Role of cardiolipin alterations in mitochondrial dysfunction and disease. *Am J Physiol Cell Physiol.* **292**, C33-44

209. Bu, S. Y., Mashek, M. T., and Mashek, D. G. (2009) Suppression of long chain acyl-CoA synthetase 3 decreases hepatic de novo fatty acid synthesis through decreased transcriptional activity. *J Biol Chem.* **284**, 30474-30483

210. Kuwata, H., Yoshimura, M., Sasaki, Y., Yoda, E., Nakatani, Y., Kudo, I., and Hara, S. (2013) Role of long-chain acyl-coenzyme A synthetases in the regulation of arachidonic acid metabolism in interleukin 1beta-stimulated rat fibroblasts. *Biochim. Biophys. Acta* **1841**, 44-53

211. Klett, E. L., Chen, S., Edin, M. L., Li, L. O., Ilkayeva, O., Zeldin, D. C., Newgard, C. B., and Coleman, R. A. (2013) Diminished acyl-CoA synthetase isoform 4 activity in INS 832/13 cells reduces cellular epoxyeicosatrienoic acid levels and results in impaired glucose-stimulated insulin secretion. *J. Biol. Chem.* **288**, 21618-21629

212. Bu, S. Y., and Mashek, D. G. (2010) Hepatic long-chain acyl-CoA synthetase 5 mediates fatty acid channeling between anabolic and catabolic pathways. *J Lipid Res.* **51**, 3270-3280

213. Meller, N., Morgan, M. E., Wong, W. P., Altemus, J. B., and Sehayek, E. (2013) Targeting of Acyl-CoA synthetase 5 decreases jejunal fatty acid activation with no effect on dietary long-chain fatty acid absorption. *Lipids in health and disease* **12**, 88

214. Kim, H. C., Lee, S. W., Cho, Y. Y., Lim, J. M., Ryoo, Z. Y., and Lee, E. J. (2009) RNA interference of long-chain acyl-CoA synthetase 6 suppresses the neurite outgrowth of mouse neuroblastoma NB41A3 cells. *Molecular medicine reports* **2**, 669-674

215. Wu, Q., Kazantzis, M., Doege, H., Ortegon, A. M., Tsang, B., Falcon, A., and Stahl, A. (2006) Fatty acid transport protein 1 is required for nonshivering thermogenesis in brown adipose tissue. *Diabetes* **55**, 3229-3237

216. Chekroud, K., Guillou, L., Gregoire, S., Ducharme, G., Brun, E., Cazevieille, C., Bretillon, L., Hamel, C. P., Brabet, P., and Pequignot, M. O. (2012) Fatp1 deficiency affects retinal light response and dark adaptation, and induces age-related alterations. *PloS one* **7**, e50231

217. Mishima, T., Miner, J. H., Morizane, M., Stahl, A., and Sadovsky, Y. (2011) The expression and function of fatty acid transport protein-2 and -4 in the murine placenta. *PloS one* **6**, e25865

218. Pei, Z., Sun, P., Huang, P., Lal, B., Laterra, J., and Watkins, P. A. (2009) Acyl-CoA synthetase VL3 knockdown inhibits human glioma cell proliferation and tumorigenicity. *Cancer Res.*

219. Lin, M. H., Hsu, F. F., and Miner, J. H. (2013) Requirement of fatty acid transport protein 4 for development, maturation, and function of sebaceous glands in a mouse model of ichthyosis prematurity syndrome. *J. Biol. Chem.* **288**, 3964-3976

220. Moulson, C. L., Lin, M. H., White, J. M., Newberry, E. P., Davidson, N. O., and Miner, J. H. (2007) Keratinocyte-specific expression of fatty acid transport protein 4 rescues the wrinkle-free phenotype in Slc27a4/Fatp4 mutant mice. *J. Biol. Chem.* **282**, 15912-15920

221. Pei, Z., Oey, N. A., Zuidervaart, M. M., Jia, Z., Li, Y., Steinberg, S. J., Smith, K. D., and Watkins, P. A. (2003) The acyl-CoA synthetase "bubblegum" (lipidosin): further characterization and role in neuronal fatty acid beta-oxidation. *J. Biol. Chem.* **278**, 47070-47078

222. Sheng, Y., Tsai-Morris, C. H., Li, J., and Dufau, M. L. (2009) Lessons from the gonadotropin-regulated long chain acyl-CoA synthetase (GR-LACS) null mouse model: a role in steroidogenesis, but not result in X-ALD phenotype. *The Journal of steroid biochemistry and molecular biology* **114**, 44-56

223. Tang, P.-Z., Tsai-Morris, C.-H., and Dufau, M. L. (2001) Cloning and characterization of a homonally regulated rat long chain acyl-CoA synthetase. *Proc. Natl. Acad. Sci. U.S.A.* **98**, 6581-6586

224. Berg, J., Tymoczko, J., and Stryer, L. (2006) *Biochemistry*, 6 ed., W.H. Freeman and Company

225. Piquereau, J., Caffin, F., Novotova, M., Lemaire, C., Veksler, V., Garnier, A., Ventura-Clapier, R., and Joubert, F. (2013) Mitochondrial dynamics in the adult cardiomyocytes: which roles for a highly specialized cell? *Frontiers in physiology* **4**, 102

226. Gomez, L. A., Monette, J. S., Chavez, J. D., Maier, C. S., and Hagen, T. M. (2009) Supercomplexes of the mitochondrial electron transport chain decline in the aging rat heart. *Arch Biochem Biophys.* **490**, 30-35

227. Ellis, J. M., Mentock, S. M., Depetrillo, M. A., Koves, T. R., Sen, S., Watkins, S. M., Muoio, D. M., Cline, G. W., Taegtmeyer, H., Shulman, G. I., Willis, M. S., and Coleman, R. A. (2011) Mouse cardiac acyl coenzyme a synthetase 1 deficiency impairs Fatty Acid oxidation and induces cardiac hypertrophy. *Molecular and cellular biology* **31**, 1252-1262

228. Li, L. O., Ellis, J. M., Paich, H. A., Wang, S., Gong, N., Altshuller, G., Thresher, R. J., Koves, T. R., Watkins, S. M., Muoio, D. M., Cline, G. W., Shulman, G. I., and Coleman, R. A. (2009) Liver-specific loss of long chain acyl-CoA synthetase-1 decreases triacylglycerol synthesis and beta-oxidation and alters phospholipid fatty acid composition. *J Biol Chem.* **284**, 27816-27826

229. Alexandre, H., Mathieu, B., and Charpentier, C. (1996) Alteration in membrane fluidity and lipid composition, and modulation of H(+)-ATPase activity in Saccharomyces cerevisiae caused by decanoic acid. *Microbiology.* **142 (Pt 3)**, 469-475

230. Kimelberg, H. K., and Papahadjopoulos, D. (1974) Effects of phospholipid acyl chain fluidity, phase transitions, and cholesterol on (Na+ + K+)-stimulated adenosine triphosphatase. *The Journal of biological chemistry* **249**, 1071-1080

231. Stulnig, T. M., Huber, J., Leitinger, N., Imre, E. M., Angelisova, P., Nowotny, P., and Waldhausl, W. (2001) Polyunsaturated eicosapentaenoic acid displaces proteins from membrane rafts by altering raft lipid composition. *The Journal of biological chemistry* **276**, 37335-37340

232. Coleman, R. A., Lewin, T. M., Van Horn, C. G., and Gonzalez-Baro, M. R. (2002) Do long-chain acyl-CoA synthetases regulate fatty acid entry into synthetic versus degradative pathways? *J Nutr.* **132**, 2123-2126

233. Fry, M., and Green, D. E. (1981) Cardiolipin requirement for electron transfer in complex I and III of the mitochondrial respiratory chain. *J Biol Chem.* **256**, 1874-1880

234. Eble, K. S., Coleman, W. B., Hantgan, R. R., and Cunningham, C. C. (1990) Tightly associated cardiolipin in the bovine heart mitochondrial ATP synthase as analyzed by 31P nuclear magnetic resonance spectroscopy. *J. Biol. Chem.* **265**, 19434-19440

235. Ban, T., Heymann, J. A., Song, Z., Hinshaw, J. E., and Chan, D. C. (2010) OPA1 disease alleles causing dominant optic atrophy have defects in cardiolipin-stimulated GTP hydrolysis and membrane tubulation. *Hum Mol Genet.* **19**, 2113-2122

236. Montessuit, S., Somasekharan, S. P., Terrones, O., Lucken-Ardjomande, S., Herzig, S., Schwarzenbacher, R., Manstein, D. J., Bossy-Wetzel, E., Basanez, G., Meda, P., and Martinou, J. C. (2010) Membrane remodeling induced by the dynamin-related protein Drp1 stimulates Bax oligomerization. *Cell* **142**, 889-901

237. Gonzalvez, F., Schug, Z. T., Houtkooper, R. H., MacKenzie, E. D., Brooks, D. G., Wanders, R. J., Petit, P. X., Vaz, F. M., and Gottlieb, E. (2008) Cardiolipin provides an essential activating platform for caspase-8 on mitochondria. *J. Cell Biol.* **183**, 681-696

238. Schlame, M., Towbin, J. A., Heerdt, P. M., Jehle, R., DiMauro, S., and Blanck, T. J. (2002) Deficiency of tetralinoleoyl-cardiolipin in Barth syndrome. *Ann. Neurol.* **51**, 634-637

239. Schlame, M., Acehan, D., Berno, B., Xu, Y., Valvo, S., Ren, M., Stokes, D. L., and Epand, R. M. (2012) The physical state of lipid substrates provides transacylation specificity for tafazzin. *Nat. Chem. Biol.* **8**, 862-869

240. Cao, J., Liu, Y., Lockwood, J., Burn, P., and Shi, Y. (2004) A novel cardiolipin-remodeling pathway revealed by a gene encoding an endoplasmic reticulum-associated Acyl-CoA:lysocardiolipin acyltransferase (ALCAT1) in mouse. *J Biol. Chem.* **279**, 31727-31734

241. Li, H. H., Willis, M. S., Lockyer, P., Miller, N., McDonough, H., Glass, D. J., and Patterson, C. (2007) Atrogin-1 inhibits Akt-dependent cardiac hypertrophy in mice via ubiquitin-dependent coactivation of Forkhead proteins. *J. Clin. Invest.* **117**, 3211-3223

242. Anderson, E. J., Thayne, K. A., Harris, M., Shaikh, S. R., Darden, T. M., Lark, D. S., Williams, J. M., Chitwood, W. R., Kypson, A. P., and Rodriguez, E. (2014) Do fish oil omega-3 fatty acids enhance antioxidant capacity and mitochondrial fatty acid oxidation in human atrial myocardium via PPARgamma activation? *Antioxid. Redox Signal.* **21**, 1156-1163

243. Vaden, D. L., Gohil, V. M., Gu, Z., and Greenberg, M. L. (2005) Separation of yeast phospholipids using one-dimensional thin-layer chromatography. *Analytical biochemistry* **338**, 162-164

244. Ames, B. N., and Dubin, D. T. (1960) The role of polyamines in the neutralization of bacteriophage deoxyribonucleic acid. *J Biol Chem.* **235**, 769-775

245. Bligh, E. G., and Dyer, W. J. (1959) A rapid method of total lipid extraction and purification. *Can J Biochem Physiol.* **37**, 911-917

246. Fujino, T., Kang, M.-J., Suzuki, H., Iijima, H., and Yamamoto, T. (1996) Molecular characterization and expression of rat acyl-CoA synthetase 3. *J Biol Chem.* **271**, 16748-16752

247. Rimessi, A., Giorgi, C., Pinton, P., and Rizzuto, R. (2008) The versatility of mitochondrial calcium signals: from stimulation of cell metabolism to induction of cell death. *Biochim. Biophys. Acta* **1777**, 808-816

248. De, K., Ghosh, G., Datta, M., Konar, A., Bandyopadhyay, J., Bandyopadhyay, D., Bhattacharya, S., and Bandyopadhyay, A. (2004) Analysis of differentially expressed genes in hyperthyroid-induced hypertrophied heart by cDNA microarray. *J Endocrinol.* **182**, 303-314

249. Paradies, G., Ruggiero, F. M., Petrosillo, G., and Quagliariello, E. (1994) Enhanced cytochrome oxidase activity and modification of lipids in heart mitochondria from hyperthyroid rats. *Biochim Biophys Acta.* **1225**, 165-170

250. Saini-Chohan, H. K., Holmes, M. G., Chicco, A. J., Taylor, W. A., Moore, R. L., McCune, S. A., Hickson-Bick, D. L., Hatch, G. M., and Sparagna, G. C. (2009) Cardiolipin biosynthesis and remodeling enzymes are altered during development of heart failure. *J Lipid Res.* **50**, 1600-1608

251. Sparagna, G. C., Johnson, C. A., McCune, S. A., Moore, R. L., and Murphy, R. C. (2005) Quantitation of cardiolipin molecular species in spontaneously hypertensive heart failure rats using electrospray ionization mass spectrometry. *J Lipid Res.* **46**, 1196-1204

252. Sprecher, H., Luthria, D. L., Mohammed, B. S., and Baykousheva, S. P. (1995) Reevaluation of the pathways for the biosynthesis of polyunsaturated fatty acids. *J. Lipid Res.* **36**, 2471-2477

253. Shindou, H., Hishikawa, D., Harayama, T., Eto, M., and Shimizu, T. (2013) Generation of membrane diversity by lysophospholipid acyltransferases. *J. Biochem.* **154**, 21-28

254. Richter-Dennerlein, R., Korwitz, A., Haag, M., Tatsuta, T., Dargazanli, S., Baker, M., Decker, T., Lamkemeyer, T., Rugarli, E. I., and Langer, T. (2014) DNAJC19, a mitochondrial cochaperone associated with cardiomyopathy, forms a complex with prohibitins to regulate cardiolipin remodeling. *Cell Metab.* **20**, 158-171

255. Ye, C., Lou, W., Li, Y., Chatzispyrou, I. A., Huttemann, M., Lee, I., Houtkooper, R. H., Vaz, F. M., Chen, S., and Greenberg, M. L. (2014) Deletion of the cardiolipin-specific phospholipase Cld1 rescues growth and life span defects in the tafazzin mutant: implications for Barth syndrome. *J. Biol. Chem.* **289**, 3114-3125

256. Mulligan, C. M., Sparagna, G. C., Le, C. H., De Mooy, A. B., Routh, M. A., Holmes, M. G., Hickson-Bick, D. L., Zarini, S., Murphy, R. C., Xu, F. Y., Hatch, G. M., McCune, S. A., Moore, R. L., and Chicco, A. J. (2012) Dietary linoleate preserves cardiolipin and attenuates mitochondrial dysfunction in the failing rat heart. *Cardiovasc. Res.* **94**, 460-468

257. Li, L. O., Grevengoed, T. J., Paul, D. S., Ilkayeva, O., Koves, T. R., Pascual, F., Newgard, C. B., Muoio, D. M., and Coleman, R. A. (2015) Compartmentalized Acyl-CoA Metabolism in Skeletal Muscle Regulates Systemic Glucose Homeostasis. *Diabetes* **64**, 23-35

258. Mashek, D. G., Li, L. O., and Coleman, R. A. (2006) Rat long-chain acyl-CoA synthetase mRNA, protein, and activity vary in tissue distribution and in response to diet. *J. Lipid Res.* **47**, 2004-2010

259. Kiebish, M. A., Han, X., Cheng, H., Chuang, J. H., and Seyfried, T. N. (2008) Cardiolipin and electron transport chain abnormalities in mouse brain tumor mitochondria: lipidomic evidence supporting the Warburg theory of cancer. *J. Lipid Res.* **49**, 2545-2556

260. Acehan, D., Vaz, F., Houtkooper, R. H., James, J., Moore, V., Tokunaga, C., Kulik, W., Wansapura, J., Toth, M. J., Strauss, A., and Khuchua, Z. (2011) Cardiac and skeletal muscle defects in a mouse model of human Barth syndrome. *J Biol Chem.* **286**, 899-908

261. Phoon, C. K., Acehan, D., Schlame, M., Stokes, D. L., Edelman-Novemsky, I., Yu, D., Xu, Y., Viswanathan, N., and Ren, M. (2012) Tafazzin knockdown in mice leads to a developmental cardiomyopathy with early diastolic dysfunction preceding myocardial noncompaction. *J. Am. Heart Assoc.* **1**

262. Barth, P. G., Scholte, H. R., Berden, J. A., van der Klei-van Moorsel, J. M., Luyt-Houwen, I. E. M., van 'T Veer-Korthof, E. T., van der Harten, J. J., and Sobotka-Plojhar, M. A. (1983) An X-linked mitochondrial disease affecting cardiac muscle, skeletal muscle and neutrophil leucocytes. *J Neurological Sci.* **62**, 327-355

263. Kolwicz, S. C., Jr., and Tian, R. (2009) Metabolic therapy at the crossroad: how to optimize myocardial substrate utilization? *Trends Cardiovasc. Med.* **19**, 201-207

264. Sen, S., Kundu, B. K., Wu, H. C., Hashmi, S. S., Guthrie, P., Locke, L. W., Roy, R. J., Matherne, G. P., Berr, S. S., Terwelp, M., Scott, B., Carranza, S., Frazier, O. H., Glover, D. K., Dillmann, W. H., Gambello, M. J., Entman, M. L., and Taegtmeyer, H. (2013) Glucose regulation of load-induced mTOR signaling and ER stress in mammalian heart. *J. Am. Heart Assoc.* **2**, e004796

265. Sharma, S., Guthrie, P. H., Chan, S. S., Haq, S., and Taegtmeyer, H. (2007) Glucose phosphorylation is required for insulin-dependent mTOR signalling in the heart. *Cardiovasc. Res.* **76**, 71-80

266. Paul, D. S., Grevengoed, T. J., Pascual, F., Ellis, J. M., Willis, M. S., and Coleman, R. A. (2014) Deficiency of cardiac Acyl-CoA synthetase-1 induces diastolic dysfunction, but pathologic hypertrophy is reversed by rapamycin. *Biochim. Biophys. Acta* **1841**, 880-887

267. Zhang, D., Contu, R., Latronico, M. V., Zhang, J., Rizzi, R., Catalucci, D., Miyamoto, S., Huang, K., Ceci, M., Gu, Y., Dalton, N. D., Peterson, K. L., Guan, K. L., Brown, J. H., Chen, J., Sonenberg, N., and Condorelli, G. (2010) MTORC1 regulates cardiac function and myocyte survival through 4E-BP1 inhibition in mice. *J. Clin. Invest.* **120**, 2805-2816

268. Zhu, Y., Pires, K. M., Whitehead, K. J., Olsen, C. D., Wayment, B., Zhang, Y. C., Bugger, H., Ilkun, O., Litwin, S. E., Thomas, G., Kozma, S. C., and Abel, E. D. (2013) Mechanistic target of rapamycin (Mtor) is essential for murine embryonic heart development and growth. *PLoS One.* **8**, e54221

269. Brown, N. F., Stefanovic-Racic, M., Sipula, I. J., and Perdomo, G. (2007) The mammalian target of rapamycin regulates lipid metabolism in primary cultures of rat hepatocytes. *Metabolism.* **56**, 1500-1507

270. Zhu, Y., Soto, J., Anderson, B., Riehle, C., Zhang, Y. C., Wende, A. R., Jones, D., McClain, D. A., and Abel, E. D. (2013) Regulation of fatty acid metabolism by mTOR in adult murine hearts occurs independently of changes in PGC-1alpha. *Am. J. Physiol. Heart Circ. Physiol.* **305**, H41-51

271. Wu, J. J., Liu, J., Chen, E. B., Wang, J. J., Cao, L., Narayan, N., Fergusson, M. M., Rovira, II, Allen, M., Springer, D. A., Lago, C. U., Zhang, S., DuBois, W., Ward, T., deCabo, R., Gavrilova, O., Mock, B., and Finkel, T. (2013) Increased mammalian lifespan and a segmental and tissue-specific slowing of aging after genetic reduction of mTOR expression. *Cell. Rep.* **4**, 913-920

272. Morita, M., Gravel, S. P., Chenard, V., Sikstrom, K., Zheng, L., Alain, T., Gandin, V., Avizonis, D., Arguello, M., Zakaria, C., McLaughlan, S., Nouet, Y., Pause, A., Pollak, M., Gottlieb, E., Larsson, O., St-Pierre, J., Topisirovic, I., and Sonenberg, N. (2013) mTORC1 controls mitochondrial activity and biogenesis through 4E-BP-dependent translational regulation. *Cell Metab.* **18**, 698-711

273. Goo, C. K., Lim, H. Y., Ho, Q. S., Too, H. P., Clement, M. V., and Wong, K. P. (2012) PTEN/Akt signaling controls mitochondrial respiratory capacity through 4E-BP1. *PLoS One.* **7**, e45806

274. Schieke, S. M., Phillips, D., McCoy, J. P., Jr., Aponte, A. M., Shen, R. F., Balaban, R. S., and Finkel, T. (2006) The mammalian target of rapamycin (mTOR) pathway regulates mitochondrial oxygen consumption and oxidative capacity. *J. Biol. Chem.* **281**, 27643-27652

275. Aschenbrenner, B., Druyan, R., Albin, R., and Rabinowitz, M. (1970) Haem a, cytochrome c and total protein turnover in mitochondria from rat heart and liver. *Biochem J.* **119**, 157-160

276. Gross, N. J., Getz, G. S., and Rabinowitz, M. (1969) Apparent turnover of mitochondrial deoxyribonucleic acid and mitochondrial phospholipids in the tissues of the rat. *J Biol Chem.* **244**, 1552-1562

277. Lamming, D. W., Ye, L., Katajisto, P., Goncalves, M. D., Saitoh, M., Stevens, D. M., Davis, J. G., Salmon, A. B., Richardson, A., Ahima, R. S., Guertin, D. A., Sabatini, D. M., and Baur, J. A. (2012) Rapamycin-induced insulin resistance is mediated by mTORC2 loss and uncoupled from longevity. *Science.* **335**, 1638-1643

278. Barlow, A. D., Nicholson, M. L., and Herbert, T. P. (2013) Evidence for rapamycin toxicity in pancreatic beta-cells and a review of the underlying molecular mechanisms. *Diabetes.* **62**, 2674-2682

279. Willis, M. S., Homeister, J. W., Rosson, G. B., Annayev, Y., Holley, D., Holly, S. P., Madden, V. J., Godfrey, V., Parise, L. V., and Bultman, S. J. (2012) Functional redundancy of SWI/SNF catalytic subunits in maintaining vascular endothelial cells in the adult heart. *Circ. Res.* **111**, e111-122

280. Wittig, I., Karas, M., and Schagger, H. (2007) High resolution clear native electrophoresis for in-gel functional assays and fluorescence studies of membrane protein complexes. *Mol. Cell. Proteomics* **6**, 1215-1225

281. He, L., Kim, T., Long, Q., Liu, J., Wang, P., Zhou, Y., Ding, Y., Prasain, J., Wood, P. A., and Yang, Q. (2012) Carnitine palmitoyltransferase-1b deficiency aggravates pressure overload-induced cardiac hypertrophy caused by lipotoxicity. *Circulation.* **126**, 1705-1716

282. Fullekrug, J., Ehehalt, R., and Poppelreuther, M. (2012) Outlook: membrane junctions enable the metabolic trapping of fatty acids by intracellular acyl-CoA synthetases. *Front Physiol.* **3**, 401

283. Cunningham, J. T., Rodgers, J. T., Arlow, D. H., Vazquez, F., Mootha, V. K., and Puigserver, P. (2007) mTOR controls mitochondrial oxidative function through a YY1-PGC-1alpha transcriptional complex. *Nature.* **450**, 736-740

284. Mizushima, N., Yoshimori, T., and Levine, B. (2010) Methods in mammalian autophagy research. *Cell.* **140**, 313-326

285. Sarkar, S., Ravikumar, B., and Rubinsztein, D. C. (2009) Autophagic clearance of aggregate-prone proteins associated with neurodegeneration. *Methods Enzymol.* **453**, 83-110

286. Klionsky, D. J., and al., e. (2012) Guidelines for the use and interpretation of assays for monitoring autophagy. *Autophagy.* **8**, 445-544

287. Komatsu, M., Waguri, S., Koike, M., Sou, Y. S., Ueno, T., Hara, T., Mizushima, N., Iwata, J., Ezaki, J., Murata, S., Hamazaki, J., Nishito, Y., Iemura, S., Natsume, T., Yanagawa, T., Uwayama, J., Warabi, E., Yoshida, H., Ishii, T., Kobayashi, A., Yamamoto, M., Yue, Z., Uchiyama, Y., Kominami, E., and Tanaka, K. (2007) Homeostatic levels of p62 control cytoplasmic inclusion body formation in autophagy-deficient mice. *Cell.* **131**, 1149-1163

288. Pankiv, S., Clausen, T. H., Lamark, T., Brech, A., Bruun, J. A., Outzen, H., Overvatn, A., Bjorkoy, G., and Johansen, T. (2007) p62/SQSTM1 binds directly to Atg8/LC3 to facilitate degradation of ubiquitinated protein aggregates by autophagy. *J. Biol. Chem.* **282**, 24131-24145

289. Goodwin, G. W., Taylor, C. S., and Taegtmeyer, H. (1998) Regulation of energy metabolism of the heart during acute increase in heart work. *J. Biol. Chem.* **273**, 29530-29539

290. Osorio, J. C., Stanley, W. C., Linke, A., Castellari, M., Diep, Q. N., Panchal, A. R., Hintze, T. H., Lopaschuk, G. D., and Recchia, F. A. (2002) Impaired myocardial fatty acid oxidation and reduced protein expression of retinoid X receptor-alpha in pacing-induced heart failure. *Circulation.* **106**, 606-612

291. Bugger, H., Schwarzer, M., Chen, D., Schrepper, A., Amorim, P. A., Schoepe, M., Nguyen, T. D., Mohr, F. W., Khalimonchuk, O., Weimer, B. C., and Doenst, T. (2010) Proteomic remodelling of mitochondrial oxidative pathways in pressure overload-induced heart failure. *Cardiovasc. Res.* **85**, 376-384

292. Pereira, R. O., Wende, A. R., Olsen, C., Soto, J., Rawlings, T., Zhu, Y., Anderson, S. M., and Abel, E. D. (2013) Inducible overexpression of GLUT1 prevents mitochondrial dysfunction and attenuates structural remodeling in pressure overload but does not prevent left ventricular dysfunction. *J. Am. Heart Assoc.* **2**, e000301

293. Dyck, J. R., Hopkins, T. A., Bonnet, S., Michelakis, E. D., Young, M. E., Watanabe, M., Kawase, Y., Jishage, K., and Lopaschuk, G. D. (2006) Absence of malonyl coenzyme A decarboxylase in mice increases cardiac glucose oxidation and protects the heart from ischemic injury. *Circulation.* **114**, 1721-1728

294. Yan, J., Young, M. E., Cui, L., Lopaschuk, G. D., Liao, R., and Tian, R. (2009) Increased glucose uptake and oxidation in mouse hearts prevent high fatty acid oxidation but cause cardiac dysfunction in diet-induced obesity. *Circulation* **119**, 2818-2828

295. Laplante, M., and Sabatini, D. M. (2012) mTOR Signaling in Growth Control and Disease. *Cell* **149**, 274-293

296. Murakami, M., Ichisaka, T., Maeda, M., Oshiro, N., Hara, K., Edenhofer, F., Kiyama, H., Yonezawa, K., and Yamanaka, S. (2004) mTOR is essential for growth and proliferation in early mouse embryos and embryonic stem cells. *Mol. Cell. Biol.* **24**, 6710-6718

297. Song, X., Kusakari, Y., Xiao, C. Y., Kinsella, S. D., Rosenberg, M. A., Scherrer-Crosbie, M., Hara, K., Rosenzweig, A., and Matsui, T. (2010) mTOR attenuates the inflammatory response in cardiomyocytes and prevents cardiac dysfunction in pathological hypertrophy. *Am. J. Physiol. Cell. Physiol.* **299**, C1256-1266

298. Aoyagi, T., Kusakari, Y., Xiao, C. Y., Inouye, B. T., Takahashi, M., Scherrer-Crosbie, M., Rosenzweig, A., Hara, K., and Matsui, T. (2012) Cardiac mTOR protects the heart against ischemia-reperfusion injury. *Am. J. Physiol. Heart Circ. Physiol.* **303**, H75-85

299. Shen, W. H., Chen, Z., Shi, S., Chen, H., Zhu, W., Penner, A., Bu, G., Li, W., Boyle, D. W., Rubart, M., Field, L. J., Abraham, R., Liechty, E. A., and Shou, W. (2008) Cardiac restricted overexpression of kinase-dead mammalian target of rapamycin (mTOR) mutant impairs the mTOR-mediated signaling and cardiac function. *J. Biol. Chem.* **283**, 13842-13849

300. McMullen, J. R., Sherwood, M. C., Tarnavski, O., Zhang, L., Dorfman, A. L., Shioi, T., and Izumo, S. (2004) Inhibition of mTOR signaling with rapamycin regresses established cardiac hypertrophy induced by pressure overload. *Circulation.* **109**, 3050-3055

301. Shioi, T., McMullen, J. R., Tarnavski, O., Converso, K., Sherwood, M. C., Manning, W. J., and Izumo, S. (2003) Rapamycin attenuates load-induced cardiac hypertrophy in mice. *Circulation.* **107**, 1664-1670

302. Schwarzer, M., Schrepper, A., Amorim, P. A., Osterholt, M., and Doenst, T. (2013) Pressure overload differentially affects respiratory capacity in interfibrillar and subsarcolemmal mitochondria. *Am. J. Physiol. Heart Circ. Physiol.* **304**, H529-537

303. Matsui, Y., Takagi, H., Qu, X., Abdellatif, M., Sakoda, H., Asano, T., Levine, B., and Sadoshima, J. (2007) Distinct roles of autophagy in the heart during ischemia and reperfusion: roles of AMP-activated protein kinase and Beclin 1 in mediating autophagy. *Circ. Res.* **100**, 914-922

304. Das, A., Salloum, F. N., Durrant, D., Ockaili, R., and Kukreja, R. C. (2012) Rapamycin protects against myocardial ischemia-reperfusion injury through JAK2-STAT3 signaling pathway. *J. Mol. Cell. Cardiol.* **53**, 858-869

305. Choi, J. C., and Worman, H. J. (2013) Reactivation of autophagy ameliorates LMNA cardiomyopathy. *Autophagy.* **9**, 110-111

306. Ramos, F. J., Kaeberlein, M., and Kennedy, B. K. (2013) Elevated mTORC1 signaling and impaired autophagy. *Autophagy.* **9**, 108-109

307. Xu, X., Hua, Y., Nair, S., Bucala, R., and Ren, J. (2014) Macrophage migration inhibitory factor deletion exacerbates pressure overload-induced cardiac hypertrophy through mitigating autophagy. *Hypertension.* **63**, 490-499

308. Dutta, D., Xu, J., Kim, J. S., Dunn, W. A., Jr., and Leeuwenburgh, C. (2013) Upregulated autophagy protects cardiomyocytes from oxidative stress-induced toxicity. *Autophagy.* **9**, 328-344

309. Kane, L. A., Youngman, M. J., Jensen, R. E., and Van Eyk, J. E. (2010) Phosphorylation of the F(1)F(o) ATP synthase beta subunit: functional and structural consequences assessed in a model system. *Circ. Res.* **106**, 504-513

310. Vassilopoulos, A., Pennington, J. D., Andresson, T., Rees, D. M., Bosley, A. D., Fearnley, I. M., Ham, A., Flynn, C. R., Hill, S., Rose, K. L., Kim, H. S., Deng, C. X., Walker, J. E., and Gius, D. (2014) SIRT3 deacetylates ATP synthase F1 complex proteins in response to nutrient- and exercise-induced stress. *Antioxid. Redox Signal.* **21**, 551-564

311. Rahman, M., Nirala, N. K., Singh, A., Zhu, L. J., Taguchi, K., Bamba, T., Fukusaki, E., Shaw, L. M., Lambright, D. G., Acharya, J. K., and Acharya, U. R. (2014) Drosophila Sirt2/mammalian SIRT3 deacetylates ATP synthase beta and regulates complex V activity. *J. Cell. Biol.* **206**, 289-305

312. Taylor, S. W., Fahy, E., Murray, J., Capaldi, R. A., and Ghosh, S. S. (2003) Oxidative post-translational modification of tryptophan residues in cardiac mitochondrial proteins. *J. Biol. Chem.* **278**, 19587-19590

313. Phillips, C. M., Goumidi, L., Bertrais, S., Field, M. R., Cupples, L. A., Ordovas, J. M., Defoort, C., Lovegrove, J. A., Drevon, C. A., Gibney, M. J., Blaak, E. E., Kiec-Wilk, B., Karlstrom, B., Lopez-Miranda, J., McManus, R., Hercberg, S., Lairon, D., Planells, R., and Roche, H. M. (2010) Gene-nutrient interactions with dietary fat modulate the association between genetic variation of the ACSL1 gene and metabolic syndrome. *J Lipid Res.* **51**, 1793-1800

314. Gertow, K., Rosell, M., Sjogren, P., Eriksson, P., Vessby, B., de Faire, U., Hamsten, A., Hellenius, M. L., and Fisher, R. M. (2006) Fatty acid handling protein expression in adipose tissue, fatty acid composition of adipose tissue and serum, and markers of insulin resistance. *Eur J Clin Nutr.* **60**, 1406-1413

315. Bouchard, C., Sarzynski, M. A., Rice, T. K., Kraus, W. E., Church, T. S., Sung, Y. J., Rao, D. C., and Rankinen, T. (2011) Genomic predictors of the maximal O(2) uptake response to standardized exercise training programs. *J Appl Physiol.* **110**, 1160-1170

316. Le, C. (2013) *Influence of cardiolipin remodeling on mitochondrial respiratory function in the heart.* PhD PhD Dissertation, Colorado State University

317. Varadarajan, S. G., An, J., Novalija, E., Smart, S. C., and Stowe, D. F. (2001) Changes in [Na(+)](i), compartmental [Ca(2+)], and NADH with dysfunction after global ischemia in intact hearts. *Am. J. Physiol. Heart Circ. Physiol.* **280**, H280-293

318. Porter, G. A., Urciuoli, W. R., Brookes, P. S., and Nadtochiy, S. M. (2014) SIRT3 deficiency exacerbates ischemia-reperfusion injury: implication for aged hearts. *Am. J. Physiol. Heart Circ. Physiol.* **306**, H1602-1609

319. Ruan, Y., Dong, C., Patel, J., Duan, C., Wang, X., Wu, X., Cao, Y., Pu, L., Lu, D., Shen, T., and Li, J. (2015) SIRT1 suppresses doxorubicin-induced cardiotoxicity by regulating the oxidative stress and p38MAPK pathways. *Cell Physiol Biochem.* **35**, 1116-1124

320. Li, L. O., Grevengoed, T. J., Paul, D. S., Ilkayeva, O., Koves, T. R., Pascual, F., Newgard, C. B., Muoio, D. M., and Coleman, R. A. (2015) Compartmentalized acyl-CoA metabolism in skeletal muscle regulates systemic glucose homeostasis. *Diabetes.* **64**, 23-35